

Impacts of Biochar Application to a Douglas-fir Forest Soil on Greenhouse Gas Fluxes and
Water Quality

by

Iain Hawthorne

A THESIS SUBMITTED IN PARTIAL FULFILLMENT OF THE REQUIREMENTS FOR
THE DEGREE OF

Doctor of Philosophy

in

The Faculty of Graduate and Postdoctoral Studies

(Geological Sciences)

THE UNIVERSITY OF BRITISH COLUMBIA
(Vancouver)

April 2017

© Iain Hawthorne, 2017

Abstract

Forest management for carbon sequestration is a valuable tool to combat rising greenhouse gas (GHG) concentrations in the Earth's atmosphere. This thesis examined the use of *biochar*, a product of the thermal decomposition of waste organic matter in a reduced oxygen environment (i.e. pyrolysis) that is applied to soil, as an option for increasing carbon sequestration in a Coastal Douglas-fir forest soil in British Columbia when applied with and without urea fertilizer at 200 kg N ha⁻¹. Biochar produced from Douglas-fir forestry slash materials was used in this study to address this from a systems-based perspective.

A soil incubation study showed that biochar application at high rates (10% oven dry soil basis) significantly increased CO₂ and N₂O emissions when applied without fertilizer and at both low (1%) and high rates (10%) decreased CH₄ consumption without fertilization. In terms of carbon dioxide equivalent emissions (CO₂e), it was shown that CO₂ accounted for >98% from all treatments. In a field study, GHG fluxes were measured after application of 5 t ha⁻¹ of biochar to a Douglas-fir forest soil in the first year followed by urea-N fertilization in the second year. The results showed that 5 t ha⁻¹ of biochar had little effect on GHG fluxes and their total CO₂e fluxes. Applying biochar prior to fertilizer application following industry-standard practices did not significantly change treatment CO₂e fluxes. It was concluded that low rates of biochar application to this forest soil would improve soil C sequestration with or without fertilization.

In the field and laboratory experiments, soil pore water was extracted and analyzed for C and N concentrations and dissolved organic carbon using spectral indices. The results showed that low biochar application rates could be beneficial for both increasing C-sequestration and N-retention. Changes in spectral indices measured in the laboratory suggested that alterations in the dissolved organic matter pool could lead to changes in GHG emissions due to changing substrate

supply for microbes as application rates increased. There is a recognized need for further studies prior to large-scale industrial applications; however, as result of this work it is possible to provide recommendations for large-scale pilot studies.

Preface

Chapter 2 is based on work conducted in UBC laboratories. The author designed and conducted an experiment utilizing a state-of-the-art measurement system capable of quantifying difficult-to-detect greenhouse gas (GHG) fluxes of carbon dioxide (CO₂), methane (CH₄) and nitrous oxide (N₂O) using a novel soil incubation system. This development facilitated a first of its kind comparison of treatment effects on soil GHG fluxes after treatment of a Douglas-fir forest soil with 0%, 1% and 10% Douglas-fir derived biochar with and without a 200 kg ha⁻¹ urea-N fertilizer application. This work was presented at the 2016 Canadian Society of Soil Science and Pacific Society of Soil Science Joint Annual General Meeting 16th May 2016. The author collected and analyzed the data, and wrote a paper, to which Drs. M.S. Johnson, T.A. Black, R. S. Jassal, S. M. Smukler and N. J. Grant made editorial contributions that is published in the *Journal of Environmental Management*: Hawthorne, I., Johnson, M. S., Jassal, R. S., Black, T. A., Grant, N. J., and Smukler, S. M. (2017), Application of biochar and nitrogen influences fluxes of CO₂, CH₄ and N₂O in a forest soil, *Journal of Environmental Management*, 192, 203-214, doi:<http://dx.doi.org/10.1016/j.jenvman.2016.12.066>.

Chapter 3 is based on work conducted near a well-established micrometeorology and stream water quality research site, jointly operated by the UBC Biometeorology and Soil Physics Research Group and UBC Ecohydrology Research Group, in a Coastal Douglas-fir forest near Campbell River on Vancouver Island, Canada. The author, with field help from undergraduate and laboratory associates, conducted an experiment using non-steady-state chamber techniques and gas chromatography to measure fluxes of CO₂, CH₄ and N₂O over 1 year following a surface application of Douglas-fir derived biochar (5 t ha⁻¹) and a surface application of urea fertilizer

(200 kg N ha⁻¹) in the following year. The author collected and analyzed the data and wrote a paper draft, which was guided and contributed to by Drs. M.S Johnson, T.A. Black, and R. S. Jassal, with additional input at the later editing stages from N.J. Grant. This work was presented at the American Geophysical Union 2013 Annual General Meeting on 16th December 2013. It was also presented at the Western Silvicultural Contractors' Association on 2nd February 2017, which stimulated discussion with government and private companies on how to increase the scale and scope of biochar research for enhancing carbon sequestration using forest management in BC. The goal is to publish this chapter in a suitable peer-reviewed journal. Of significance were the installation, development and maintenance of the laboratory gas chromatography system. The author acted as supervisor of instrument operations for more than 10 undergraduate and graduate projects collaborating with the Faculty of Forestry, Faculty of Land and Food Systems and the Department of Geography at UBC, and) and with two other university organizations (Quest University, Squamish, BC and Cornell University, Ithaca, New York) to facilitate affordable GHG analysis, helping to promote environmental science across in North America.

Chapter 4 is based on work done using the laboratory incubation system described in Chapter 2 and the field research site described in Chapter 3. The author describes soil pore water extractions from both studies and how the dissolved organic carbon (DOC) and total dissolved nitrogen (TDN) are affected by Douglas-fir derived biochar and urea-N fertilizer application. Measured ultraviolet-visible spectroscopy spectral indices were used to compare the dissolved organic matter molecular signals between the treatments, an area not well researched yet in the current literature available for biochar studies. The author collected and analyzed the data and

has worked on a draft of this chapter, which was guided and contributed by Drs. M.S Johnson, T.A. Black, and R. S. Jassal. This work was presented on 2nd February 2017 at the Western Silvicultural Contractors' Association annual general meeting, further stimulating discussion with government and private companies on how to increase the scale and scope of biochar research for enhancing carbon sequestration using forest management in BC. The aim is to publish this chapter in a suitable peer-reviewed journal.

Table of Contents

| | |
|--|--------------|
| Abstract | ii |
| Preface | iv |
| Table of Contents | vii |
| List of Tables | xi |
| List of Figures | xii |
| List of Abbreviations | xvi |
| List of Symbols | xviii |
| Acknowledgments | xix |
| Chapter 1: Introduction | 1 |
| 1.1 Background and study motivation | 1 |
| 1.2 Research objectives | 7 |
| 1.3 Thesis overview | 7 |
| Chapter 2: Douglas-fir forest soil incubation experiment to measure greenhouse gas emissions after biochar application at three rates with and without urea-N fertilization | 10 |
| 2.1 Introduction | 10 |
| 2.2 Materials and methods | 12 |
| 2.2.1 Soil | 12 |
| 2.2.2 Biochar | 13 |
| 2.2.3 Experimental incubations..... | 14 |
| 2.2.4 GHG flux measurements..... | 15 |

| | |
|--|-----------|
| 2.2.5 Statistical analysis..... | 17 |
| 2.3 Results and discussion | 18 |
| 2.3.1 Temporal variation in GHG fluxes..... | 18 |
| 2.3.2 Effect of biochar application rates on soil GHG fluxes from unfertilized soil..... | 20 |
| 2.3.3 Fertilizer effects on soil GHG flux responses to biochar application rates..... | 22 |
| 2.3.4 Influence of soil moisture on GHG fluxes | 24 |
| 2.3.5 Global warming potentials | 24 |
| 2.4 Conclusions | 26 |
| 2.5 Tables | 27 |
| 2.6 Figures | 28 |
| | |
| Chapter 3: In-situ measurements of greenhouse gas emissions after biochar | |
| application with and without urea-N fertilization at a Coastal Douglas-fir forest | 37 |
| 3.1 Introduction..... | 37 |
| 3.2 Methods | 41 |
| 3.2.1 Site description | 41 |
| 3.2.2 Experimental design | 42 |
| 3.2.3 Biochar and fertilizer application | 43 |
| 3.2.3 Field soil GHG emission measurements | 44 |
| 3.2.3.1 Sample collection and ancillary measurements..... | 44 |
| 3.2.3.2 Greenhouse gas analyses and flux calculations..... | 46 |
| 3.2.4 Data analysis..... | 46 |
| 3.3 Results..... | 48 |
| 3.3.1 Soil climate | 48 |
| 3.3.2 Soil greenhouse gas fluxes..... | 49 |
| 3.3.2.1 Soil CO ₂ emissions | 49 |

| | |
|--|-----------|
| 3.3.2.2 Soil CH ₄ Uptake | 52 |
| 3.3.2.3 Soil N ₂ O emission and uptake | 53 |
| 3.3.2.4 Soil CO ₂ e and GWP | 54 |
| 3.3.3 Soil greenhouse gas flux relationships to soil climate..... | 55 |
| 3.4 Discussion | 57 |
| 3.4.1 Biochar treatment effects | 57 |
| 3.4.2 Fertilizer treatment effects | 59 |
| 3.4.3 Carbon dioxide equivalent fluxes | 63 |
| 3.5 Conclusions | 64 |
| 3.6 Tables | 65 |
| 3.7 Figures | 66 |
| | |
| Chapter 4: Laboratory and field measurements of dissolved organic carbon and nitrogen after biochar application with and without urea-N fertilization to a West Coast Douglas-fir forest soil | 71 |
| 4.1 Introduction..... | 71 |
| 4.2 Materials and methods..... | 75 |
| 4.2.1 Field soil water sampling..... | 76 |
| 4.2.2 Laboratory Experimental Setup..... | 78 |
| 4.2.3 Soil pore water analysis | 78 |
| 4.2.4 Soil moisture characterization | 80 |
| 4.2.5 Statistical analysis..... | 81 |
| 4.2.5.1 Field experiment..... | 81 |
| 4.2.5.2 Laboratory experiment..... | 81 |
| 4.3 Results..... | 82 |
| 4.3.1 Field experiment..... | 82 |

| | |
|--|------------|
| 4.3.1.1 Soil climate | 82 |
| 4.3.1.2 Field ancillary measurements of soil pore water quality..... | 83 |
| 4.3.1.3 Field soil pore water DOC and TN | 84 |
| 4.3.1.4 Field soil pore water spectral indices | 86 |
| 4.3.2 Laboratory experiment..... | 87 |
| 4.3.2.1 Laboratory ancillary soil pore water quality measurements..... | 87 |
| 4.3.2.2 Laboratory soil pore water DOC and TN | 87 |
| 4.3.2.3 Laboratory soil pore water spectral indices | 89 |
| 4.3.2.4 Laboratory soil TOC, NO ₃ ⁻ and NH ₄ ⁺ post experiment | 89 |
| 4.4 Discussion | 91 |
| 4.5 Conclusions | 95 |
| 4.6 Tables | 96 |
| 4.7 Figures | 99 |
| Chapter 5: Summary and conclusions..... | 109 |
| 5.1 Future work | 111 |
| 5.2 Overall significance | 112 |
| References..... | 114 |
| Appendices..... | 130 |
| Appendix 1 Site soil description..... | 130 |
| Appendix 2 Biochar details | 133 |
| Appendix 3 Minimum detectable flux estimation | 134 |
| Appendix 4 Project instrumentation | 136 |
| Appendix 5 Site images | 137 |

List of Tables

| | |
|---|-----|
| Table 1. Summary of experimental treatments | 27 |
| Table 2. Greenhouse gas annual (Annl) and seasonal one-way ANOVA. Spring-summer (SS), Summer-fall (SF). HSD analysis indicates which treatments were determined to be significantly larger than others in list. | 65 |
| Table 3. Treatment annual dependence of R_{s10} (μ mol CO ² m ⁻² s ⁻¹) and Q_{10Rs} parameters in Eq.2. Also shown model goodness of fit parameters AIC and R^2 . Fitted relationships for all data can be seen in Figure 14. | 65 |
| Table 4. Field EC _s and EC _{SCL} , pH _{SCL} and spectral indices. All values given are mean (± 1 standard error) of all available data in 2013 | 96 |
| Table 5. DOC _{SCL} vs TN _{SCL} linear regression analysis output | 96 |
| Table 6. Laboratory EC, pH and spectral indices. All values given are mean (± 1 standard error) of all data collected after more than 1 L of DDI had been flushed through each incubation. | 97 |
| Table 7. DOC _{LAB} vs TN _{LAB} linear regression analysis output..... | 97 |
| Table 8. S ₂₇₅₋₂₉₅ vs leachate volume linear regression analysis output..... | 98 |
| Table 9. Soil characteristics literature review | 130 |
| Table 10. Soil characteristics..... | 131 |
| Table 11 Fine mineral fraction % | 131 |
| Table 12. Textural class soil organic matter content | 131 |
| Table 13. Diacarbon Douglas-fir derived biochar particle size distribution | 133 |

List of Figures

| | |
|--|-----------|
| Figure 1. Incubation units attached to the CRDS greenhouse gas analyzer comprising a closed chamber soil flux measurement system. The four replicates of the six treatments are shown in the inset photo, as (A) unamended soil (S); (B) Soil + 1% biochar (w/w) (BC1%); (C) Soil + 10% biochar (BC10%); (D) Soil + fertilizer (200 kg N ha⁻¹ equivalent of urea fertilizer) (S+F); (E) Soil + 1% biochar + fertilizer (BC1%+F); (F) Soil + 10% biochar +fertilizer (BC10%+F)..... | 28 |
| Figure 2. (A) Cumulative CO₂ effluxes during experiment by treatment (means ± 1 standard error (SE)); (B) Daily mean CO₂ flux time series plot (means ± 1 standard error (SE))..... | 29 |
| Figure 3. (B) Cumulative CH₄ effluxes during experiment by treatment (means ± 1 standard error (SE)); (B) Daily mean CH₄ flux time series plot (means ± 1 standard error (SE))..... | 30 |
| Figure 4. (A) Cumulative N₂O effluxes during experiment by treatment (means ± 1 standard error (SE)); (B) Daily mean N₂O flux time series plot (means ± 1 standard error (SE))..... | 31 |
| Figure 5. Boxplots of soil CO₂ efflux during the post-disturbance period by treatment. The thick horizontal line represents the means, the upper and lower lines of the boxes indicate the means ± 1 SE, and the whiskers extend to the maximum and minimum fluxes measured during the post-disturbance period. | 32 |
| Figure 6. Boxplots of soil CH₄ efflux during the post-disturbance period by treatment. The thick horizontal line represents the means, the upper and lower lines of the boxes indicate the means ± 1 SE, and the whiskers extend to the maximum and minimum fluxes measured during the post-disturbance period. | 33 |
| Figure 7. Boxplots of soil N₂O efflux during the post-disturbance period by treatment. The thick horizontal line represents the means, the upper and lower lines of the boxes indicate the means ± 1 SE, and the whiskers extend to the maximum and minimum fluxes measured during the post-disturbance period. | 34 |
| Figure 8. Principal component analysis of experimental variables..... | 35 |
| Figure 9. Effect of treatments on net GHG emissions in terms of CO_{2e} relative to unamended soil. The magnitude of the CH₄ consumption is subtracted from the CO₂ plus N₂O total..... | 36 |

Figure 10. Site soil climate variables. (A) Daily cumulative precipitation measured at a nearby climate station. Dashed lines indicate biochar application (27th Feb 2012) and fertilizer application (27th Mar 2013); (B) Daily mean T_{s15} from averaging each MPS-2 and GS3 measurements; (C) Daily mean θ_{s15} from averaging GS3 measurements; (D) Logarithm of the daily mean Ψ_{s15} from MPS-2 measurements. Dashed lines indicate sample dates..... 66

Figure 11. Mean treatment CO₂ fluxes for soil (S), biochar (BC), fertilizer (F) and Biochar plus Fertilizer (BC+F). During 2012 when only the biochar treatment was applied (top panel); Measurements during 2013 when all treatment were applied (bottom panel). Error bars indicate \pm one standard error of the mean treatment value and points have been spread evenly for each sample date to ease comparison..... 67

Figure 12. Methane 2012:2013 seasonal treatment effect (mean \pm 1 SE). Spring-summer (SS), Summer-fall (SF). Lettering (a-b) indicates pairwise differences detected in HSD analysis when $p < 0.05$ 68

Figure 13. Nitrous oxide 2012:2013 seasonal treatment fluxes (Mean \pm 1 SE). Summer-spring (SS), Spring-fall (SF). Lettering (a-b) indicates pairwise differences detected in HSD analysis when $p < 0.05$ 69

Figure 14. Relationship of soil CO₂ efflux (R_s) to soil temperature at 15-cm depth for different treatments. 70

Figure 15. Suction cup lysimeter (SCL) sample date (dashed lines) daily (month-day) soil climate at 15-cm depth. (A) Daily precipitation with cumulative precipitation prior to each sample date is provided above and below this the cumulative amount of precipitation since fertilization; (B) Treatment EC_s, mean (± 1 SE), 1 and 2 asterisks indicates where one way ANOVA detected statistical differences between treatments at $p < 0.01$ and $p < 0.5$ respectively; (C) Soil temperature, site mean (± 1 standard deviation); (D) Volumetric soil water content site mean (± 1 SD); (E) Soil water matric potential, site mean (± 1 SD). In plots B-E values shown are the mean values from soil sensors with one in each of 12 plots, evenly distributed between treatments. The red dashed line indicates timing of fertilization..... 99

| | |
|--|-----|
| Figure 16. Field sample date treatment surface EC measurements, mean (± 1 standard error). (i) 2-days. (ii) 9-days. (iii) 16-days and (iv) 21-days after fertilization on 26 March 2013. There is a significant response to fertilization in F and BC+F treatment plots 9-days and less so 16-days after fertilization. | 100 |
| Figure 17. Field sample date treatment mean DOC _{SCL} (± 1 standard error). (A) 2012; (B) 2013 | 100 |
| Figure 18. Field sample date (month-day) treatment mean TN (± 1 standard error). (A) 2012; (B) 2013 | 101 |
| Figure 19. Suction cup lysimeter mean (± 1 standard error) DOC and TN observations from data collected during 2013 (A) DOC _{SCL} ; (B) TN _{SCL} ; (C) Treatment DOC vs TN analysis. Colored dashed lines in panels (A) and (B) indicate the treatment to be used as an aid to identifying dataset outliers..... | 102 |
| Figure 20. Suction cup lysimeter mean (± 1 standard error) (A) $S_{275-295}$; (B) SUVA ₂₅₄ | 103 |
| Figure 21. Soil incubation pore water treatment mean EC (A) and pH (B) measurements over the course of the leaching experiment. Error bars indicate one standard error..... | 104 |
| Figure 22. Soil incubation pore water treatment mean DOC (A) and TN (B) measurements over the course of the leaching experiment. Error bars indicate one standard error..... | 105 |
| Figure 23. Soil incubation pore water treatment boxplots of (A) DOC and (B) TN after >1 L volume of leachate collected. Error bars are one standard error. (C) Relationship between DOC and TN. The coloured dashed lines are the lines of best fit for each treatment following treatment color conventions in (A) and (B). | 106 |
| Figure 24. Soil incubation pore water treatment UV-Vis spectroscopy-based indicators of DOC quality (A) $S_{275-295}$ and (B) SUVA ₂₅₄ | 107 |
| Figure 25. (A) Amount of nitrogen species (NH ₄ ⁺ -N and NO ₃ ⁻ -N) remaining in soil following the soil incubation experiment for each treatment; (B) Mean treatment ratio of nitrogen species (NH ₄ -N/NO ₃ -N). Error bars are one standard error. | 108 |
| Figure 26. This image shows a slash piles in the foreground, with eight more visible in the background at a near-by (within 500 m of research location) harvested forest location that could have been feedstock for biochar production. | 137 |

Figure 27. This image shows the slash piles burned to improve access for replanting and reduce forest fire hazard. 137

Figure 28. Research site soil profile 138

Figure 29. This image shows a static non-steady state chamber between two large trees with the chamber lid on during a site greenhouse gas flux measurement campaign. 138

Figure 30. This image shows the ancillary GS3 instrument in use for surface soil electrical conductivity (EC_s), volumetric water content and temperature measurements in close proximity to a static non-steady state chamber collar. Also seen are 5 vials used for greenhouse gas sample storage in preparation for chamber flux measurements. 139

Figure 31. Biochar being hand applied on date of application (27th Feb 2012). 139

Figure 32. Completed biochar application, showing contrasting color with untreated surrounding area. 140

List of Abbreviations

ANOVA – analysis of variance

AIC – Akaike information criterion

UBC – the University of British Columbia

C - carbon

CO₂ – carbon dioxide

CO_{2e} – carbon dioxide equivalent

CH₄ - methane

CEC – cation exchange capacity

DDI – deionized distilled water

df – Degrees of freedom

EC – electrical conductivity

F – F statistic

DOC – dissolved organic carbon

FID – flame ionization detector

GC – gas chromatograph

GHG – greenhouse gas

GPP – gross primary productivity

GWP – global warming potential

HCL - hydrochloric acid

IBI – international biochar initiative

IPCC – Intergovernmental Panel on Climate Change

KCL – potassium chloride

μ ECD – micro-electron capture device

MC – molecular weight

N – nitrogen

NEP – net ecosystem productivity

NH_4^+ - ammonium

NO_3^- – nitrate

N_2O – nitrous oxide

NPOC – non-purgeable organic carbon

p - probability value

PTFE - polytetrafluoroethylene

SCL – suction cup lysimeter

SE – standard error

SNSS – static non-steady state chamber

SOC – soil organic carbon

SOM – soil organic matter (~58% carbon)

SUVA_{254} – specific UV absorbance at 254 nm

TN – total nitrogen

TOC – Total organic carbon

Tukey HSD – Tukey honest significant difference test

UV-vis – Ultraviolet visible

List of Symbols

T_s - soil temperature (0-5 cm)

θ_s - volumetric soil water content (0-5 cm)

σ_s - bulk electrical conductivity (0-5 cm)

θ_{15} - volumetric soil water content (15-cm depth)

σ_{15} - bulk electrical conductivity (15-cm depth)

T_{15} - soil temperature (15-cm depth)

Ψ_{15} - soil water matric potential (15-cm depth)

R_a – autotrophic soil respiration

R_e – ecosystem respiration

R_h – heterotrophic soil respiration

R_s – total soil respiration

R_{s10} – reference respiration rate at 10 °C

Q_{10R_s} - relative change in R_s for 10 °C change in shallow surface soil temperature

Acknowledgments

This research in this thesis was financially supported through a Natural Resources and Applied Sciences Research Team Grant from the BC Innovation Council to MSJ and TAB, with additional support from the Natural Sciences and Engineering Research Council Discovery grants to MSJ and TAB. The author is thankful to Decagon Devices, Inc. for support through the Grant A. Harris Fellowship.

The work carried out in this thesis could not have been achieved without the network of support that I receive at UBC. Thank you to all of the undergraduate students and graduate students, in particular Cameron Webster and Mathias Meyer, who have helped chip away at the task in hand. The UBC Biometeorology and Soil Physics Group and members, Nicholas Grant, Zoran Nestic, Hughie Jones and past member Rick Ketler have been instrumental in providing essential field, laboratory and moral support. Thanks guys!

I would like to thank Dr. Mark Johnson for much more than being my supervisor, his support and guidance has been bottomless, Dr. Andrew T. Black for guiding me academically to value the attention to detail that he applies to every endeavor and Dr. Ulrich Meyer for responding promptly, effectively and kindly whenever called.

I would like to thank my family for always believing in me. Finally, Christine, THANK YOU, you have kept me in check, making me a stronger and happier person.

I would like to dedicate this thesis to David Gaumont-Guay (1972-2016) and Thomas Hilker (1976-2016). They remain inspirational.

Chapter 1: Introduction

1.1 Background and study motivation

Global climate change caused by increasing concentrations of greenhouse gases (GHGs) in the Earth's atmosphere is creating an uncertain climate future for generations to come (IPCC, 2014). There are no human systems exempt from a direct or indirect dependency on natural resource supply and climate. A broad recognition of this has pushed forward the issue of how to best reduce the anthropogenic contribution to global warming through quantifying sinks and sources of GHGs, finding ways to maximize the efficiency with which we manage natural resources and acknowledging ecosystems for their services (Foley et al., 2005). The most significant long-lived GHGs in terms of atmospheric concentrations are carbon dioxide (CO₂), methane (CH₄) and nitrous oxide (N₂O). It is estimated that CO₂ accounts for >65% of the increase in radiative forcing when expressed over a 100 year time period (IPCC, 2014). Referencing the radiative forcing of other non-CO₂ gases to the radiative forcing of CO₂ provides a metric commonly referred to as the global warming potential (GWP) which can be used to compare emissions from different sources/sectors and landscape treatments on different spatial scales (IPCC, 2014; Lashof and Ahuja, 1990; Montzka et al., 2011). The GWP is calculated on a mass basis with CH₄ and N₂O each having 28 and 298 times the radiative forcing of CO₂ over a 100 year time period, respectively (IPCC, 2014).

One way to reduce the global climatic impact of increasing CO₂ and other GHGs is to store carbon (C) in forms other than as CO₂ in the atmosphere. Soil C, at 4.5 times the size of the biotic C pool and 3.3 times the size of the atmospheric C pool, is hugely important in the global C cycle (Lal et al., 2004). Forests absorb CO₂ through photosynthesis then release a portion of it back through respiration. On balance, forests in recent decades have acted as a net sink for as

much as 30 % of annual anthropogenic CO₂ emissions (Houghton, 2000, Pan et al., 2011). Reducing CO₂ emissions from deforestation and forest degradation, enhancing C sequestration rates in existing and new forests, substituting wood fuels for fossil fuels, and providing wood products in place of more energy-intensive materials are all recognized options for improving forest management to help mitigate climate change (IPCC, 2014). Increasing soil C stocks through *biochar* addition provides an additional option that has been receiving increasing attention in recent years (IPCC, 2014).

Biochar is a product of the thermal decomposition of organic matter in a reduced oxygen environment (i.e. pyrolysis). Biochar typically has high C content and has the potential to be used as a climate change mitigation strategy by reducing the amount of CO₂ in the atmosphere through increased C sequestration in soils (Lehman *et al.*, 2006). It is resistant to decomposition in soils due to a prevalence of aromatic structures containing few functional groups (Dai et al., 2005, Zimmerman, 2010), which has been shown to be particularly true when the O:C ratio of the biochar is less than 0.2 (Spokas, 2010). Biochar has a lower specific density compared to mineral soils, with larger surface areas (Brewer et al., 2014). When incorporated into soil, biochar alters the physical structure of soil, generally decreasing its bulk density (Major et al., 2010; Lim et al., 2016), increasing the exposure of chemically reactive surfaces, and providing refugia for microbes (Lehmann et al., 2011). Changes to the physical structure of soils impacts soil water-holding characteristics, and leads to alterations in biotic and abiotic processes affecting fluxes of soil CO₂, CH₄ and N₂O (Major et al., 2010; Sohi et al., 2010). Biochar is known to affect soil inorganic nitrogen (N) dynamics differently when applied with or without fertilizers (Nguyen et al., 2017), affecting N contents in plants (Ling et al., 2017). It is advisable therefore that agronomic and silvicultural systems needing to increase productivity where

inorganic N is limited must consider effects of biochar application with and without fertilization, as well as the timing of applications (Nguyen et al., 2017). To do this, policy makers need clear information from a broad range of identifiably important forest and soil types.

The global forest resource assessment in 2015 determined that deforestation has slowed and reforestation has increased globally since 1990, though not in poorer tropical countries (Sloan and Seyer, 2015). In 2015, Natural Resources Canada reported in their annual State of Canada's forests report (Natural Resources Canada, 2016), that Canada has 9 % of the world's forests, exceeded only by Russia and Brazil. This equates to 347 million hectares of forest cover of which 166 million hectares is independently certified as being sustainably managed and 24 million hectares are protected. Notably, the Canadian forest industry generated more than \$20 billion CAD in 2015 towards the gross domestic product and provided more than 200,000 jobs. This puts Canada in a unique position to act as a global economic leader in forest C management.

In Canada, some of the most productive and economically valuable second-growth forests are the stands of Coastal Douglas-fir in British Columbia, where active forestry is an essential part of the local, provincial and national economy. These production forests in the coastal region of British Columbia are typically N-limited systems, and have been found to respond significantly to N-fertilizer additions (Chappell et al., 1991). Fertilizing Coastal Douglas-fir forests remains a common silvicultural practice in British Columbia's Coastal Forest Action Plan offers fiscal incentives to increase productivity of second-growth coastal forests using fertilization to provide a potential benefit of reducing GHG emissions through increased C sequestration while maintaining employment levels in the forest product sector (BCMFR, 2007). While fertilization can significantly increase gross primary productivity, not all fertilizer applied is taken up by the trees, with estimates of up to 20% of the applied fertilizer lost as N₂O gas or

through leaching losses of ammonium (NH_4^-) and nitrate (NO_3^-). Strategies to increase soil C sequestration for mitigating climate change that also improve the sustainability of the production of forest products and minimize nutrient losses are urgently needed. Biochar has been suggested as a means for doing so, though studies of biochar use in forested systems are currently limited (Thomas and Gale, 2015).

Soil CO_2 emissions, also termed soil respiration (R_s), are controlled by a complicated balance of biotic and abiotic processes that encompass the cumulative release of CO_2 from autotrophic (root and rhizosphere, R_a) and heterotrophic (soil organisms, R_h) respiration and some chemical weathering of carbon compounds (Kuzyakov, 2006). Many studies have shown strong and significant positive correlations between R_s and near surface soil temperature (T_s) (Davidson and Janssens, 2006). It is uncertain if surface applied biochar would alter or change this soil $R_s - T_s$ relationship. It is possible that the biochar surface application could reduce the surface albedo leading to changes in thermal soil properties (Usowicz et al., 2016) and potentially increase surface warming and enhance T_s and R_s .

In terms of other primary biogenic GHGs, forest soils can be a source or sink of CH_4 and N_2O depending on the balance of biotic and abiotic processes, in particular those that regulate microbial activity. For CH_4 , two pathways exist: methanogenesis that produces methane under anoxic, often water saturated, conditions, and methanotrophy by bacteria that consume CH_4 under oxic conditions. Both pathways can exist in the same soil and the resultant CH_4 flux is the net balance between them (Hiltbrunner et al., 2012). Studies have found that biochar can increase CH_4 oxidation, possibly through improving soil aeration (Van Zwieten et al., 2009, Spokas and Reicosky, 2009), although decreases in CH_4 oxidation have also been observed due to reductions

in methanotrophic activity (Spokas, 2013), possibly attributable to biochar inhibiting microbial intracellular signaling (Masiello et al., 2013).

The soil surface flux of N₂O represents the net balance between nitrification, occurring under aerobic conditions, and denitrification, occurring where low O₂ conditions exist (Parton et al 1996; Hang Wei et al., 2015). In N deficient soils, emissions of N₂O are typically small, with net consumption overall being possible (Chapius-Lardy et al., 2007; Jassal et al., 2010). Studies have shown that biochar additions to soil can reduce N₂O emissions, and some of this reduction could be due to N retention directly onto the surfaces of the biochar (Jassal et al., 2015). Biochar has often been reported to reduce N₂O emissions from soils (Spokas et al., 2010; Cayuela, 2010; Cayuela, 2014; Harter et al., 2014), although biochar with high N content (e.g., biochar made from animal manure or food waste), has been observed to stimulate N₂O fluxes (Spokas and Reicosky, 2009; Singh et al., 2010; Van Zweiten et al., 2010). With uncertainty surrounding how biochar application will influence net GHG fluxes, and with very few field studies in forest soils, there is a need to quantify these fluxes when biochar is applied with and without fertilizer N application.

The impact of biochar application on soil water dynamics depends on the structure and surface properties of the biochar, as controlled by the feedstock type and pyrolysis conditions, as well as by the rate of application and how it is applied, and the characteristics of the soil it is applied to. The porous nature of biochar could improve a soil's ability to retain moisture by reducing the unsaturated hydraulic conductivity of a soil, though the exact mechanism of such a result remains elusive (Novak et al., 2009). This effect could also help reduce loss of dissolved ions and suspended solids as well as ease crop moisture stress potentially providing higher yields. It may also regulate ammonium-N (NH₄⁺-N) availability through increases in redox

potential and cation exchange capacity (CEC). The likely increase in CEC over time resulting from biochar inputs (Lehmann, 2007; Liang et al., 2006) and subsequent absorption of positively charged N-based ions (e.g., NH_4^+) in biochar amended soils could result in a reduction of dissolved N, causing an initial decrease in plant N availability followed by increasing availability to plants over longer time periods. As the biochar becomes saturated with positive ions, its ability to retain nutrients will decrease. Specifically, NH_3 formation after urea-N fertilization and its subsequent adsorption onto the biochar could reduce the inorganic-N pool available for nitrifiers and thus NO_3^- concentrations in leachate may be reduced.

Biochar application studies in the laboratory have reported differing effects on GHG emissions, soil pore water quality and plant growth over a broad range of mainly agricultural soils. There has been less study of biochar effects on forest soils (which are typically more heterogeneous than agricultural soils), and so there is a need to investigate its potential benefits and pitfalls. Applying biochar to a site could have broad implications for GHG emissions and nutrient leaching, some of which may not be beneficial and may change over time depending on initial biochar physical and chemical properties and resulting interactions with the surrounding soil. Complex interactions between applied biochar and prevailing biogeochemical nutrient cycles and climate restricts our ability to forecast exact effects of biochar application at any site. Thus, field-based studies are needed for establishing feedstock and reaction parameters where organic waste is available. In particular, biochar applications should be investigated as part of a system based approach, where biochar produced from specific site-based biomass waste can be applied on site, which could be the most cost effective for climate change mitigation taking into account additional economic and carbon costs of transportation.

The abundant supply of woody materials left on-site after forest harvesting represents a potential feedstock for biochar and energy production via pyrolysis. At present, forest harvest residues are burned in coastal British Columbia to facilitate replanting and reduce fire hazards during warm-dry months, reducing the C sequestration potential of the forest life cycle by releasing significant amounts of GHGs rapidly back to the atmosphere (British Columbia, Ministry of Environment, 2012). However, positive results are being reported from the utilization of biochars derived from woody debris for improving carbon sequestration, and soil water and nutrient dynamics.

1.2 Research objectives

This thesis presents a series of studies focused on evaluating the effects of application of Douglas-fir derived biochar in combination with N-fertilizer on the biogeochemistry and hydrology of a forest soil from an intermediate aged Douglas-fir (*Pseudotsuga menziesii* [Mirbel] Franco) stand on Vancouver Island. The specific research objectives were to:

1. Evaluate impacts of differing biochar application rates on soil fluxes of CH₄, N₂O and CO₂ in combination with fertilizer application.
2. Determine effects of biochar application on dissolved organic concentrations of C and N in leachate in relation to fertilizer application.

1.3 Thesis overview

Chapter 2 describes a laboratory based soil incubation experiment utilizing a state of the art measurements system capable of quantifying difficult to detect GHG fluxes of carbon dioxide CO₂, CH₄ and N₂O using laser-based cavity ring-down spectroscopic (CRDS) GHG analyzer (G2508 Greenhouse Gas Analyzer, Picarro Inc., Santa Clara, CA, USA). A comparison of treatment effects on soil GHG effluxes after application of a Douglas-fir forest soil with 0%, 1%

and 10% biochar derived from Douglas-fir residual materials was evaluated with and without 200 kg ha⁻¹ urea-N fertilizer. Measurements were performed over a 4-week period, with soil mixtures being kept consistently warm (23 °C) and moist (~40% relative saturation) and open to the atmosphere between measurements. The results of this study demonstrated that CO₂ was the dominant gas controlling net GHG fluxes from the soils, with CO₂ representing more than 98% contribution to the total calculated CO_{2e} flux for all treatments. Emissions of CO₂ and N₂O were found to be significantly greater than the control soil for the 10% mixtures without fertilization, while both low (1%) and high biochar application rates (10%) resulted in decreased CH₄ consumption. The techniques outlined in this chapter offer a fast and effective way to quantify GHG fluxes in soil incubations, and could be expanded to any mixture of soils and treatments.

Chapter 3 presents a field experiment conducted with a biochar surface application rate of 5 t ha⁻¹ biochar (<1% biochar incorporation in top 10 cm of soil with bulk density close to 1.35 g cm⁻³) with and without fertilization. Using static non-steady state chamber flux measurements techniques analyzed with an Agilent 7890A (G3440A) Gas Chromatograph (GC) system, flux determinations for three GHGs of interest (CO₂, CH₄ and N₂O) was possible. Temperature was found to be the dominant control on CO₂ emissions from the field plots. Biochar application was found to have little impact on the GHG fluxes from the soil, although slightly reduced CO₂ emissions were observed for the biochar-amended plots during drought conditions in late summer and fall. Fertilizer applications to the forest soil plots following industry-standard practices neither significantly increased nor decreased the treatment CO_{2e} fluxes in relation to biochar additions. Therefore, in agreement with Chapter 2, low rates of biochar addition to this forest soil were found to improve soil C sequestration, both with or without fertilization.

In **Chapter 4**, effect of the biochar and fertilizer applications on laboratory and field soil pore water DOC, TN and spectral indices were evaluated. Methods included utilizing a vacuum manifold in the laboratory, and suction cup lysimeters in the field. Samples were analyzed using a UV-vis spectrophotometer immediately after collection, followed by DOC and TN analysis. Data from the laboratory data showed that the high rate biochar addition significantly increased DOC in free draining water after a period of drying while helping reduce TN leaching, with and without fertilization. Furthermore, the high rate biochar treatments were shown to have decreasing values $S_{275-295}$ with successive flushed of deionized water, as well as significantly lower $SUVA_{254}$ values. This suggests that more labile forms of DOM were being flushed out first, and that biochar additions resulted in a significant contribution of highly aromatic molecules to the DOC. However, the losses of DOC relative to the total amount of C added as biochar were extremely low (<1%). In the laboratory study, there was a significant difference detected in the N species retained, with increased retention of N as both NH_4^+ -N and NO_3^- -N in 10% biochar applications (with and without fertilization). No significant treatments effects on DOC or TN were observed in the field study. **Chapter 5** presents a summary of the conclusions drawn from research described in Chapters 2, 3 and 4.

Chapter 2: Douglas-fir forest soil incubation experiment to measure greenhouse gas emissions after biochar application at three rates with and without urea-N fertilization

2.1 Introduction

The relationship between soil respiration (i.e., CO₂ emissions from soils) and biochar additions to soil is central to understanding the sequestration potential of biochar-amended soil in specific systems. Since soil respiration is one of the largest fluxes of the global terrestrial C cycle, representing about 70% of total ecosystem respiration in temperate forests (Ryan and Law, 2005), soil management strategies such as biochar addition should be carefully evaluated with respect to changes in soil CO₂ fluxes. (Ryan and Law, 2005) In a meta-analysis of 46 studies, Sagrilo et al. (2015) found when studies were grouped by the ratio of added biochar C to soil organic C (SOC), only those with a ratio > 2 showed a significant increase in CO₂ emissions.

Biochar has been shown to have the potential to reduce methane (CH₄) emissions in water-logged rice paddies (Liu et al., 2011) and enhance CH₄ uptake in aerobic soils (Karhu et al., 2011). However, clear patterns in the impact of biochar applications on CH₄ dynamics have been difficult to identify (Gurwick et al., 2013). A recent study evaluating the impacts of biochar addition on greenhouse gas (GHG) fluxes from a temperate forest soil found no differences in CH₄ fluxes between biochar-amended soil and control soil (Sackett et al., 2015).

Similarly, nitrous oxide (N₂O) emissions from soils are also an important consideration for soil management (Zhang et al., 2015). Biochar has shown significant potential for reducing N₂O fluxes, with factors such as biochar feedstock, pyrolysis conditions, and soil C/N ratio

influencing the efficacy of biochar addition (Cayuella et al., 2014; Case et al., 2015). However, some studies have found that biochar with high nitrogen (N) content, or biochar applied with urea can increase soil N₂O emissions (Chen et al., 2015). The likelihood for reduction or enhancement of soil N₂O fluxes is strongly linked to which N₂O formation pathway is followed, which is soil specific (Sánchez-García et al., 2014).

It is important to note that the majority of biochar studies related to GHG fluxes have been performed on agricultural soils (Spokas et al., 2009). However, little is known about the effect of biochar additions on forest soil GHG fluxes despite the potential of biochar to enhance the size of the forest C sink by increasing forest productivity (Thomas and Gale, 2015). Of particular relevance to this study is that slash material remaining after forest harvest is commonly burnt to facilitate replanting and reduce fire hazard, and that this directly releases large amounts of GHGs (~8 Mt CO₂ equivalent annually) into the atmosphere (British Columbia Ministry of Environment, 2012). An alternative would be to adopt a systems-based approach and convert the slash into biochar that could be incorporated back into the forest soil to enhance soil quality for the subsequent rotation and help reduce the large C footprint of forest harvesting on managed land (de Ruiter et al., 2014). Fertilization is a common forest management practice to enhance biomass production rates of N-limited forests in the Pacific North West of North America, with typical application rates of 200 kg N ha⁻¹ (Hanley et al., 1996; Jassal et al., 2010). In these circumstances, excess N can result in large N₂O emissions from soils during the first year following fertilizer application (Jassal et al., 2008; Jassal et al., 2010; Shrestha et al., 2014) that significantly reduce the global warming benefit of additional forest C uptake in response to fertilizer addition (Jassal et al., 2011). However, very little biochar research to date has been conducted on forest soils using a systems-based approach, and none to our knowledge has

addressed N fertilizer interactions with biochar and the resulting GHG emissions for a forested humo-ferric podzol, the dominant forested podzol great group in Canada.

In order to evaluate the potential for biochar incorporation into forest management practices in British Columbia, Canada, where a forest carbon offset protocol is already in place and under critical review (Peterson St-Laurent et al., 2017), we measured the GHG fluxes from a forest soil amended with different rates of biochar produced from Douglas-fir harvest residuals, in combination with unfertilized soil and soil receiving an N fertilizer application of 200 kg N ha⁻¹. We designed a laboratory incubation study using a state-of-the-art cavity ring-down spectroscopic (CRDS) gas analyzer to simultaneously measure soil CO₂, CH₄ and N₂O fluxes in relation to different rates of biochar and urea-N application under controlled laboratory conditions. We tested the hypotheses that (i) biochar application would increase CO₂ emissions from an N-fertilized soil, (ii) biochar application would suppress N₂O emissions from an N-fertilized forest soil, and (iii) biochar would enhance CH₄ uptake by the forest soil regardless of N fertilization. We also sought to determine the influence of biochar and fertilizer applications on soil CO₂ fluxes, and to quantify the relative magnitude of GHG fluxes by accounting for their individual global warming potentials (i.e., CO₂ equivalent fluxes), and relative to C added as biochar.

2.2 Materials and methods

2.2.1 Soil

Soil was collected from a coastal Douglas-fir (*Pseudotsuga menziesii* (Mirbel) Franco var. *menziesii*) forest located near Campbell River on Vancouver Island, British Columbia (BC), Canada (49° 52'N, 125 20'W, 320 m.a.s.l.). Stand density in the area is typically ~1100 trees ha⁻¹, less than 60 years old and composed primarily of Douglas-fir (80%), western red cedar (*Thuja*

plicata Donn, 17%) and western hemlock (*Tsuga heterophylla* (Raf.) Sarg., 3%) (Humphreys et al., 2006). The majority of the old-growth forest in this area was harvested in the early 1900s with land being managed for forest products on a 50 to 90 year rotation thereafter (Spittlehouse, 2003).

The soil is classified as a humo-ferric podzol with a gravelly loamy-sand texture and is described in more detail in Appendix 1. The top 20 cm of the mineral soil layer was collected from an area of the forest that was not previously fertilized. During collection, the soil was sieved to 1 cm, removing large stones and roots. Soil was transported to the laboratory and stored in darkness at 5 °C for one week before being sieved to <2 mm for use in the experiment.

2.2.2 Biochar

The biochar used was supplied by Diacarbon Inc. (Burnaby, Canada) and was made from Douglas-fir slash feedstock, chipped to 2-cm pieces and pyrolyzed for 30 min at 420 °C. The C content of the biochar was 78% on a dry matter basis, with low volatiles and ash contents (18.8 and 2.4%, respectively). The biochar was sieved to <2 mm for use in the experiment, and comprised a wide range of particle sizes. The largest fraction (32%) was in the range of 425 to 991 μm , and the next largest fraction (<150 μm) was 24%. Biochar pH and electrical conductivity were determined following the International Biochar Initiative (IBI) protocols (International Biochar Initiative, 2012), and were found to be 6.86 (\pm 0.04) and 86 (\pm 2) $\mu\text{S}/\text{cm}$, respectively. The skeletal (i.e., particle) density of the sieved biochar was 1.33 (\pm 0.03) g cm^{-3} which is within the range of other wood derived biochar investigated in Brewer et al., (2014). The biochar had been stored for more than two years after production in airtight steel drums, which were opened occasionally for use in other experiments.

2.2.3 Experimental incubations

The incubation study was conducted using 250 cm³ Steri-fil® Asceptic filtration units (EMD Millipore, Darmstadt, Germany) coupled in line with the laser-based CRDS GHG analyzer (G2508 Greenhouse Gas Analyzer, Picarro Inc., Santa Clara, CA, USA). Mixtures of air-dry soil, biochar and fertilizer in different proportions were added to the incubation units in 20-cm³ volumes until reaching a total volume of 200 cm³. Mixtures were compacted and the upper surface loosened to avoid layering between each addition.

Six experimental mixtures, consisting of combinations of soil, biochar (application rates of 0, 1% and 10% biochar on a mass basis) and fertilizer (application rates of 0 and 200 kg N ha⁻¹ equivalent of urea fertilizer) (Table 1), were replicated four times, yielding a total of 24 incubation units. Soil and biochar components for each of the six treatments were mixed independently in batches, with fertilizer applied to the assigned treatments at the initial wetting of the soil-biochar mixture before packing. Using a soil mineral particle density of 2.65 g cm⁻³, the total porosity of the mixture when packed to 200 cm³ was ~0.61 cm³ cm⁻³. The initial wetting using deionized water raised the relative saturation to ~40%.

During the experiment, water was added to the incubation units to maintain the relative saturation in the range of 15-40%. The incubation units were weighed daily during the week to estimate soil evaporation, with deionized water added on Mondays, Wednesdays and Fridays to return incubations to soil water contents equivalent to ~40% relative saturation. In this way, the units were rewetted every 48 hours from Monday to Friday, and after 72 hours over weekends. Added water was allowed to spread throughout the incubation units for 24 hours prior to the GHG flux measurements.

GHG fluxes and incubation masses were measured daily for four weeks from Monday to Friday. Wetting of the soil in the incubation units occurred immediately following the GHG flux measurements on Tuesdays and Fridays, with subsequent flux measurements made ~24, 48 and 72 hours after wetting. The incubation units were left open to the atmosphere in a dark laboratory at 23 °C between measurements. Relative saturation was determined for each flux measurement based upon incubation masses. At the end of the experiment, the incubation units were destructively sampled and their oven dry (105 °C for 24 hours) mass was used to calculate bulk density.

2.2.4 GHG flux measurements

GHG flux measurements were made on each incubation unit daily between 10 AM and 12 PM over a 25-day period during November and December 2014. This length of time was chosen based on biochar incubation studies that have shown relatively constant CO₂ fluxes during 100-day incubations (Spokas and Reicosky, 2009) and stabilized N₂O fluxes within 30 days of fertilizer application (Cayuela et al., 2013). The non-steady state flow-through incubation system (Figure 1) was constructed to permit in-line measurements of CO₂, CH₄ and N₂O fluxes. Each incubation unit headspace was sealed using Steri-fill caps during flux measurements. The caps were additionally sealed with Parafilm and secured by firmly pressing down on the cap during measurements to ensure ambient air did not enter the air stream circulating between the incubation headspace and the CRDS analyzer. Rubber septa were placed to block two of the four ports in the caps, leaving two ports for air entry and exit. Air was circulated between the incubation unit headspace and the CRDS analyzer at 250 mL min⁻¹ using a low-leak diaphragm pump (A0702, Picarro, Santa Clara, CA, USA). The total volume of the system was 215 mL comprising the 105 mL Picarro G2508 standard system configuration volume, 30 mL comprised

of 24 cm of 3.175 mm (1/8") ID Bev-A-Line® (manufacturer) tubing including a 1.0- μm inlet filter, and the 80 mL incubation unit headspace. The twenty-four incubation units were analyzed in random order each day, with each unit coupled to the analyzer for five minutes.

During the 5-min flux measurement closure time, CO_2 , CH_4 and N_2O mixing ratios (mol of GHG per mol of dry air) were measured every 2 s. Default analyzer settings used in others studies (Fleck et al., 2013, Christiansen et al., 2015) were used throughout the experiment. Immediately after lid closure, the headspace was flushed via a three-way valve for 1 minute at 1 L min^{-1} with laboratory reference air (mixing ratios of $420 \mu\text{mol mol}^{-1} \text{ CO}_2$, $1.96 \mu\text{mol mol}^{-1} \text{ CH}_4$ and $0.72 \mu\text{mol mol}^{-1} \text{ N}_2\text{O}$) to provide the same ambient conditions in all treatments. Prior to the experiment, this reference air was obtained as air that was pumped from outside a laboratory window overlooking a lightly treed lawn using an air compressor system to fill an empty gas cylinder. The laboratory reference air was analyzed on a gas chromatograph (Agilent 7890A, Mississauga, CA) that was calibrated using certified standards (Air Liquide America Specialty Gases LLC, Houston, USA).

The hourly fluxes (F_x , $\mu\text{mol g}^{-1} \text{ h}^{-1}$) for GHG_x , where x represents each GHG, at time t_0 after flushing with reference gas were calculated using Eq. (1) which is the same as Eq. (6) in Jassal et al. (2012), except that ground surface area has been replaced by sample mass, the mass of soil ($\sim 200 \text{ g}$) inside each incubation unit (m_s , kg):

$$F_x = (\rho_a V / m_s) ds_x / dt \quad (1)$$

where ρ_a is the density of dry air (mol m^{-3}), V is the total system volume (m^3), and ds_x/dt is the rate of change of the mixing ratio of GHG_x ($\mu\text{mol mol}^{-1} \text{ s}^{-1}$). ρ_a is given by $P/[RT(1 + s_w)]$, where s_w is the water vapour mixing ratio ($\mu\text{mol mol}^{-1}$) (average value during the measurement), P is atmospheric pressure (Pa), and T is absolute temperature (K). Using a hand-held infrared

thermometer, we found the soil surface temperature was not affected by contact with air warmed by the CRDS during the measurement interval.

To track system drift and leakages during headspace air circulation through the measurement system, a non-soil control incubation unit containing acid-washed glass beads rather than soil was used. GHG fluxes were measured daily using the same method as for the soil incubation units, and fluxes from the glass beads unit, were subtracted from the daily soil incubation measurements.

The starting time (t_0) for rate of change of mixing ratio determination was 5 s after the completion of air flushing to avoid associated pressure perturbations. This also permitted enough time for air to circulate through the system to remove any lag effect. Generally, the rate of change in mixing ratio (ds_x/dt) for CO₂ was non-linear, declining with time because the gradient declined as the volume filled, and so the exponential model described by Jassal et al. (2012) was used to determine ds_x/dt at t_0 for this gas. A linear fit was used for determination of ds_x/dt for CH₄ and N₂O since linear changes were observed for these gases. The manual switching of incubation units, flushing with laboratory reference gas and closures did result in occasional time series for which calculated fluxes were unreliable. After testing the flux-filtering approaches of Jassal et al (2012) and Christiansen et al (2015), only extreme outliers (defined as fluxes with RMSE more than 3 standard deviations from the mean RMSE for all fluxes for each GHG_x) were removed, which corresponded to <3% of data. Cumulative fluxes were calculated using the procedure outlined by Yang and Cai (2005).

2.2.5 Statistical analysis

Data were analyzed using a one-way analysis of variance (ANOVA) to test for significant differences. Biochar treatments (S, BC1%, and BC10%) were compared independently of

fertilization treatments (S+F, BC1%+F and BC10%+F). When *F* values indicated significant differences, a post-hoc Tukey's Honest Significant Differences (HSD) test was conducted to determine which pair-wise differences were statistically significant.

Independent samples t-tests were conducted to further compare biochar with and without fertilization (BC1%, BC1%+F, BC10%, BC10%+F). Following this, independent samples t-tests were conducted to compare the responses of unamended soil (S) and soil with a low biochar application rate (BC1%) to fertilizer application (i.e., S + F and BC1% +F).

Differences in soil moisture between treatments were investigated using measurements of relative saturation as the main factor in an ANOVA for the three GHGs. Where *F* values indicated significant difference, a post-hoc Tukey's Honest Significant Differences (HSD) was conducted. The effect of soil moisture on GHG fluxes was then investigated within each treatment by performing independent linear regressions.

The net GHG flux in terms of CO₂ equivalent (CO_{2e}) was calculated for each treatment using mean fluxes from the last two weeks of the experiment using global warming potentials (GWP) of 1 for CO₂, 34 for CH₄, and 298 for N₂O (IPCC, 2014). To evaluate net CO_{2e} of soil GHG fluxes relative to C added in the biochar treatments (g biochar (g soil)⁻¹), soil gas fluxes without biochar were subtracted from soil gas fluxes with biochar using the differences determined from the treatment post-hoc Tukey's HSD tests and converted to CO_{2e} fluxes. Greenhouse gas flux calculations and statistical analyses were performed in R version 3.3.1 (2016-06-21) (RCore Team, 2016)

2.3 Results and discussion

2.3.1 Temporal variation in GHG fluxes

For all treatments, the measured CO₂ fluxes were high on the first day of incubation

(DOI-1), decreasing substantially through DOI-3, after which values remained lower for all treatments (Figure 2). The highest CO₂ flux (0.75 μmol CO₂ (g soil)⁻¹ h⁻¹) was measured on one of BC10%+F samples on DOI-2, with an average value of approximately 0.55 μmol CO₂ (g soil)⁻¹ h⁻¹) obtained for both BC10% and BC10%+F. Although these high CO₂ effluxes did not persist past DOI-3, the cumulative efflux over the three days was a major contributor to total CO₂ emissions during the experiment, representing 18% - 25% of total CO₂ effluxes for the treatments (Figure 2).

In general, the unamended soil (S) had the lowest CO₂ effluxes measured during the disturbance period (i.e. over the first 3-days), as well as over the remaining 22-days (Figure 2). The biochar treatments BC10% and BC10%+F had the largest CO₂ fluxes of all treatments in the first few days of the experiment, with the rank order treatments for CO₂ fluxes persisting throughout the experiment as BC10%+F > BC10% > BC1%+F > S+F > BC1% > S (Figure 2). Overall, the cumulative soil CO₂ flux from BC10%+F was 55% larger than S.

Soil CH₄ fluxes were mainly negative, indicating net consumption of CH₄ by methanotrophic soil microbes in all treatments. Differences in treatment responses were pronounced and consistent throughout the entire experiment (Figure 3). A disturbance effect was also observed during the first 3 days for CH₄, which can be observed in the rapid increases in CH₄ uptake (e.g. more negative CH₄ fluxes) for DOI-3 compared to DOI-1. The BC10% and BC10%+F treatments clearly exhibited the lowest rates of CH₄ consumption, and in some cases showed signs of net CH₄ production, particularly for BC10%+F (Figure 3). The cumulative values at the end of the experiment in ranked order from highest to lowest CH₄ consumption varied as: S > BC1% > S+F > BC1%+F > BC10% > BC10%+F (Figure 3). The S treatment consistently had the strongest CH₄ consumption, followed by BC1%, which had 35% less CH₄

consumption compared to the unamended soil (treatment S). The highest rate of CH₄ consumption ($-6.41 \times 10^{-5} \mu\text{mol CH}_4 (\text{g soil})^{-1} \text{h}^{-1}$) was measured for the S treatment on DOI-16.

Unlike the CO₂ fluxes, there was little initial disturbance effect in N₂O flux magnitudes, which were generally highest towards the end of the experiment (Figure 4). The cumulative values at the end of the experiment in ranked order from largest to smallest are BC10% > BC10%+F ~ S+F > BC1%+F > S = BC1% (Figure 4). While emissions were highest for BC10% and BC10%+F throughout the experiment, an increase in emissions can be observed towards the end of the experiment for S+F after DOI-14. Total N₂O emissions from the largest emitters, BC10% and BC10%+F were 191% and 169% greater, respectively, than S. However, there were clear reductions in N₂O fluxes when biochar was applied to N-fertilized soil at the 1% rate, as cumulative N₂O fluxes for BC1%+F were 28% lower than for S+F (Figure 4).

2.3.2 Effect of biochar application rates on soil GHG fluxes from unfertilized soil

Comparing individual treatment pairs after the disturbance effect diminished (Figure 5), we found that CO₂ fluxes in BC10% were significantly larger than in BC1% ($p < 0.01$) and BC1% was significantly larger than S ($p < 0.01$, Figure 5).

Studies have reported that biochar addition can at first increase soil respiration rates, but then result in a decline over the following weeks to years (Cross and Sohi, 2011; Major et al., 2010; Steinbeiss et al., 2009). Specifically, some incubation studies have shown that, after subtracting measured raw biochar CO₂ emission from those measured from soil biochar mixtures, biochar reduces soil CO₂ emissions (Spokas et al., 2009, Zimmerman et al., 2011) or does not effect it, and where increases have been recorded they have been attributed to abiotic CO₂ release directly from the biochar (Thomazini et al., 2015). Additionally, Zimmerman et al. (2011) found increased CO₂ emission more likely during early stages of incubation (<90 days)

for soils treated with biochar produced at lower temperature (250 – 400 °C) and from grasses. In contrast, Spokas (2013) investigated the effect of weathering on soil CO₂ emission response after wood-derived biochar addition and concluded that biochar increases soil CO₂ emissions in the long-term, suggesting that there was an enhancement in the rate of microbial mineralization of weathered biochar. In a meta-analysis of 106 studies, Wang et al. (2015) concluded that biochar additions stimulated soil organic matter mineralization in nutrient poor sandy soils by as much as 20% and suggested that this would largely be due to biochar stimulating microbial activity.

Biochar application significantly decreased CH₄ uptake (AOV $F_{2,214} = 470.99$, $p < 0.01$, Figure 6), with the net CH₄ consumption decreasing with increasing rates of biochar application ($F_{(1,167)}$, $p < 0.01$, $R^2 = 0.87$). The post-hoc Tukey HSD test showed that the BC1% and BC10% differed significantly from S and from each other ($p < 0.01$). This is at first surprising given that biochar is expected to improve conditions for CH₄ oxidation and uptake by soil microbes, and by reducing bulk density and increasing porosity (Van Zwieten et al., 2009). However, we ensured that bulk density was not significantly different between control and biochar application treatments, so it is possible that differences observed in this study are due to biochar increasing pH thereby improving conditions for methanogens (Inubushi et al., 2005). This remains to be proven and our results differ from those described in Jeffery et al. (2016) where biochar addition increased CH₄ uptake in soils of pH < 5 with no effect in soils with pH > 5. Spokas et al. (2009) also found reductions in CH₄ oxidation after wood derived biochar was applied to a silt loam soil, hypothesizing that there could be an inhibitor to methanotrophic activity found on the biochar particle surface area or that the methanotrophs are selectively using another organic compound sorbed to the biochar surface before potentially returning to CH₄ over time.

There was a significant effect of biochar additions on N₂O fluxes (AOV $F_{2,214} = 23$, $p < 0.01$), with the BC10% having significantly higher emissions than BC1% and the unamended soil (S) (Figure 7). The post-hoc Tukey HSD test showed that N₂O emissions from BC1% were not significantly different from S ($p > 0.97$). Other studies have shown that biochar addition reduces N₂O emissions (Cayuela et al., 2010) in relation to soil moisture (Yanai et al., 2007; Spokas et al., 2009). Spokas (2013) found that field-aged biochar did not suppress N₂O emissions. Nitrification, converting ammonium to nitrate and releasing N₂O and nitric oxide (NO), occurs in well-aerated soils. Sanchez-Garcia et al., (2014) suggested that the fact that biochar increased measured N₂O emissions in a Haplic Calcisol soil may have resulted from improved conditions for microbial ammonia-oxidizer populations. Similarly, Gundale and Deluca (2006) found that Douglas-fir derived biochar applied to Western Montana forest soil (sandy-skeletal, mixed, frigid Typic Dystrustep) increased ammonification and nitrification rates. In this study, where relative saturation was generally low, it is possible that the increase in N₂O emissions was due to an improvement in conditions favouring nitrification, and it is unlikely that this is due to improved oxygen availability (Prommer et al., 2014).

2.3.3 Fertilizer effects on soil GHG flux responses to biochar application rates

T-tests were performed on treatment pairs S vs. S+F, BC1% vs. BC1%+F and BC10% vs. BC10%+F to test the influence of fertilizer on CO₂ fluxes. In contrast to the significant increase in CO₂ efflux ($p < 0.05$) for fertilized soil (S+F) compared to soil without fertilizer (S), we found no significant difference between BC1% and BC1%+F, or between BC10% and BC10%+F (Figure 5). In a meta analysis Liu et al. (2016) found that biochar in combination with synthetic-N fertilizers led to the most significant increases in soil CO₂ emissions and microbial biomass-C, likely due to a shift in the C/N ratio favoring microbial soil C mineralization.

Comparing fertilized and non-fertilized treatments, fertilizer addition appeared to decrease CH₄ uptake, with significant differences ($p < 0.01$) for S vs. S+F and BC1% vs. BC1%+F, but not for BC10% vs. BC10%+F (Figure 6). Adding Fertilizer appears to further reduce CH₄ uptake. This is in agreement with Jassal et al (2011) for this forest soil. While biochar is generally expected to improve conditions for CH₄ uptake, we did not find this to be the case in this study (i.e., BC1% +F and BC10% +F were virtually the same as S + F).

Fertilizer application significantly increased N₂O fluxes (S vs. S+F, Figure 7), which is similar to measurements made in the field (Jassal et al., 2010, Jassal et al 2011) close to where the soil used in this study was collected. When fertilized, biochar addition at the 1% application rate (BC1%+F) reduced N₂O emissions relative to the fertilized soil with no biochar (S+F) ($p < 0.05$); however, N₂O fluxes for BC10%+F were not significantly different than from S+F. Furthermore, N₂O fluxes for BC10%+F were not significantly different from those measured for BC10% (Figure 7). This suggests that for high biochar application rates, large N₂O fluxes resulting from biochar additions overwhelmed any reduction in N₂O emissions resulting from fertilizer additions observed at the lower biochar application rate. Lan et al. (2017) found that different biochar significantly reduced N₂O emissions after N-fertilization in Australian Tenosols and this was not consistent in Ferrosols. They concluded that this was a result of modification in the ratio of dissolved organic-C and nitrate. Our results suggest that there may be a maximum rate at which biochar can be added in combination with urea-N fertilizer for which reductions in N₂O emissions can be expected. As with treatments with only biochar, this could be the result of high rates of biochar improving conditions for nitrification, while fertilizer provides more available N enhancing N₂O emissions.

2.3.4 Influence of soil moisture on GHG fluxes

We performed a principal component analysis for the post-disturbance period to identify patterns between dependent and independent variables (Figure 8). The incubation length (e.g. day of experiment) was strongly related to N₂O fluxes, but less associated with CO₂ and CH₄ fluxes. Time since wetting was not a significant factor for either of the principal components (standardized loadings of 0.02 and -0.01 of PC1 and PC2, respectively). Among dynamic parameters, relative saturation was the strongest explanatory variable (whereas biochar application rate and bulk density represent static parameters). Exploring the relationships between soil moisture and soil GHG fluxes, we found a significant, though weak, correlation between soil CO₂ fluxes and relative saturation ($p < 0.001$, $R^2 = 0.09$). The relationship was stronger between CH₄ fluxes and relative saturation ($p < 0.001$, $R^2 = 0.27$). There was not a significant relationship between N₂O fluxes and soil moisture ($p > 0.05$, Figure). Any differences in saturation between treatments during the experiment were limited to the high (10%) biochar application rate and were not significant. Relationships between GHG fluxes and soil moisture were not detected within treatments.

2.3.5 Global warming potentials

The total global warming potential (GWP) for each treatment was determined by summing the 100-year radiative forcings associated with each of the three measured GHGs (GWP factors of 1 for CO₂, 34 for CH₄, and 298 for N₂O, respectively (IPCC, 2014)). In this experiment, soil CO₂ effluxes represented >95% of the total GWP for all treatments (Figure 9). Cayuela et al., (2010) also showed that CO₂ contributed the largest percentage to the GWP, when biochar was added to a sandy soil. The increases in N₂O emissions after biochar and fertilizer additions increase total GWPs, as do the reductions in CH₄ consumption. However, the effects of

these two GHGs had very little impact on the total CO_{2e} of any treatment (Figure 9). The BC10% treatment had the largest total CO_{2e} emissions, followed by BC10%+F > BC1%+F > BC1% > S+F > 1% > S.

We also estimated the net climate change impact of biochar additions by considering both the C addition represented by biochar amendments in addition to the GWP resulting from changes in GHG fluxes. This calculation was based on the mean flux measured during the last two weeks of the experiment, which we used to provide a first-order approximation of the length of time during which the enhanced C sequestration due to biochar additions would be “offset” due to the enhanced CO_{2e} emissions of the treatments relative to the unamended soil. We subtracted the CO_{2e} of the unamended soil from the CO_{2e} of treatments receiving biochar additions. This provided a metric for characterizing the impacts of biochar additions on the net GWP of a soil (Wang et al, 2015).

The treatment with the longest time interval before the C sequestration resulting from biochar additions was offset by the total CO_{2e} of GHG emissions from the soil was the BC10%+F at 17.7 years. This was slightly longer than the value calculated for the BC10% treatment (16.3 years). Though these high biochar application rates have the highest CO_{2e} values (Figure 9), they also represent the highest C additions. Repeating the calculation using the radiative forcings of CH₄ and N₂O for a 20-year period (GWP of 72 and 289, respectively) (IPCC, 2014), the C-neutrality time remained similar: 17.4 and 16.1 years for BC10%+F and BC10%, respectively. This is due to the fact that CO₂ fluxes dominate the total GWP. For the lower biochar addition rate (BC1%), CO_{2e} from added biochar would be lost through soil GHG fluxes after 6.7 years. With fertilization (BC1%+F), the climate benefit of biochar to soil is reduced to just 3.9 years of equivalent C sequestration.

Steinbeiss et al. (2009) calculated the mean residence time for biochar added to a forest soil to be 6 and 12 years, with results differing based on biochar feedstock material. These values are similar to the offset periods calculated in the present study. In a meta-analysis of 24 studies Wang et al. (2015) concluded that the mean residence time of biochar-C ranged from 108 days and 556 years for labile and recalcitrant biochar C pools, respectively. The high rates of C loss we measured could be the result of stimulated soil organic matter mineralization and the labile component of the biochar being more readily mineralized.

Clearly, short-term laboratory incubation studies are not representative of the ecosystem responses to biochar, which would include vegetation dynamics, seasonal climate drivers, and other factors influencing the overall climate impact of biochar amendments with and without fertilizer. Field studies should include these considerations in future measurements in order to provide policy guidance based on the effects of each environmental variable on a soil receiving biochar additions.

2.4 Conclusions

1. Biochar application at high (10%) application rates increased CO₂ and N₂O emissions when applied without urea-N fertilizer.
2. Biochar application at both low (1%) and high (10%) application rates decreased CH₄ consumption when applied without urea-N fertilizer.
3. Biochar application with urea-N fertilization did not increase CO₂ emissions compared to biochar amended soil without fertilizer.
4. In terms of CO_{2e}, net change in GHG emissions was mainly controlled by CO₂ emissions with CH₄ and N₂O together accounting for less than 1.5% of the total emissions.

2.5 Tables

Table 1. Summary of experimental treatments

| Treatment code | Treatment details |
|-----------------------|---------------------------------|
| S | Soil with no amendments |
| BC1% | Soil + 1% biochar ¹ |
| BC10% | Soil + 10% biochar |
| S+F | Soil + fertilizer ² |
| BC1%+F | Soil + 1% biochar + fertilizer |
| BC10%+F | Soil + 10% biochar + fertilizer |

¹ Biochar mixed with soil as a percentage of total mass

² 200 kg N ha⁻¹ equivalent of urea fertilizer

2.6 Figures

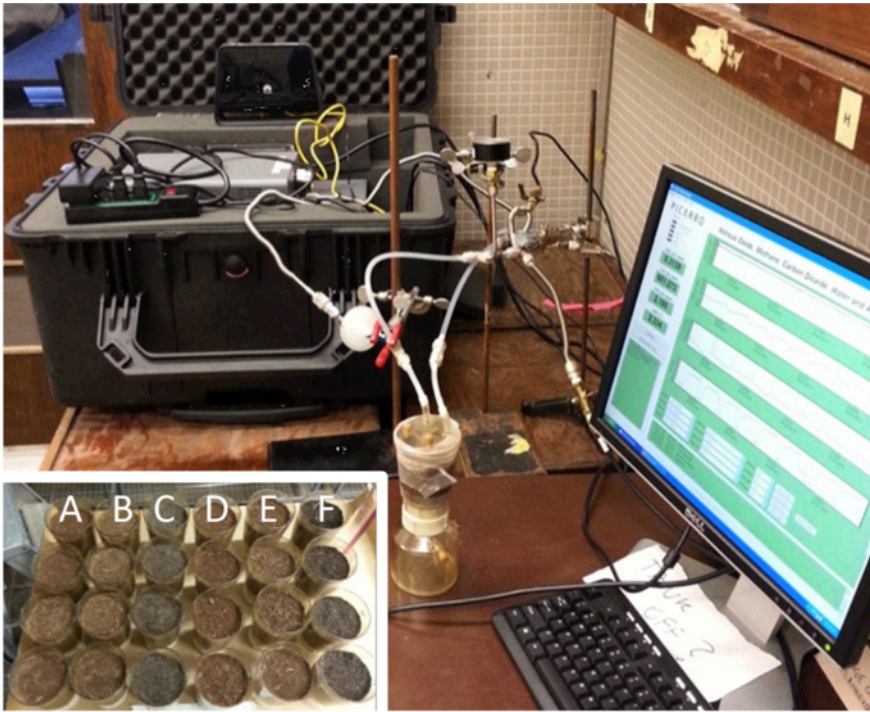


Figure 1. Incubation units attached to the CRDS greenhouse gas analyzer comprising a closed chamber soil flux measurement system. The four replicates of the six treatments are shown in the inset photo, as (A) unamended soil (S); (B) Soil + 1% biochar (w/w) (BC1%); (C) Soil + 10% biochar (BC10%); (D) Soil + fertilizer (200 kg N ha⁻¹ equivalent of urea fertilizer) (S+F); (E) Soil + 1% biochar + fertilizer (BC1%+F); (F) Soil + 10% biochar +fertilizer (BC10%+F).

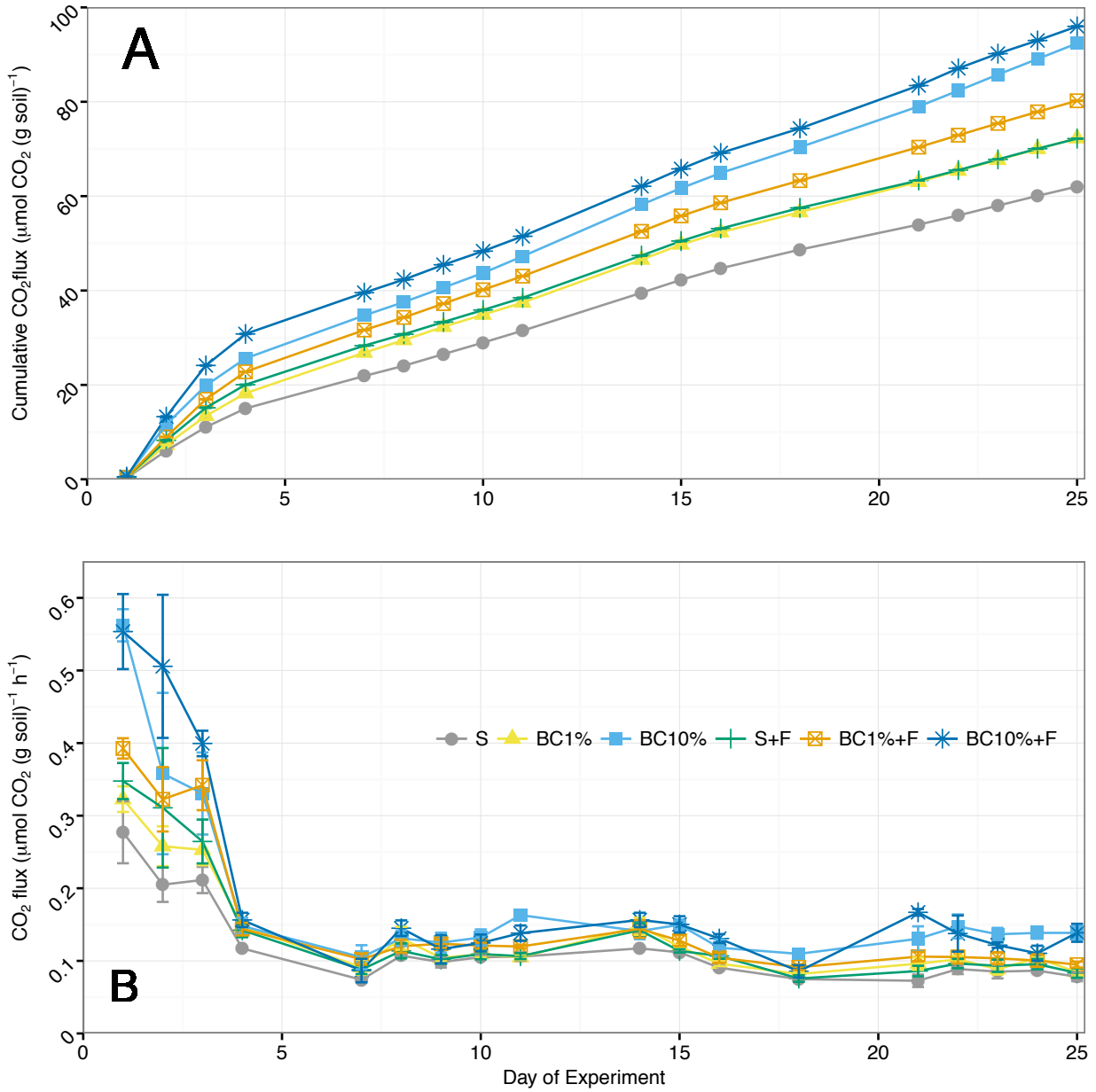


Figure 2. (A) Cumulative CO₂ effluxes during experiment by treatment (means ± 1 standard error (SE)); (B) Daily mean CO₂ flux time series plot (means ± 1 standard error (SE)).

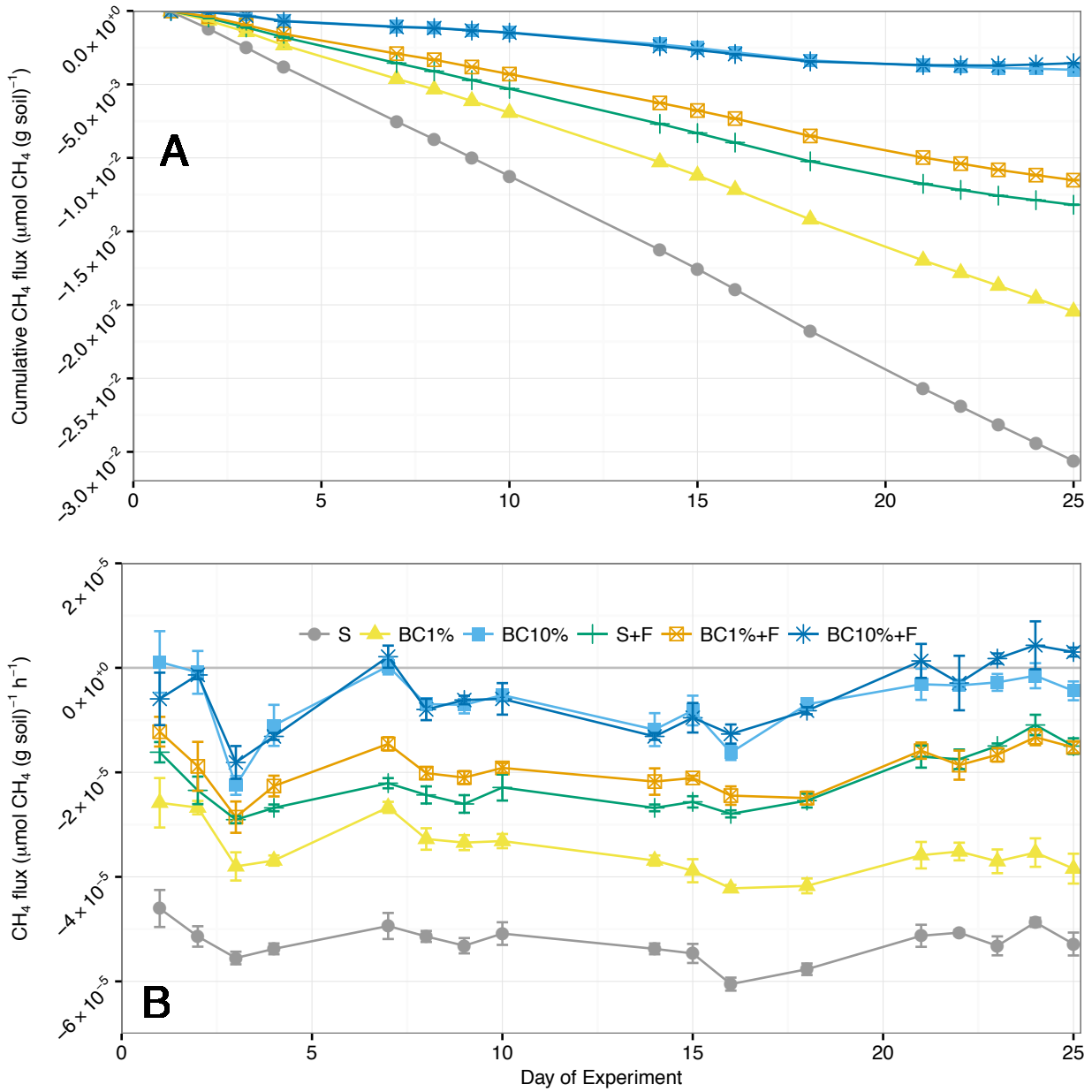


Figure 3. (A) Cumulative CH₄ effluxes during experiment by treatment (means \pm 1 standard error (SE)); (B) Daily mean CH₄ flux time series plot (means \pm 1 standard error (SE)).

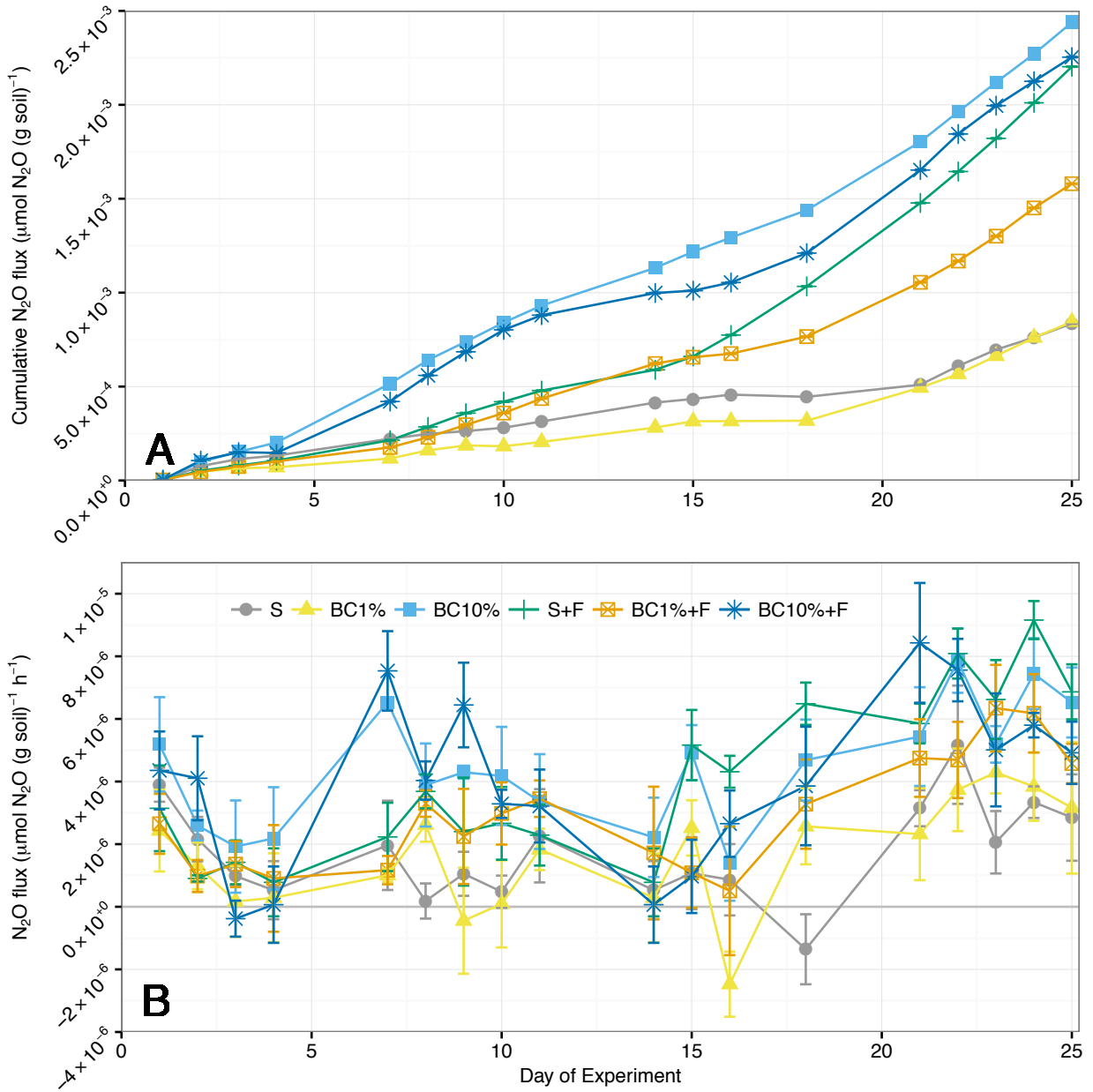


Figure 4. (A) Cumulative N₂O effluxes during experiment by treatment (means ± 1 standard error (SE)); (B) Daily mean N₂O flux time series plot (means ± 1 standard error (SE)).

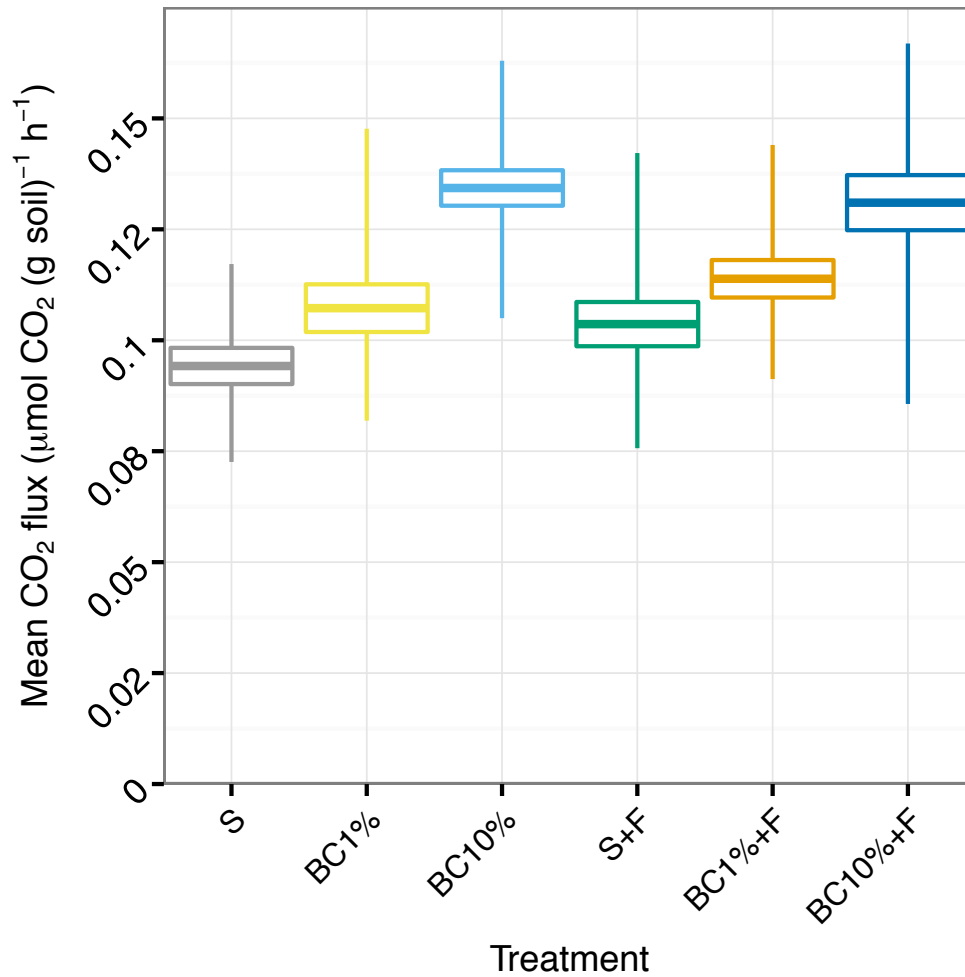


Figure 5. Boxplots of soil CO₂ efflux during the post-disturbance period by treatment. The thick horizontal line represents the means, the upper and lower lines of the boxes indicate the means \pm 1 SE, and the whiskers extend to the maximum and minimum fluxes measured during the post-disturbance period.

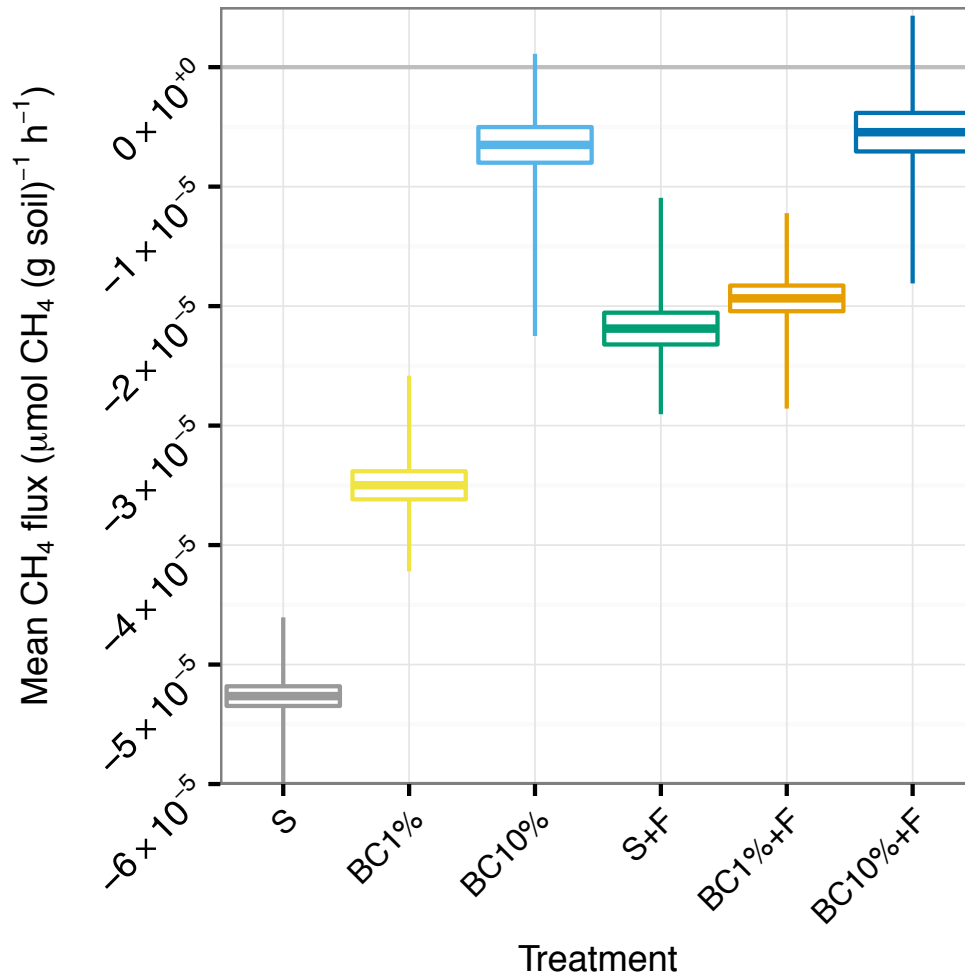


Figure 6. Boxplots of soil CH₄ efflux during the post-disturbance period by treatment. The thick horizontal line represents the means, the upper and lower lines of the boxes indicate the means \pm 1 SE, and the whiskers extend to the maximum and minimum fluxes measured during the post-disturbance period.

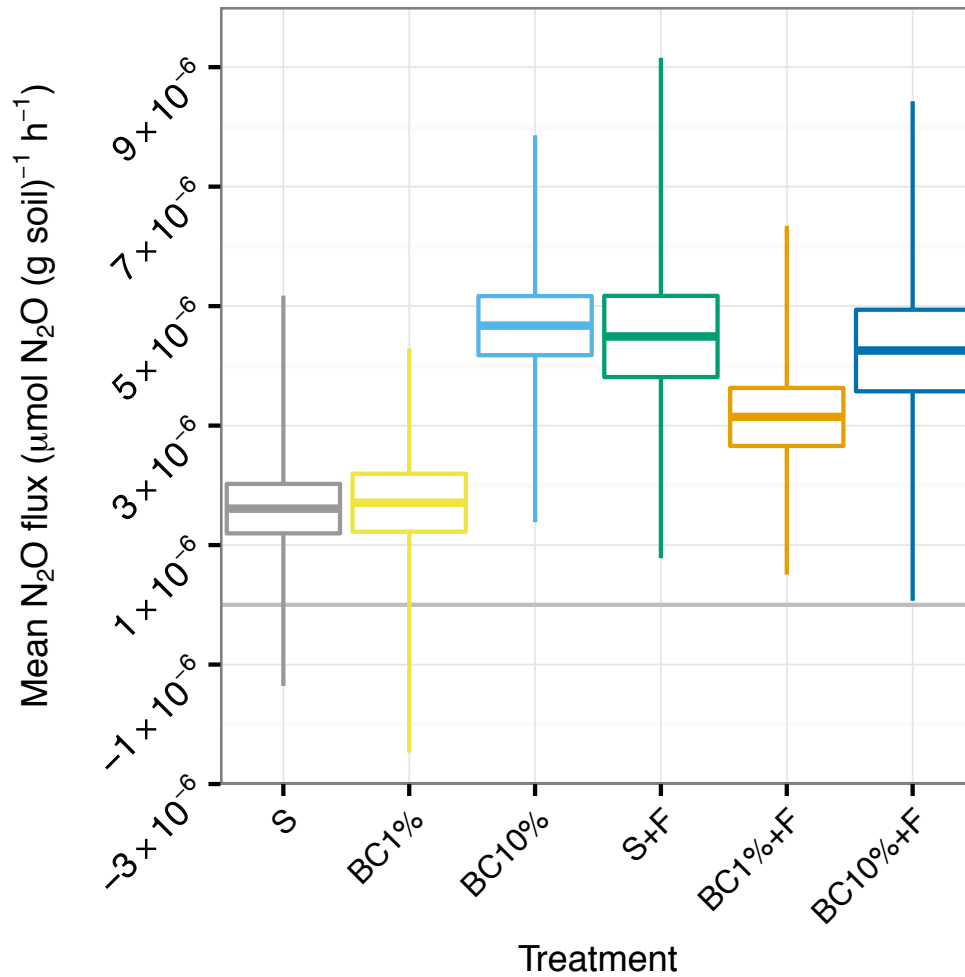


Figure 7. Boxplots of soil N₂O efflux during the post-disturbance period by treatment. The thick horizontal line represents the means, the upper and lower lines of the boxes indicate the means \pm 1 SE, and the whiskers extend to the maximum and minimum fluxes measured during the post-disturbance period.

Variables factor map (PCA)

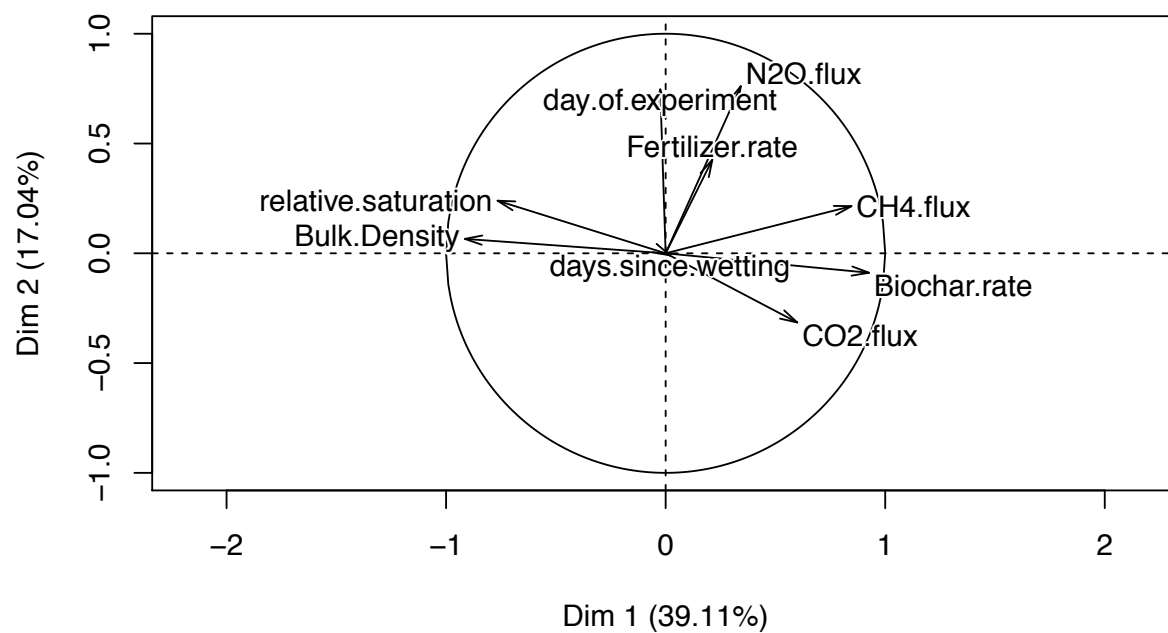


Figure 8. Principal component analysis of experimental variables.

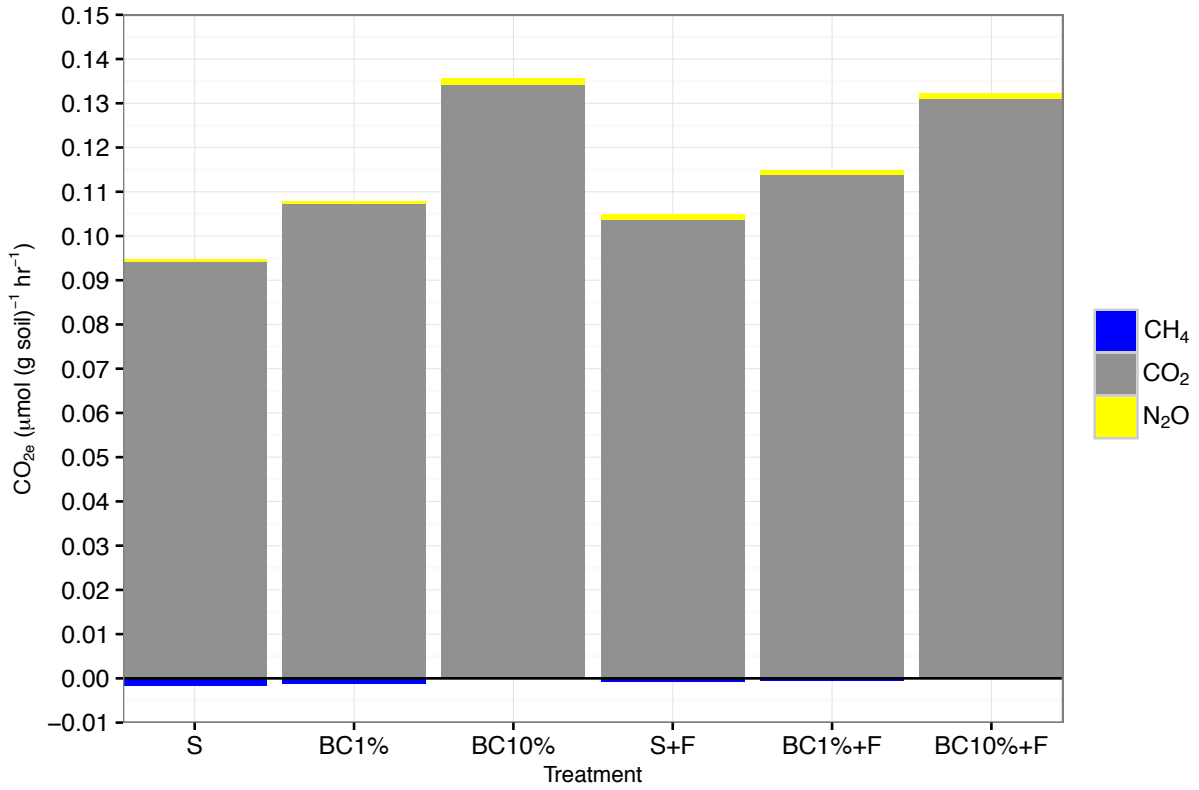


Figure 9. Effect of treatments on net GHG emissions in terms of CO_{2e} relative to unamended soil. The magnitude of the CH₄ consumption is subtracted from the CO₂ plus N₂O total.

Chapter 3: In-situ measurements of greenhouse gas emissions after biochar application with and without urea-N fertilization at a Coastal Douglas-fir forest

3.1 Introduction

Rising atmospheric concentrations of greenhouse gases (GHGs) - carbon dioxide (CO₂), methane (CH₄) and nitrous oxide (N₂O) - linked to climate change have stimulated a global effort to mitigate atmospheric concentrations of these gases. There is an urgent need to increase awareness of land management impacts on GHG flux dynamics to facilitate the development of mitigation strategies that minimize GHG emissions, and to reduce concentrations of CO₂, CH₄, and N₂O in the atmosphere, as land management strategies can have significant impacts on soil GHG fluxes. Forest management options for climate adaptation and mitigation include reducing emissions from deforestation and forest degradation, enhancing the carbon (C) sequestration rate in existing and new forests, substituting wood fuels as a substitute for fossil fuels, and providing wood products in place of more energy-intensive materials. Increasing soil C stocks through biochar addition is an additional option (IPCC, 2014) that has yet to be extensively investigated in forest ecosystems. To determine if biochar addition to forest soil is a beneficial climate action requires information on its effect on both C stocks and soil GHG fluxes.

Biochar is produced through the thermal decomposition of organic matter in a reduced oxygen environment (i.e. pyrolysis). Biochar typically has high C content and has the potential to be used as a climate change mitigation strategy by reducing the amount of CO₂ in the atmosphere through increased C sequestration in soils (Lehman *et al.*, 2006). It is resistant to decomposition

in soils due to a prevalence of aromatic structures containing few functional groups (Dai et al., 2005; Zimmerman, 2010), which has been shown to be particularly true when the O:C ratio of the biochar is less than 0.2 (Spokas, 2010). Biochar has a lower specific density compared to mineral soils, with larger surface areas (Brewer et al., 2014). When incorporated into soil, biochar alters the physical structure of soil, generally decreasing its bulk density (Major et al., 2010; Lim et al., 2016) increasing the exposure of chemically reactive surfaces, and providing refugia for microbes (Lehmann et al., 2011). Changes to the physical structure of soils impacts soil water-holding characteristics, and leads to alterations in biotic and abiotic processes affecting fluxes of soil CO₂, CH₄ and N₂O (Major et al., 2010; Sohi et al., 2010).

Biochar has been shown to reduce soil CO₂ emissions when applied at a ratio less than twice the level of soil organic carbon stock (SOC), but can increase soil CO₂ fluxes at higher application rates (Sagrilo et al., 2015). These reductions are possibly the result of biochar's ability to sorb soluble organic matter and stabilize SOC, reducing the amount of organic substrates available for respiration (Lehman and Joseph, 2012; Spokas et al., 2009; Chintala et al., 2014; Chang et al., 2016). Other studies have concluded that biochar can stimulate soil CO₂ emission potentially due to increased mineralization of the labile fraction of biochar C, changes in the soil C:N ratio and nutrient availability, and enhanced microbial mineralization of weathered biochar (Kolb et al., 2009; Zimmerman et al., 2011, Spokas, 2013).

Soil CO₂ emissions, also termed soil respiration (R_s), are controlled by a complicated balance of biotic and abiotic processes that encompass the cumulative release of CO₂ from autotrophic (root and rhizosphere, R_a) and heterotrophic (soil organisms, R_h) respiration and some chemical weathering of carbon compounds (Kuzyakov, 2006). Many studies have shown strong and significant positive correlations between R_s and near surface soil temperature (T_s)

(Davidson and Janssens, 2006). It is uncertain if surface applied biochar would alter or change this soil $R_s - T_s$ relationship. It is possible that the biochar surface application could reduce the surface albedo (Usowicz et al., 2016) and potentially increasing surface warming and enhancing R_s .

In terms of other primary biogenic GHGs, forest soils can be a source or sink of CH_4 and N_2O depending on the balance of biotic and abiotic processes, in particular those that regulate microbial activity. For CH_4 , two pathways exist; methanogenesis that produces methane under anoxic, often water saturated, conditions, and methanotrophy by bacteria that consume CH_4 under oxic conditions. Both pathways can exist in the same soil and the resultant CH_4 flux is the net balance between them (Hiltbrunner et al., 2012). Studies have found that biochar can increase CH_4 oxidation, possibly through improving soil aeration (Van Zwieten et al., 2009, Spokas and Reicosky, 2009), although decreases in CH_4 oxidation have also been observed due to reductions in methanotrophic activity (Spokas, 2013), possibly attributable to biochar inhibiting microbial intracellular signaling (Masiello et al., 2013).

The soil surface flux of N_2O represents the net balance between nitrification, occurring under aerobic conditions, and denitrification, occurring where low O_2 conditions exist (Parton et al 1996; Hang Wei et al., 2015). In nitrogen (N) deficient soils, net emissions of N_2O are typically small, while net consumption could be possible (Chapius-Lardy et al., 2007; Jassal et al., 2010). Studies have shown that biochar addition to soil can reduce N_2O emissions, and some of this reduction could be due to N retention directly onto the surfaces of the biochar (Jassal et al., 2015). Biochar has often been reported to reduce N_2O emissions from soils (Spokas et al., 2010; Cayuela, 2010; Cayuela, 2014; Harter et al., 2014), although biochar with high N content (e.g., biochar made from animal manure or food waste), has been observed to stimulate N_2O

fluxes (Spokas and Reicosky, 2009; Singh et al., 2010; Van Zwaiten et al., 2010). With uncertainty surrounding how biochar application will influence net GHG fluxes, and with very few field studies in forest soils, there is a need to quantify these fluxes when biochar is applied with and without fertilizer N application.

Production forests in the coastal region of British Columbia are typically N-limited systems, and have been found to respond significantly to N-fertilizer additions (Chappell et al., 1991). British Columbia's Coastal Forest Action Plan offers fiscal incentives to increase productivity of second-growth coastal forests using fertilization to provide a potential benefit of reducing GHG emissions through increased C sequestration while maintaining employment levels in the forest product sector (BCMFR, 2007). While fertilization can significantly increase gross primary productivity, it also comes at a cost to the climate system in terms of N₂O emissions resulting from fertilizer additions: these N₂O emissions have been found to negate much of the climatic benefit of increased C uptake in response to forest fertilization in the first year after application (Jassal et al., 2008). If biochar additions reduced fertilization-related N₂O emissions the potential would exist to maximize the benefits of forest management strategies by including changes to soil C stocks and net GHG fluxes on a CO₂ equivalent (CO₂e) basis (relative to CO₂, CH₄ and N₂O have global warming potentials (GWP) of 34 and 298, respectively, on a 100-yr basis (IPCC, 2013)).

The abundant supply of woody materials left on-site after forest harvesting is a potential pyrolysis feedstock for biochar and energy production. At present, harvest residues are burned in coastal British Columbia to facilitate replanting and reduce fire hazards during warm-dry months, reducing the C sequestration potential of the forest life cycle by releasing significant

amounts of GHGs rapidly back to the atmosphere (British Columbia, Ministry of Environment, 2012).

In this paper, we report on a controlled field-based experiment that we conducted to investigate the effects of biochar application to a forest soil, with and without N fertilization, on soil fluxes of CO₂, CH₄ and N₂O in a Pacific Northwest Douglas-fir forest. We hypothesized that biochar additions would (i) increase CO₂ emissions irrespective of fertilizer additions, (ii) increase CH₄ uptake (or decrease CH₄ emissions) in fertilized and unfertilized soils, and (iii) reduce N₂O emissions in fertilized soils, but increase N₂O emissions in un-fertilized soils in this N-limited system. The overall objective was to determine whether biochar additions could reduce net soil GHG fluxes on a CO₂e basis in response to fertilizer application.

3.2 Methods

3.2.1 Site description

The research site is a Douglas-fir forest on the eastern side of Vancouver Island 10 km SW of Campbell River, British Columbia and close to a long-term eddy-covariance site (Paul-Limoges et al., 2015) where local climate data was measured (49°52'N, 125°20'W, 300 m.a.s.l.). Located in the dry maritime Coastal Western Hemlock Biogeoclimatic subzone, the forest has been classified as seasonally dry temperate rain forest--a region that experiences cool summers and relatively warm winters--with a mean annual temperature of 9.1 °C and annual precipitation of 1500 mm yr⁻¹ (Pojar, 1987). The second-growth forest stand was planted in 1949 and comprises 80% Douglas-fir, 17% western red cedar (*Thuja plicata* Donn), and 3% western hemlock (*Tsuga heterophylla* (Raf.) Sarg) with a relatively sparse understory (Humphreys et al., 2006, Morgenstern et al., 2004). The stand is tall (30-35 m) and dense (1100 stems ha⁻¹) (Hilker et al., 2010), with a leaf area index of 7.3 m² m⁻² (Chen et al., 2006) keeping the soil surface well

shaded. Understory vegetation is sparse ($LAI < 1$), consisting mainly of salal (*Gaultheria shallon* Pursh.), Oregon grape (*Berberis nervosa* Pursh.), vanilla-leaf dear foot (*Archlys triphylla* DC) and a shallow mat (< 1 cm) of ferns and mosses. The soil is classified as duric humo-ferric podzol of morainal origin with a Quimper gravelly-loamy-sand texture commencing below a variable, litter-fermented-humified (LFH) organic layer that ranges in depth from 9 to 19 cm. More detailed information, summarized from available publications and sampling is available in Appendix 1.

3.2.2 Experimental design

A previously unfertilized area of the forest stand was selected and sixteen 4 m x 4 m plots were assigned in a randomized complete-block design with four blocks each of the following four treatments: i) soil only (S; i.e. control), ii) 5 Mg ha⁻¹ biochar (BC), iii) 200 kg N ha⁻¹ urea fertilizer pellets (F), and iv) 5 Mg ha⁻¹ biochar with 200 kg N ha⁻¹ urea pellets (BC + F). Each plot was positioned to have two large trees with diameter at 1.3 m > 31 cm within its boundary (Jassal et al., 2011).

Each plot contained a PVC collar to be used with a static non-steady-state (SNSS) chamber (for details see below) for the measurement of soil CH₄, CO₂ and N₂O fluxes at the soil surface. Measurements from the SNSS chambers commenced in September 2011, with monthly measurements during September to December 2011 prior to snowfall, and biweekly measurements following snowmelt in April 2012. Measurements continued until September, 2013.

Additional instrumentation was used to monitor soil properties in twelve of the 16 plots (three replicates for each of the four treatments), starting in April 2012. This instrumentation consisted of sensor clusters at the 15-cm depth to measure volumetric water content (θ_{15}), bulk

electrical conductivity (σ_{15}), and soil temperature (T_{15}) (model GS3, Decagon Devices Inc. Pullman, WA), and soil matric potential (Ψ_{15} , model MPS-2 sensors, Decagon Devices Inc.). Sensors were installed at the 15-cm depth on opposing sides of a trench (50 cm long x 25 cm wide x 15 cm deep), which was then backfilled. Signals were measured using a CR1000 data logger (Campbell Scientific Inc, Logan, UT) powered by a 12-V-DC 70-amp-hour lead-acid battery. The battery charge was maintained using a 60-W solar panel with a charge controller, supplemented through winter months (October-April) by recharging using a portable generator. Measurements were made at 5-min intervals and average output tabulated every 30 min.

3.2.3 Biochar and fertilizer application

The biochar used was supplied by Diacarbon Inc. (Burnaby, Canada) and was made from Douglas-fir slash feedstock, chipped to 2-cm pieces and pyrolyzed for 30 min at 420 °C. The C content of the biochar was 78% on a dry matter basis, with low volatiles and ash contents (18.8 and 2.4%, respectively). Biochar pH (6.86 ± 0.04 , mean ± 1 SD) and electrical conductivity (σ , $86 \pm 2 \mu\text{S cm}^{-1}$) were determined following the International Biochar Initiative (IBI) protocols (International Biochar Initiative, 2012). The skeletal (i.e., particle) density of the sieved biochar was $1.33 (\pm 0.03) \text{ g cm}^{-3}$ which is within the range of other wood derived biochars investigated in Brewer et al., (2014). The biochar had a wide range of particle sizes, with the largest fraction (32%) in the 425-991 μm range. Additional information describing the biochar is available in Appendix 2. Prior to application, the biochar was stored for up to 2 years in 55 gallon steel drums sealed from the atmosphere.

The biochar was applied in late February 2012 following a strategy recommended by J. Lehmann (pers. comm.) as specific methodologies for best practices in applying biochar to forest soils are not yet established. We used a drip-bag surface application approach. Plastic bags

containing 3 kg of biochar for application over 4 m² (5 t ha⁻¹) were prepared with an additional 1500 ml of tap-water (< 3 mg L⁻¹ C and < 0.2 mg L⁻¹ N) to prevent loss of airborne particles during application. The biochar was spread over a plot by cutting a hole in the corner of the sealed bag and slowly walking along a 4-m line distributing the biochar over a 1-m wide swath. In this way a homogeneous application equivalent to 5 t ha⁻¹ of biochar (3.95 t C ha⁻¹) was consistently applied to plots. Images taken at the site immediately after biochar application can be found in Appendix 5.

Urea-based fertilizer (N:P₂O₅:K₂O, 46:0:0) (Agrium Inc.) was carefully applied by hand in late March 2013 at a rate equivalent to 200 kg N ha⁻¹ (Hanley et al., 1996). The delay in the fertilizer application was intended to allow the biochar to become activated with local microbial communities, and to ensure N application during typically cool moist conditions, which is recommended for forest fertilization in BC (Lousier et al., 1991). This approach facilitates the rapid transfer of urea-N into the deeper soil profile near the roots and avoids N loss through NH₃ volatilization. Hence, the timing of N application provides 1-year window to investigate the short-term biochar application effects on GHG fluxes prior to fertilization.

3.2.3 Field soil GHG emission measurements

3.2.3.1 Sample collection and ancillary measurements

The SNSS chambers consisted of a permanent chamber collar (21-cm inner diameter x 10-cm long PVC pipe) installed to 5-cm depth or until contact with the mineral soil (Schiller and Hastie, 1996, Jassal et al., 2008). The chambers cover a total area (A) of 350 cm² with a headspace volume (V) of ~1.72 L, depending on depth of insertion limited by coarse soil fraction and tree roots. Headspace volumes were determined for each measurement date by measuring collar height. Soil cover within the collars included small ground herbs or grasses. Measurements

were made by placing an acrylic lid (0.4-cm thickness) with high-density foam attached to seal the outside edge of the collar. A small fan powered by a 9-V battery and a 10-cm-long venting tube (6.35 mm OD) attached to the lid were used to keep headspace air well mixed and equilibrate the internal volume of the chamber with atmospheric pressure (Hutchinson & Livingston, 2001), respectively.

Headspace gas samples (20-ml) were drawn from the chamber using a medical grade plastic syringe with needle (23-gauge) and piercing a 2-cm diameter butyl-rubber septum in the lid. Samples were injected into 12-cm³ pre-evacuated exetainers (Labco Limited, Buckinghamshire, UK). Samples were collected from the chambers at discrete time intervals to enable flux calculations. Initially, samples were collected at 0, 3, 10, 20, and 30-minutes after placing the lid on the collar (i.e. the total gas removal was 100 ml). Based on initial data analysis and logistical considerations, samples for 2012 onwards were collected at 0, 3, 6, 9 and 12 minutes following chamber closure. This approach allowed greater precision in GHG flux determination by focusing sampling closer to when the lid was placed on the collar during the time of the most rapid change in chamber headspace GHG concentrations. .

In combination with the sampling for GHG flux calculations, measurements of surface (0-5 cm) soil temperature (T_s), volumetric water content (θ_s), and bulk electrical conductivity (σ_s) were also made. This was done using a mobile hand-held unit equipped with a GS3 sensor (with factory calibration to convert the dielectric permittivity measurement to θ_s) at three locations triangulated within a radius of 20 cm centered on each chamber immediately after chamber measurements were made. Half-hourly measurements of precipitation and air temperature were obtained from the nearby climate station (Paul-Limoges et al., 2015).

3.2.3.2 Greenhouse gas analyses and flux calculations

GHG analyses were performed using a 100-vial autosampler connected to an Agilent 7890A (G3440A) Gas Chromatograph (GC) system fitted with a flame ionisation detector (FID) for detecting CH₄ and CO₂ following conversion to CH₄ with an inline methanizer. A micro-electron capture detector (μ ECD) was used to measure N₂O. The GC system thus evaluated the three GHGs (CO₂, CH₄, and N₂O) from each sample vial using a single injection split between parallel flowpaths to the FID and the μ ECD. Mixing ratio values were calculated from calibration curves determined from autosampler injections sampled from vials filled with certified standards (Air Liquide Inc, Burnaby, BC and Praxair, Aldergrove, WA), as were methodological standards for QA/QC, which to simulate actual field sampling, were sampled in the field (Air Liquide Inc, Burnaby, BC GC Calibration Standard mix of 1 ppm N₂O, 5 ppm CH₄, 600 ppm CO₂) and analyzed in parallel with the collected samples. All calibration standards were prepared as mixtures blended with pure N₂.

GHG fluxes for the SNSS chambers were calculated for each plot from GHG mixing ratios determined by the GC using linear and non-linear techniques with the HMR package for Flux Estimation with Static Chamber Data (Pedersen et al., 2010). The linear and non-linear fits for each chamber closure were compared independently for each of the three GHGs, with flux calculations discarded for the few closures for which fits were not obtained.

3.2.4 Data analysis

Data were analyzed using a one-way analysis of variance (ANOVA) to test for significant differences between treatments and corresponding GHG fluxes, the total treatment GWP (the sum of CO₂, CH₄-CO₂e and N₂O-CO₂e) and soil climate variables (T_s , T_{15} , θ_s , θ_{15} , σ_s , σ_{15} and Ψ_{15}). This was followed by Tukey's Honest Significant Differences (HSD) test when Treatment

was found to be a significant source of variance. It was possible to investigate the effects of BC treatments relative to S (i.e., control) plots using data from 2012 as well as 2012 and 2013 data combined. From data collected in 2013 after spring fertilization it was possible to investigate the newly fertilized treatments including F and BC+F. Date was included as an interacting factor with treatment in a two-way ANOVA. The peak in annual T_a occurred on 25 July for both years. This date was used to segregate sampling periods for both years into the spring through early summer time-period (pre 25 July; hereafter referred to as spring-summer, SS) and post 25 July time periods (referred to hereafter as summer-fall, SF).

Annual and seasonal relationships between GHG fluxes with T_s , T_{15} , θ_s , θ_{15} , σ_s , σ_{15} and Ψ_{15} were explored using linear regression. Additionally, for CO₂ we calculated the reference respiration rates (R_s at 10 °C, R_{s10}) and the temperature sensitivity parameters Q_{10} (the relative change in R_s for a 10 °C change in shallow surface soil temperature) after Davidson et al. (1998):

$$R_s = R_{s10} Q_{10R_s}^{(T_{15}-10)/10} \quad (2)$$

Equation 2 was fit to treatment CO₂ flux data and T_{15} using nonlinear least-squares estimates. While this approach does not ensure unbiased estimates of respiration rates (Lloyd and Taylor, 1994; Howard and Howard, 1979), it can be useful for comparisons between and within study sites. In this study we used it to compare differences between fitted values for the different treatments.

The net GHG flux in CO₂ equivalent terms (CO₂e as g CO₂e m⁻² s⁻¹) was calculated for each treatment using mean SNSS measured fluxes from all sampling dates and the 100-yr GWP of 1 for CO₂, 34 for CH₄, and 298 for N₂O (IPPC, 2013) using equation 3:

$$F_{CO_2e} = (F_{CO_2} \times M_{CO_2}) + (F_{CH_4} \times M_{CH_4} \times 34) + (F_{N_2O} \times M_{N_2O} \times 298) \quad (3)$$

where the F_{CO_2} , F_{CH_4} and F_{N_2O} are molar fluxes ($\text{mol m}^{-2} \text{s}^{-1}$) and, M_{CO_2} , M_{CH_4} and M_{N_2O} are molar masses (g mol^{-1}) and GWPs are global warming potentials. All calculations and statistical analyses were performed in R version 3.3.1 (2016-06-21) (RCore Team, 2016).

3.3 Results

3.3.1 Soil climate

The study site on eastern Vancouver Island typically experiences cool and wet winters with warm and dry summers. The mean annual T_a ($^{\circ}\text{C}$) was 8.1 ± 6.9 (mean ± 1 SD) in 2012 and 8.7 ± 7.0 in 2013. Both years were within one SD (standard deviation) of the 30-year mean recorded at the near-by Campbell River airport. The spring-summer mean T_a calculated from measurement days was similar for 2012 and 2013 (12.8 ± 2.6) and 11.6 ± 3.0), respectively. However, summer-fall T_a calculated from measurement days was higher in 2013 (19.6 ± 2.1) than in 2012 (15.4 ± 5.8). Precipitation in 2012 (1434 mm) was 40% more than in 2013 (840 mm), which was characterized by fewer intense (>15 mm/day) rainfall events. However, in 2013 precipitation was more evenly distributed with several small rainfall events (< 10 mm) throughout the growing season, and >50 mm in August, which is typically a very dry month.

Daily mean values of T_{15} , θ_{15} , and Ψ_{15} in the experimental area, and daily P measurements at a nearby (0.5 km) climate station, are presented during the two years when flux data were collected (Figure 10). Soil volumetric water content (θ_{15}) in early spring in both years shows drying trends frequently replenished by > 5 mm rainfall events. Both years experienced their driest periods from July to October. However, the more even distribution of rainfall during 2013, though lower in total compared to 2012, served to maintain θ_{15} at marginally higher values and Ψ_{15} at much higher values during summer-fall sample dates in 2013 (mean ± 1 standard deviation, $\theta_{15} = 0.22 \pm 0.04 \text{ cm}^3 \text{ cm}^{-3}$; $\Psi_{15} = -406 \pm 550 \text{ kPa}$) than in 2012 ($\theta_{15} = 0.20 \pm 0.06 \text{ cm}^3$

cm^{-3} ; $\Psi_{15} = -1944 \pm 2117 \text{ kPa}$). The volumetric water content values measured at the surface (θ_s) were also marginally larger in summer-fall sample dates of 2013 ($\theta_s = 0.14 \pm 0.03 \text{ cm}^3 \text{ cm}^{-3}$) compared to 2012 ($0.12 \pm 0.04 \text{ cm}^3 \text{ cm}^{-3}$).

ANOVA analyses revealed that θ_s during spring-summer in 2013 was significantly different between treatments ($F_{(3,136)} = 8.05, p \ll 0.01$), and HSD analysis showed that it was lower in BC+F compared to BC and F ($p < 0.05$), while θ_s in S it was significantly less than in BC ($p < 0.05$). The effect of biochar application on measured θ_{15} was undetected.

Using the ANOVA to assess surface σ during summer-fall in 2012 and 2013 was found to be 37% greater in the biochar plots than the control plots ($F_{(1,28)} = 3.843, p = 0.054$ in 2012 and $F_{(1,30)} = 3.794, p = 0.061$ in 2013). This could be explained by increased concentrations of exchangeable anions or cations compared to the control soil (Liang et al., 2006). After fertilization in 2013, σ_s was significantly greater (>35 %) in both the F and BC+F compared to the BC and S treatments ($F_{(3, 204)}, p \ll 0.001$), which was possibly due to increased NH_4^+ following hydrolysis of applied urea; σ_s subsequently decreased due to NH_4^+ uptake by plant roots, volatilization of NH_4^+ as NH_3 gas or immobilization as a result of binding to soil organic matter or, (in the case of the BC+F), the biochar surface. Depending on the soil conditions influencing the rate of urea oxidation (temperature, moisture and pH) this increase could also be indicative of both increasing NO_2^- and NO_3^- after nitrification of NH_4^+ .

3.3.2 Soil greenhouse gas fluxes

3.3.2.1 Soil CO_2 emissions

Mean CO_2 emissions from control (S) and biochar treated (BC) plots increased from 1.35 (± 0.86 , SE) and 1.1 (± 0.78) $\mu\text{mol CO}_2 \text{ m}^{-2} \text{ s}^{-1}$, respectively, on 11 May 2012 to 4.25 (± 1.70) and 3.2 (± 2.17) $\mu\text{mol CO}_2 \text{ m}^{-2} \text{ s}^{-1}$, respectively on 25 July 2012 (Figure 11). From all sample dates

prior to 25 July 2012, CO₂ emissions from S were on average 11 % higher than BC, peaking at nearly 33 % higher on 25 July 2012.

After the 2012 spring-summer period, CO₂ emissions from S and BC decreased to mean values of 1.537 (± 0.471) and 0.897 (± 0.868) $\mu\text{mol CO}_2 \text{ m}^{-2} \text{ s}^{-1}$, respectively on 9 October 2012, coinciding the lowest Ψ_{s15} values and decreasing temperatures (Figure 10). Fluxes were, on average, 19 % greater from S than BC during the summer-fall. The mean flux from all measurements was 2.55 (± 1.53) for S and 2.17 (± 1.644) $\mu\text{mol CO}_2 \text{ m}^{-2} \text{ s}^{-1}$ for BC. These results, especially for S, are consistent with those obtained in other studies investigating soil CO₂ emission at the site (Drewitt et al., 2002; Jassal et al., 2005, 2008, 2010) from measurements at research plots within 500-m of the study location.

Table 2 summarizes the one-way ANOVA for annual and seasonal CO₂ fluxes. In 2012, there was a statistically significant ($p < 0.1$) effect of treatments on CO₂ emissions during summer-fall months. The HSD analysis determined that fluxes from S were 0.57 $\mu\text{mol CO}_2 \text{ m}^{-2} \text{ s}^{-1}$ higher ($p = 0.082$) than from BC, suggesting that biochar decreased net CO₂ emissions towards the end of summer into fall. Including date as the second factor in the two-way ANOVA with treatment as the main factor, a significant effect for sampling date ($F_{(9,134)} = 4.23, p < 0.001$) was identified, indicating pronounced seasonal dynamics.

Results showed the CO₂ emissions from S during 2013 had similar seasonal trends as in 2012, with maximum CO₂ fluxes occurring for July through August (Figure 11). Both the fertilizer treated plots (F) and biochar plus fertilizer treated plots (BC + F) had a noticeably early season peak on 28 March 2013 shortly after fertilization (26 March 2013), with these treatment fluxes being about 75 and 60 % higher than from S, respectively. This increase could be the result of a CO₂ flux from the hydrolysis of the applied urea ($(\text{NH}_2)_2\text{CO} + 3\text{H}_2\text{O} \rightarrow 2\text{NH}_4^+ + \text{CO}_2$

+ 2OH⁻) as well as increased R_a and R_h from fertilization. The F treatment had the largest CO₂ emissions throughout 2013, in particular for July to September with a summer peak on 25 July 2013 of 10.60 (± 2.35) $\mu\text{mol CO}_2 \text{ m}^{-2} \text{ s}^{-1}$. The CO₂ flux from S reached a maximum of 4.60 (± 1.59) $\mu\text{mol CO}_2 \text{ m}^{-2} \text{ s}^{-1}$ on the same date. The emissions of CO₂ measured from S were generally smaller than all other treatments throughout the year. The CO₂ emissions from BC peaked somewhat later than S at 5.91 (± 4.03) $\mu\text{mol CO}_2 \text{ m}^{-2} \text{ s}^{-1}$ on 2013-09-05 and showed similar flux magnitudes as the BC+F, with the latter also reaching a maximum on that date of 5.21 (± 2.83) $\mu\text{mol CO}_2 \text{ m}^{-2} \text{ s}^{-1}$.

During 2013, there was a highly significant ($p < 0.001$) treatment effect on annual and seasonal CO₂ emissions (Table 2). The HSD analysis determined CO₂ fluxes from F were 3.31, 2.30 and 2.24 $\mu\text{mol m}^{-2} \text{ s}^{-1}$ higher than from S, BC and BC+F, respectively ($p < 0.01$). There was a significant effect for sampling date ($F_{(13,162)} = 10.31$, $p < 0.001$) when included as the second factor in ANOVA, supporting the earlier observation of temporal variability. During spring-summer 2013, the HSD analysis determined that CO₂ emissions from F were 2.94, 2.18 and 1.8 $\mu\text{mol m}^{-2} \text{ s}^{-1}$ greater than from S ($p < 0.001$), BC ($p < 0.001$) and BC+F ($p = 0.001$) treatments, respectively. Furthermore, the analysis detected significant differences between S and BC+F, with BC+F being 1.14 $\mu\text{mol m}^{-2} \text{ s}^{-1}$ greater than S. In summer-fall, the HSD analysis determined that CO₂ emissions from the F treatment were 5.69, 5.14 and 4.11 $\mu\text{mol m}^{-2} \text{ s}^{-1}$ greater than from S ($p < 0.001$), BC ($p < 0.001$) and BC+F ($p < 0.001$) treatments, respectively.

Taken together, these results strongly suggest that biochar alone did not increase CO₂ emissions compared to the control plots. They also suggest that fertilization significantly increased CO₂ emissions in early spring and summer, and that biochar applied prior to fertilization helped reduce these emissions. Furthermore, these results suggest that fertilization

significantly increased CO₂ emissions more during late summer/fall than during spring/early summer in 2013 with biochar mitigating these higher fluxes (Figure 11).

3.3.2.2 Soil CH₄ Uptake

Uptake of CH₄ in this forest soil was observed throughout 2012 for both S and BC (Figure 12). The net consumption of CH₄ increased during warmer and drier soil conditions starting in July with a maximum uptake measured in summer-fall, at 4.12 (±0.0.30) and 4.49 (±0.62) μmol CH₄ m⁻² h⁻¹ for S and BC, respectively. Mean fluxes for just S in 2012 averaged 3.58 μmol CH₄ m⁻² h⁻¹, which was close to the annual mean uptake of 4 μmol m⁻² h⁻¹ in a nearby control (without any treatment) soil surface measured by Jassal et al. (2011). On average CH₄ uptake was 15 % greater for BC when compared with S, although differences were not statistically significant (Table 2).

The CH₄ uptake for S and BC treatments in 2013 was greater and shared similar seasonal trends as found in 2012, with the maximums again being again occurring in summer-fall (Figure 12). Throughout 2013, CH₄ uptake in S was approximately 60% of that measured in F, which had a maximum uptake of 11.86 (±5.1) μmol CH₄ m⁻² h⁻¹ on 14 August 2013, closely matching that in BC with maximum uptake of 10.37 (±6.74) μmol CH₄ m⁻² h⁻¹ on 5 September 2013 (not shown).

During 2013 there was a significant effect of treatments on CH₄ uptake ($p < .05$) annually as well as seasonally. Including date as the second factor in the two-way ANOVA with treatment as the main factor, a significant effect for sampling date during 2012 and 2013 ($F_{(9,107)} = 2.16, p < 0.03, F_{(13,124)} = 2.68, p < 0.002$, respectively) was identified, supporting the observations of seasonal dynamics (Figure 12). The HSD comparisons for the one-way ANOVA determined that uptake in the F treatment was significantly larger than in S ($p = 0.012$) with an annual average of

2.21 $\mu\text{mol m}^{-2} \text{h}^{-1}$ more CH_4 uptake in F. Similar results were observed for spring-summer ($p = 0.012$) and summer-fall ($p = 0.039$) with CH_4 uptake higher in F than in S by 1.47 and 4.89 $\mu\text{mol m}^{-2} \text{hr}^{-1}$, respectively. The lack of significant difference between other treatments suggests that fertilization-induced increases in CH_4 uptake were lower if fertilizer was applied to soils pre-treated with biochar.

3.3.2.3 Soil N_2O emission and uptake

During 2012, N_2O emission and uptake were very small and well below the minimum detectable flux (Appendix 3) in most plots. Higher fluxes were more commonly found from BC during warmer days in the spring when the soil was wetter than in summer and fall (Figure 13). The N_2O emission peaked for BC on 20 June 2013 at 0.085 (± 0.053) $\mu\text{mol m}^{-2} \text{hr}^{-1}$ (not shown), while, at the same time, flux magnitudes were lower for S. There was a significant ($p < 0.1$) effect of treatments on N_2O emissions annually and during the spring-summer period in 2012 (Table 2). The HSD comparisons determined that for 2012, BC had, on average, emissions 0.027 $\mu\text{mol m}^{-2} \text{hr}^{-1}$ greater than S ($p = 0.068$).

During 2013, S displayed similar trends as in 2012, generally emitting N_2O in early spring when conditions were warm and moist, followed by a transition to N_2O uptake in summer and fall months (Figure 13). BC and F were consistently very small sources of N_2O to the atmosphere, and on average, F, BC and BC+F were 9, 11 and 19 times larger N_2O sources than S, respectively. In general, fertilization increased N_2O emissions throughout 2013, and there was a difference in peak timing with F peaking first on 26 June 2013 at 0.323 (± 0.477) $\mu\text{mol N}_2\text{O m}^{-2} \text{h}^{-1}$, followed by BC+F on 10 July 2013 at 0.266 (± 0.312) $\mu\text{mol N}_2\text{O m}^{-2} \text{h}^{-1}$ and BC on 14 August 2013 at 0.300 (± 0.560) $\mu\text{mol N}_2\text{O m}^{-2} \text{h}^{-1}$ (not shown).

There was as modest effect of treatments determined from annual and spring-summer one-way ANOVA during 2013 ($p < 0.1$). The HSD comparisons determined that the 2013 annual emissions from S were on average lower by $0.103 \mu\text{mol m}^{-2} \text{hr}^{-1}$ compared to the BC+F ($p = 0.006$) and not significantly different from F. The HSD comparisons also determined that the spring-summer emissions from S were on average lower by $0.109 \mu\text{mol m}^{-2} \text{hr}^{-1}$ compared to the BC+F ($p = 0.003$) and that the emissions from BC were on average lower by $0.074 \mu\text{mol m}^{-2} \text{hr}^{-1}$ compared to the BC+F ($p = 0.003$). The results suggest that biochar application stimulated N_2O emissions, both with and without fertilizer application.

3.3.2.4 Soil CO_2e and GWP

The seasonal pattern of the net CO_2e emissions was strongly correlated with actual CO_2 emissions. For all treatments, CO_2 emissions were almost equal to the calculated CO_2e , indicating an almost undetectable contribution from CH_4 uptake and N_2O emissions to the total treatment GWP during this study with and without biochar application. On average, the CO_2 emissions accounted for $\sim 100\%$ CO_2e emissions from S and BC and 99% from F and BC+F.

There was a significant treatment effect on CO_2e emissions only in 2013 and this mimics differences already identified in the CO_2 analysis. The annual HSD comparisons showed that F was significantly greater than all other treatments ($p < 0.001$) exceeded S by $2.93 \mu\text{mol m}^{-2} \text{s}^{-1}$, BC by 2.47 $2.36 \mu\text{mol m}^{-2} \text{s}^{-1}$ and BC+F by $2.36 \mu\text{mol m}^{-2} \text{s}^{-1}$, respectively.

In summary, in the first year after winter application of biochar it likely decreased CO_2 emissions in summer-fall, while fertilization (F) in the following year increased CO_2 emissions immediately after application, especially in summer, with BC and BC+F showing no significant difference when compared with S. From these results we would reject the hypothesis that biochar additions would increase CO_2 emissions irrespective of fertilization. Biochar application had no

effect on CH₄ uptake while fertilization increased CH₄ uptake and biochar likely reduced this enhanced uptake. From these results we would reject the hypothesis that biochar additions before fertilization would increase CH₄ uptake (or decrease CH₄ emissions) in fertilized and unfertilized soils. In the first year (2012) after winter application of biochar, N₂O emissions increased during spring-summer, while in 2013 annual N₂O emissions were larger for all treatments and during spring summer for BC+F. From these results we would accept the hypothesis that biochar additions would increase N₂O emissions in un-fertilized soils in this N-limited system and reject the hypothesis that prior biochar additions would reduce N₂O emissions in fertilized soils. The net effect on GWP was that biochar did not significantly increase emissions (with no fertilizer addition) and helped to reduce CO₂e emissions when applied before fertilization.

3.3.3 Soil greenhouse gas flux relationships to soil climate

Overall, CO₂ emissions during 2013 were positively correlated with T_{15} for all treatments ($r = 0.71, 0.49$ and 0.74 , $n = 42, 42$ and 34 , for S, BC and F, respectively at $p < 0.01$), somewhat weakly for BC+F ($r = 0.23$, $n = 34$, $p < 0.01$). During 2013, CO₂ emissions in BC and F treatments were negatively correlated with θ_{15} , particularly when $\theta_{15} > 0.25$, ($r = -0.42$ and -0.28 , $n = 37$ and 35 , respectively at $p < 0.01$), less so in S ($r = -0.08$, $n = 42$, $p = 0.07$) and not at all in BC+F treatments. Both correlations of CO₂ emissions with T_{15} and θ_{15} were heavily chamber dependent: chambers that indicated stronger correlations with T_{15} also indicated stronger correlations with θ_{15} , suggesting variability in other controlling variables was having more impact at other chamber locations. This could be due to a large number of measurements in 2013 from early spring (Figure 11) made when water availability was not limiting to stand photosynthesis and associated R_a , and may also have resulted from the wetter conditions expressed through consistently higher Ψ_{15} through summer-fall in that year.

For CH₄ uptake, there were weak but significant soil climate correlations determined for the BC and F treatments. For BC, CH₄ uptake during 2012 and 2013 was found to have a positive correlation with T_s ($r = 0.06$, $n = 92$, $p = 0.02$) and T_{15} ($r = 0.09$, $n = 78$, $p = 0.01$), and negatively correlated to θ_s ($r = 0.09$, $n = 87$, $p < 0.01$), σ_s ($r = 0.09$, $n = 96$, $p < 0.01$) and σ_{15} ($r = 0.12$, $n = 78$, $p < 0.01$). For F, CH₄ uptake during 2013 was found to have a positive correlation with T_s ($r = 0.19$, $n = 29$, $p = 0.01$) and T_{15} ($r = 0.29$, $n = 29$, $p < 0.01$), and a negative correlation with θ_{15} ($r = 0.32$, $n = 29$, $p < 0.01$) and Ψ_{15} ($r = 0.42$, $n = 6$, $p = 0.08$) and σ_{15} ($r = 0.13$, $n = 29$, $p = 0.04$). The only significant although weak correlation found for the BC+F treatment was a positive response for CH₄ uptake with σ_s ($r = 0.18$, $n = 38$, $p = 0.01$).

For N₂O emissions, very weak but significant soil climate correlations were determined for only the BC+F in 2013, which was also the only treatment during this time period where non-zero N₂O fluxes from the soil to the atmosphere were detected. Very weak positive correlations were determined between N₂O fluxes and θ_{15} ($r = 0.18$, $n = 34$, $p = 0.01$) and between N₂O fluxes and σ_{15} ($r = 0.16$, $n = 34$, $p = 0.02$).

In general, the strongest response to climate variables across treatments and individual chambers was that of CO₂ fluxes to changes in soil temperature. Figure 14 shows the fitted lines for equation 2 with the estimated F_{10} , Q_{10} values and statistics for each treatment given in Table 3. All parameter fits were significant at $p \ll 0.001$. The highest R² were observed during 2013, which, similar to the results obtained for the CO₂ response to T_{15} using linear regression, we attribute to the greater number of measurements during early spring (Figure 11) when water availability was not limiting and the wetter conditions that occurred during the summer-fall 2013. Of particular interest is the high R² value (0.75) for the F treatment compared to others (0.68 and 0.47 for S and BC, respectively) and the contrastingly low R² value for the BC+F

treatment (0.21). The F treatment showed the highest R_{s10} , followed by BC+F, BC and S with the latter almost half of the F R_{s10} . The BC treatment had the greatest sensitivity to temperature increase ($Q_{10} = 3.15$) followed by F, S, then BC+F.

3.4 Discussion

3.4.1 Biochar treatment effects

Biochar decreased net CO₂ emissions compared to control plots towards the end of summer into fall in the first year after application. Taking care to subtract the control CO₂ from the biochar emissions, Spokas et al., (2009) showed that the addition of biochar reduced R_s in an incubation experiment, while Lui et al., (2016) showed no net effect on CO₂ emissions when biochar was added to Chinese agricultural soils.

The soil C resident in the surface organic horizon is estimated to be between 244-257 mg g⁻¹ dry soil (Humphreys et al., 2006), making it more than 50% of the rate of biochar C addition in this study. The resulting decrease in CO₂ emissions is therefore in line with findings from a meta-analysis by Sagrilo et al. (2015), who concluded that biochar generally reduces CO₂ emissions when applied at rates less than twice the amount of the soil organic matter C. Studies reporting increased CO₂ emissions following biochar application to soils have attributed the rise to mineralization of the available labile C pool associated with the biochar and enhanced mineralization of weathered biochar over time by microbes. It is possible that in this study the lack of any detected increase in CO₂ emissions associated with biochar effects on soil mineralization is the result of variably charged minerals like iron (Fe) and aluminum (Al), associated with humo-ferric podzol soils (Evans and Wilson, 1985), sorbing onto typically electronegative biochar surfaces (Mukherjee et al., 2011) and serving to stabilize the biochar

(Fang et al., 2014), although this more commonly occurs in soils with high clay contents (Brodowski et al 2006).

This study found no significant effect on net CH₄ uptake after biochar addition, while there was a trend toward increased consumption following fertilizer application. The magnitude of CH₄ uptake measured during this study was comparable to measurements made at this forest site by Jassal et al., (2011), and by Crill (1991) in a temperate forest near New York, as well as at sites further afield and from other ecosystem types during summer months as summarized by Sabrekov et al. (2016). The increased CH₄ uptake in fall suggests that low soil water content did not induce a biological limitation (Del Grosso et al., 2000), but rather remained within the optimal range (70-20 %) for methane consumption in the surface soil layer (Mosier et al., 1996). The soil at this site is highly acidic and experiences short term flooding from high rainfall events (see Figure 10, year 2013), while the soil texture (gravelly-sandy-loam) also helps it to drain rapidly. In a meta-analysis by Jeffery et al (2016), biochar was found to mitigate CH₄ emission in acidic soils that are periodically flooded. Masiello et al (2013) found that biochar can stimulate a range of effects on microbial gene expression that are dependent on intercellular communication and hence it could regulate microbial-dependent soil processes like net CH₄ uptake through the balance between methanotrophic (uptake) and methanogenic activity (production).

This study showed that biochar modestly increased N₂O emissions during the first year after application. The N₂O emissions measured in this study were notably smaller than those measured at nearby (200 m away) research plots by Jassal et al., (2008, 2010 and 2011) following spring and winter fertilizations at 200 kg N ha⁻¹. From a meta-analysis, Cayuela et al (2014) concluded that biochar reduced N₂O emissions from agricultural soils in both field and laboratory studies by up to 54%. This was directly correlated to the amount of biochar applied.

Harter et al. (2014) specifically related these decreases in water-saturated soils to the structure and function of the N-cycling microbial community. Whether similar behavior holds for the soil microbial community in rapidly drained, N-deficient forest soils is unknown at present. In contrast, by utilizing microcosm experiments with the addition of different types of fertilizer-N and using stable isotope techniques with and without the use of a nitrification inhibitor, Sanchez-Garcia et al., (2014) found that biochar can increase soil N₂O emissions produced by nitrification-mediated pathways.

3.4.2 Fertilizer treatment effects

Fertilized plots were consistently large sources of CO₂ compared to all other treatments, while fertilized plots with biochar were significantly larger sources than control plots only during spring and early summer periods of relatively low fluxes (Figure 11). The significantly larger CO₂ emissions observed immediately after the fertilization of the control plots in this study are consistent with the increases in R_s observed in the field measurements of Jassal et al. (2010) and Shrethsa et al. (2014), each of whom attributed the short-term increase in R_s to increases in R_a more than from R_h , with possible contributions from CO₂ released from urea hydrolysis (Jassal et al., 2010). Raich et al. (1994) found increased root growth after fertilization of N-limited forest soils, which would be reflected in increased contributions of R_a to R_s . In this study, after an initial increase in CO₂ emissions following fertilization, differences between treatments diminished through spring into early summer, possibly due to decreased R_h as labile substrates were used up and the remaining litter quality was low (Knorr et al., 2005). Another explanation could be changes to the microbial structure after fertilization (Cleveland et al., 2007; Levy-Booth, 2016). Fray et al. (2004) detected shifts in fungal diversity; reductions in active fungal

biomass and the activity of ligninolytic enzymes (e.g., phenol oxidase), which all influence rates of degradation of recalcitrant organic material after N-fertilization of pine and hardwood forests. Significant differences between the fertilized plots and all others were found throughout the summer period when N₂O fluxes were largest. The increase in measured CO₂ emissions from fertilized plots after June 2013 suggests that there could have been increased plant productivity and associated R_a as a result of fertilization. In this study fertilizer was applied more than 15 days earlier than other in studies that measured CO₂ emissions from Douglas fir forest soils after spring fertilization (Jassal et al., 2010; Shrestha et al., 2014). Seasonal changes in microbial biomass and nutrient flush have been recorded in forest soils and complex relationships between fertilizer timing, microbial biomass, nutrient mineralization and climate could have contributed to the different CO₂ fluxes measured in this study (Diaz-Ravina et al., 1995; Levy-Booth, 2016). Unlike the fertilized plots without biochar, those with biochar did not have elevated CO₂ emissions compared to the control plots throughout the summer (Figure 11). It is possible that the biochar retained some released NH₄⁺-N after urea hydrolysis, through physical entrapment in its pores (Jassal et al., 2015) rendering it unavailable for microbial or plant uptake or subsequent nitrification to plant available NO₃⁻-N. Zheng et al. (2012), found that biochar decreased extractable NO₃⁻ in N-fertilized treatments by 8% with mixed effects on NH₄⁺ in two temperate soils. Biochar absorption of NH₄⁺ released via hydrolysis of urea would likely reduce microbial activity, decrease R_h , and slow the conversion of NH₄⁺ through nitrification to NO₃⁻, which in combination could effectively reduce R_a .

Soil fluxes of GHGs share soil temperature and soil moisture as common controlling variables (Smith et al., 2003). The effect of biochar application on these, with and without fertilization in a forest soil is unknown. Other important variables, known to affect gas diffusion

gradients and microbial activity include θ , Ψ , C/N, organic matter content, redox potentials and pH (Mosier et al., 1996; Del Grosso et al., 2000; Jassal et al., 2005; Jassal et al., 2010; Jassal et al., 2011; Hu et al., 2015). Analysis and comparison between treatments and the soil climate variables for all gases was made difficult by the large spatial and temporal variability in this heterogeneous forest soil, that is not ideally captured by SNSS chamber techniques and where these biogenic GHG fluxes are the expression of complex abiotic and biotic relationships. Analysis of the relationship between the CO₂ emissions and temperature for the different treatments indicated that this relationship was strongest in fertilized plots suggesting that the partitioning between R_h and R_a could be different between treatments. The reduced temperature sensitivity of R_s observed in the biochar plots indicates that the effects of biochar application on R_a and R_h differ from those of fertilizer application. Eberwein et al. (2015) found that the response of R_h to N-enrichment and changes in temperature was dependent on the C availability of soil substrates, and when C was abundant, N enrichment increased R_h . Furthermore, they found that while the complexity of the C source was important, abundance of C was more so. In this study we found that the addition of biochar, in the absence of fertilizer, resulted in slightly higher Q_{10} estimates during 2013 when surface conditions were generally wetter.

After fertilization of biochar treated plots, there was no noticeable differences in CH₄ uptake in BC + F compared to biochar without fertilization (BC); however, there was a noticeable increase in CH₄ uptake in fertilized plots without biochar application (F). The fertilization results differ from those observed by Jassal et al. (2011) who found that N addition reduced CH₄ uptake from an average of 4 $\mu\text{mol m}^{-2} \text{h}^{-1}$ in the control plots to 2 $\mu\text{mol m}^{-2} \text{h}^{-1}$ in the fertilized plots. Jassal et al.'s (2011) results are consistent with the likely inhibition of methanotrophic activity caused by competitive inhibition of the enzyme methane monooxygenase (MMO) by NH₄⁺. The work of

Krus and Everson (1995) may help explain the differences in the observed CH₄ uptake response to N addition between Jassal et al. (2011) and the present study. They found that fertilization of nutrient poor ecosystems may have a stimulating effect on CH₄ oxidation and associated this with likely increases in ammonium concentrations resulting from more rapid nutrient cycling (Goldman et al., 1995). Furthermore, Bodelier et al. (1999) found that urea-N fertilization stimulated methane oxidation around the roots of rice plants with an increase in Type-I methanotrophs being measured, with N known to be selective for those methane oxidizers. It is possible we detected increased CH₄ uptake and Jassal et al. (2011) detected decreased CH₄ uptake after fertilization because less mineral-N was available in the soil prior to fertilization in our study (not measured), as is indicated by the difficulties in determining significant N₂O fluxes before and after fertilization in our study as well as the recorded significant increase in CO₂ emissions, thought to be related to increase R_a and R_h after fertilization.

Using the SNSS technique, Jassal et al. (2007) measured peak emissions of 26 $\mu\text{mol N}_2\text{O m}^{-2} \text{ h}^{-1}$ on 24 July 2007, 3-months after spring fertilizer application, at a nearby (200 m away) location in this stand. Other studies have shown lesser N₂O emissions but similar timing after urea-N fertilization (Shrestha, et al., 2014). The small increase in N₂O emissions that was observed after fertilization, is unusual as it is more usual to detect increases from 20-500% after fertilization (Magill et al., 2000; Papen et al., 2001; Jassal et al., 2008; Koehler et al., 2009; Shrestha et al., 2014). It is likely that the very small amount of rain that fell immediately following fertilization (< 15 mm over 12 days, with only 1-day receiving > 5 mm), could have resulted in poor incorporation of the urea-N into the deeper soil profile and increased loss of N as NH₃ (Fox and Hoffman, 1981). Another factor contributing to the low N₂O emissions observed could be that the applied N was quickly bound to organic matter surfaces with high CEC in the

upper LFH layer, rendering it unavailable for nitrifying bacteria (Chapell et al., 1999; Prescott et al., 1993). The transient, sporadic nature of elevated N_2O emissions often associated with rainfall events and nitrifier denitrification would have been missed by the biweekly sampling (Barton et al., 2015). Furthermore, the delayed peak in N_2O emissions experienced after fertilization (Jassal et al., 2008; Shrestha et al., 2014) is often short-lived (Peng et al., 2001; 2-3 weeks) and so can be easily missed with low temporal sampling frequency.

Jassal et al. (2010) reported short-term significant increases in N_2O emissions following fertilization and hypothesized that this was due to a lack of bioavailable C in acidic forest soils which would facilitate immobilization of NH_4^+ -N in microbial assimilates (Aber et al., 1998). The small increase in N_2O emissions after biochar addition and fertilization could be the result of improved bioavailability of C. In a meta analysis, Cayuela et al (2014) found that emissions of N_2O after biochar application were influenced by the biochar feedstock, pyrolysis conditions and the C/N ratio; interactions between soil texture and the biochar, and, if applied, the chemical form of N-fertilizer, were also found to be important.

3.4.3 Carbon dioxide equivalent fluxes

In this experiment, soil CO_2 effluxes represented > 99% of the CO_2e for all treatments. The unexpected increase in net- CH_4 uptake after fertilizer additions was not sufficient to significantly decrease CO_2e , and the N_2O emissions were also not sufficiently large to have an effect. When we take into account the added biochar-C (3.9 t ha^{-1}) and consider that there was no detected increase in the CO_2 emissions after application to unfertilized plots, we can conclude that the biochar application to soil successfully sequestered more C in the short-term in the soil. Without a more thorough knowledge of the effects of fertilization on stand productivity, it is impossible to ascertain if there was an increase in C sequestration as a result of biochar

applications to a fertilized forest. Jassal *et al.* (2008) determined a net increase of 64% in net ecosystem productivity (NEP), from 3.3-5.3 Mg-C ha⁻¹ yr⁻¹ following fertilization. Based on this, and because we found that biochar reduced CO₂ emission after fertilization, we estimate that biochar would further improve C-sequestration by an additional 15% to 5.9 Mg-C ha⁻¹ during the first year after fertilization compared to fertilization alone.

3.5 Conclusions

The results presented show the effects on soil GHG emissions after application of 5 t ha⁻¹ of Douglas-fir derived biochar to a Douglas-fir forest soil in the first year followed by application of fertilizer N as urea in the second year. The results support that soil CO₂ emissions are strongly controlled by soil temperature, furthermore that the relationship is stronger after fertilization suggesting that the partitioning between R_a and R_h can vary with different treatments. Overall the results suggest that the effect of adding low amounts of Douglas-fir derived biochar to the surface of the dominant soil type supporting Douglas-fir stand growth in Western Canada, would have little effect on GHG emissions and their total CO₂e fluxes. Additionally, applying biochar prior to fertilizer applied following industry-standard practices neither significantly increased nor decreased the treatment CO₂e fluxes. Fertilization did have a significant effect, increasing CO₂ emissions. In conclusion, low rates of biochar addition to this forest soil would further improve soil C sequestration with or without fertilization.

3.6 Tables

Table 2. Greenhouse gas annual (Annl) and seasonal one-way ANOVA. Spring-summer (SS), Summer-fall (SF). HSD analysis indicates which treatments were determined to be significantly larger than others in list.

| Gas | Year | Season | df | F | p | HSD |
|------------------|------|--------|-------|--------|----------|----------------------------------|
| CO ₂ | 2012 | Annl | 1,152 | 2.155 | 0.144 | |
| | | SS | 1,76 | 0.099 | 0.750 | |
| | | SF | 1,74 | 3.106 | 0.082 | S > BC |
| | 2013 | Annl | 3,212 | 22.610 | << 0.001 | F > S, BC, BC+F |
| | | SS | 3,164 | 16.560 | << 0.001 | F > S, BC, BC+F & BC+F > S |
| | | SF | 3,44 | 14.650 | << 0.001 | F > S, BC, BC+F |
| CH ₄ | 2012 | Annl | 1,125 | 1.656 | 0.2 | |
| | | SS | 1,61 | 1.001 | 0.32 | |
| | | SF | 1,62 | 0.804 | 0.37 | |
| | 2013 | Annl | 3,173 | 4.447 | 0.005 | S > F |
| | | SS | 3,133 | 3.159 | 0.03 | S > F |
| | | SF | 3,36 | 2.703 | 0.056 | S > F |
| N ₂ O | 2012 | Annl | 1,130 | 2.241 | 0.012 | |
| | | SS | 1,71 | 3.428 | 0.068 | BC > S |
| | | SF | 1,57 | 0.231 | 0.632 | |
| | 2013 | Annl | 3,190 | 4.227 | 0.006 | BC+F > S BC+F > S & BC+F > BC |
| | | SS | 3,149 | 4.460 | 0.005 | @ p < .1 |
| | | SF | 3,37 | 1.479 | 0.235 | |

Table 3. Treatment annual dependence of R_{s10} ($\mu\text{mol CO}_2 \text{ m}^{-2} \text{ s}^{-1}$) and Q_{10Rs} parameters in Eq.2. Also shown model goodness of fit parameters AIC and R^2 . Fitted relationships for all data can be seen in Figure 14.

| Years | Treatment | R_{s10} | Q_{10Rs} | AIC | R^2 |
|-------|-----------|-----------|------------|--------|-------|
| All | S | 2.55 | 2.94 | 317.23 | 0.31 |
| All | BC | 3.36 | 3.15 | 420.89 | 0.21 |
| 2012 | S | 2.61 | 2.67 | 199.28 | 0.09 |
| 2012 | BC | 2.76 | 1.37 | 205.67 | -0.01 |
| 2013 | S | 2.48 | 3.06 | 100.67 | 0.68 |
| 2013 | BC | 4.38 | 3.13 | 193.84 | 0.47 |
| 2013 | BC+F | 3.87 | 1.97 | 159.73 | 0.21 |
| 2013 | F | 6.02 | 3.08 | 137.24 | 0.75 |

3.7 Figures

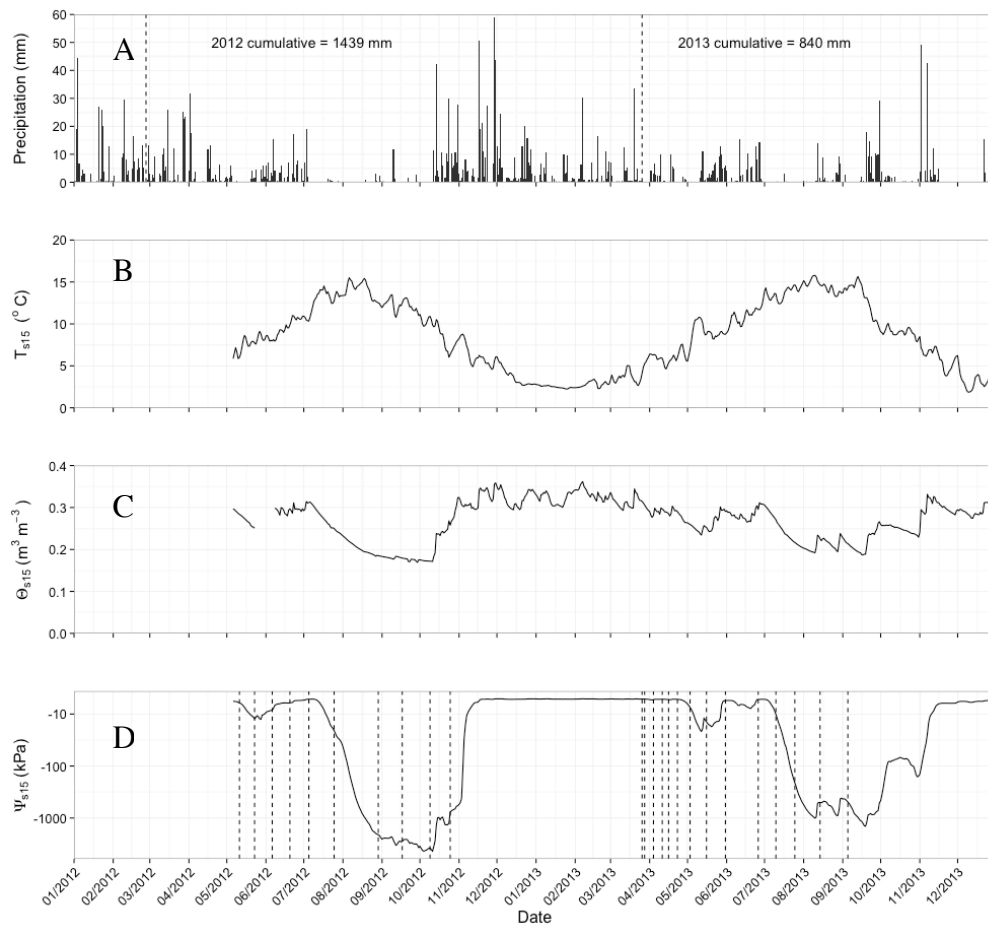


Figure 10. Site soil climate variables. (A) Daily cumulative precipitation measured at a nearby climate station. Dashed lines indicate biochar application (27th Feb 2012) and fertilizer application (27th Mar 2013); (B) Daily mean T_{s15} from averaging each MPS-2 and GS3 measurements; (C) Daily mean θ_{s15} from averaging GS3 measurements; (D) Logarithm of the daily mean Ψ_{s15} from MPS-2 measurements. Dashed lines indicate sample dates.

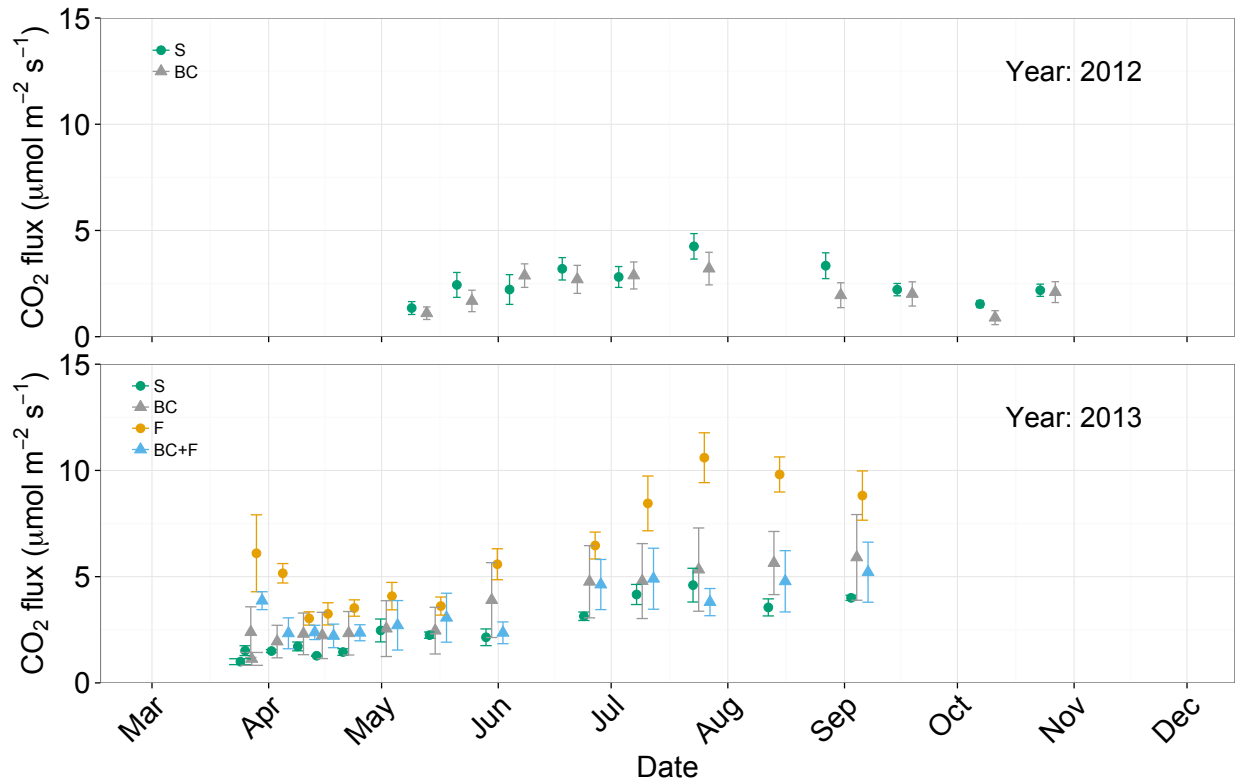


Figure 11. Mean treatment CO₂ fluxes for soil (S), biochar (BC), fertilizer (F) and Biochar plus Fertilizer (BC+F). During 2012 when only the biochar treatment was applied (top panel); Measurements during 2013 when all treatment were applied (bottom panel). Error bars indicate \pm one standard error of the mean treatment value and points have been spread evenly for each sample date to ease comparison.

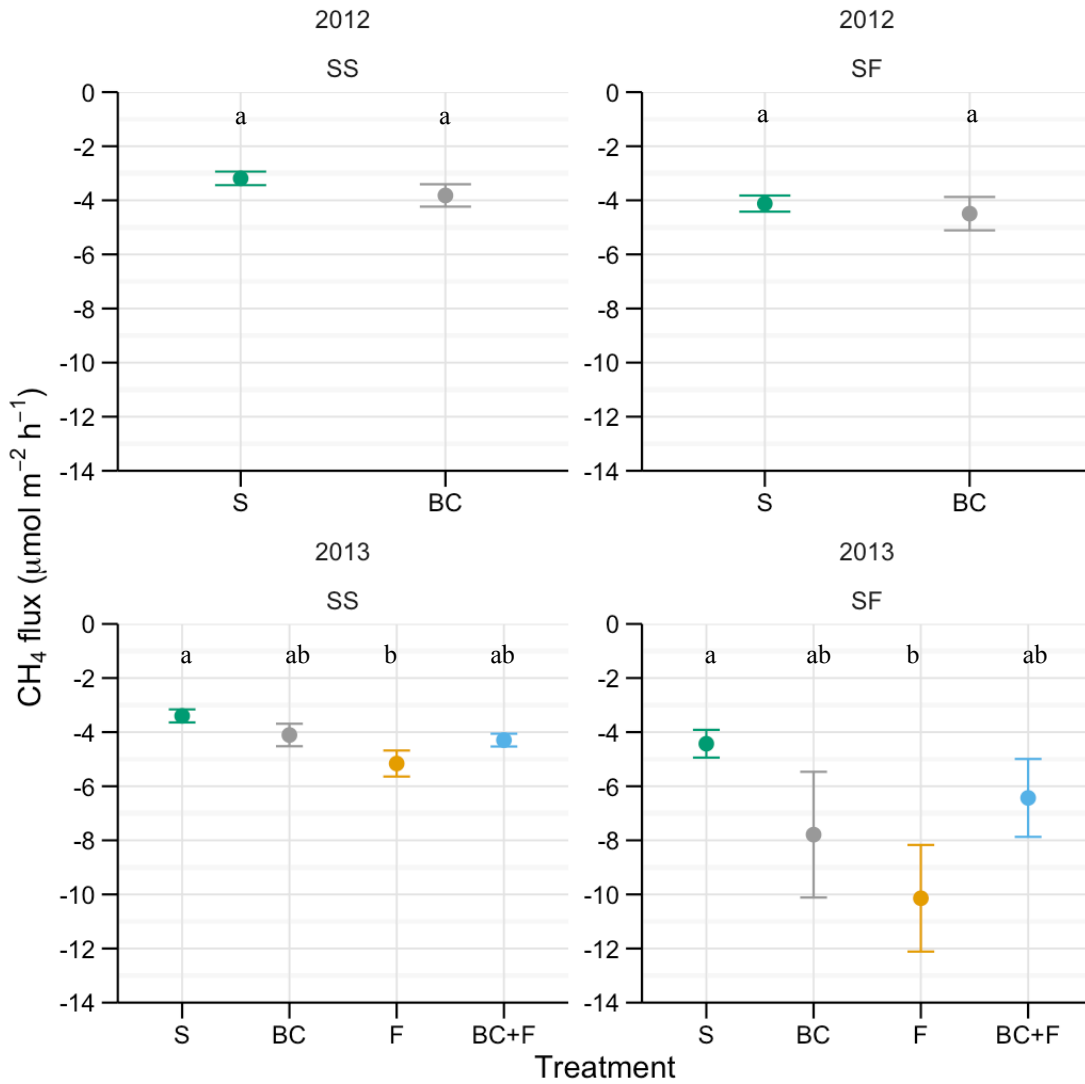


Figure 12. Methane 2012:2013 seasonal treatment effect (mean \pm 1 SE). Spring-summer (SS), Summer-fall (SF). Lettering (a-b) indicates pairwise differences detected in HSD analysis when $p < 0.05$.

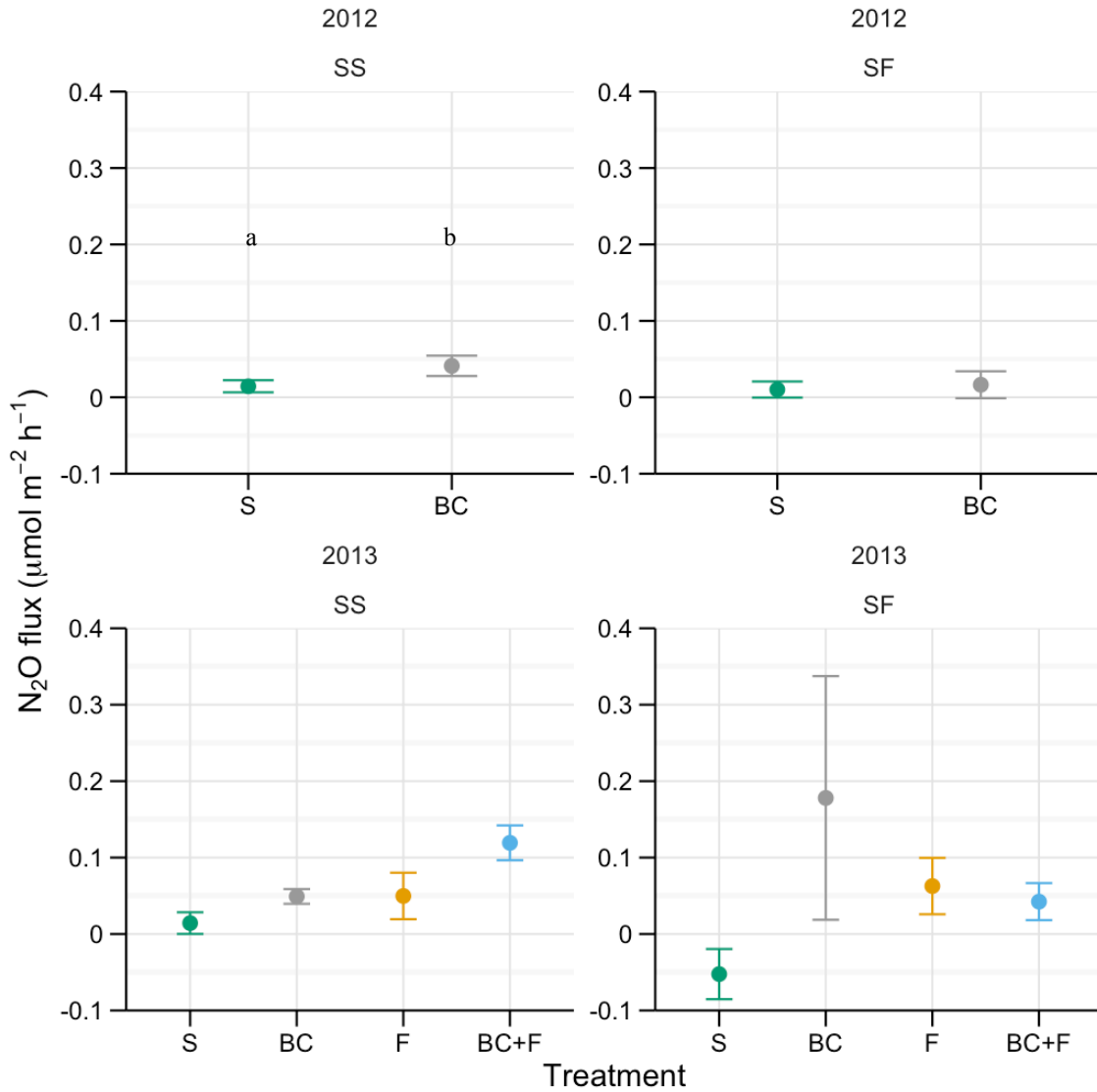


Figure 13. Nitrous oxide 2012:2013 seasonal treatment fluxes (Mean \pm 1 SE). Summer-spring (SS), Spring-fall (SF). Lettering (a-b) indicates pairwise differences detected in HSD analysis when $p < 0.05$.

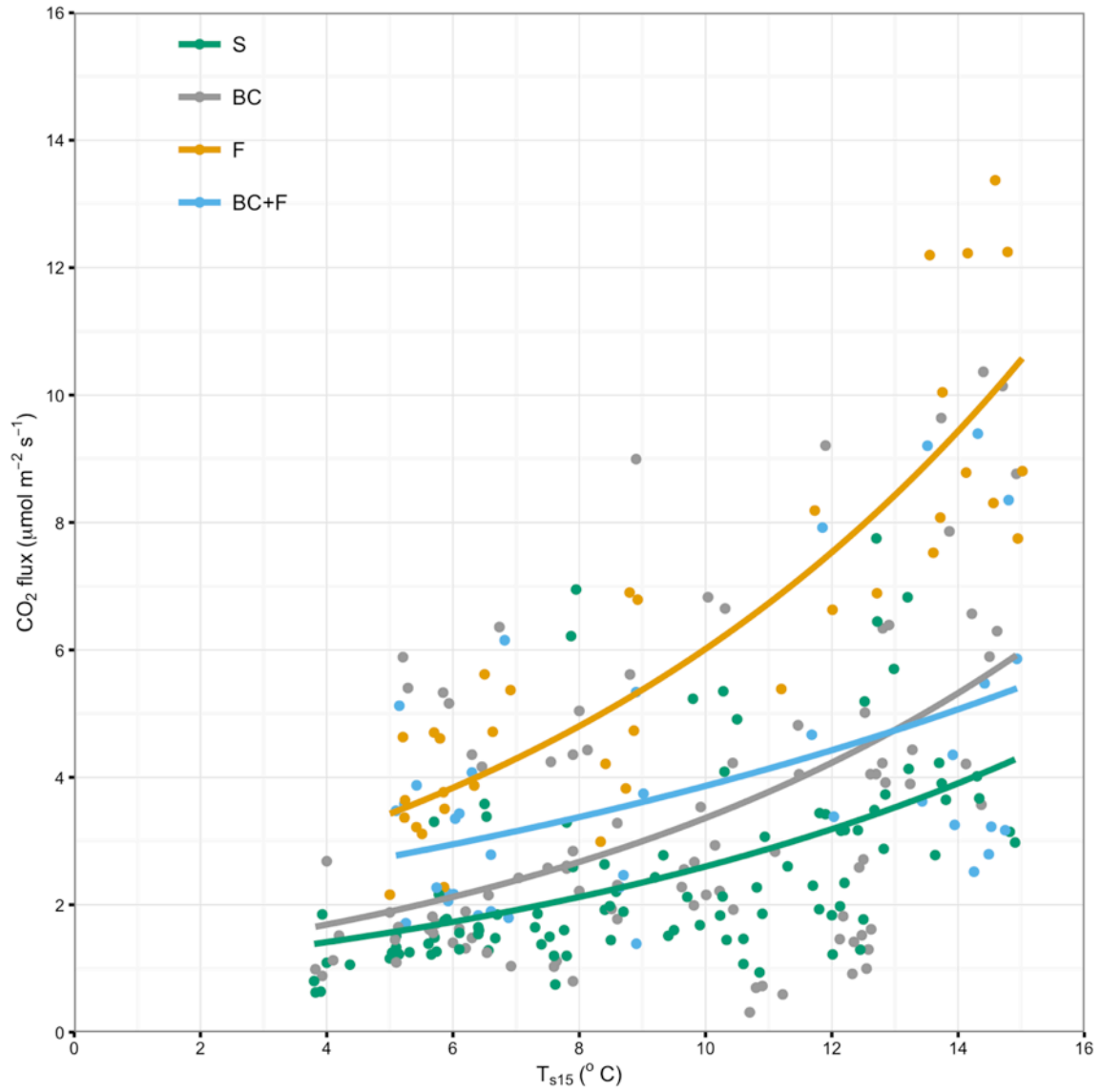


Figure 14. Relationship of soil CO_2 efflux (R_s) to soil temperature at 15-cm depth for different treatments.

Chapter 4: Laboratory and field measurements of dissolved organic carbon and nitrogen after biochar application with and without urea-N fertilization to a West Coast Douglas-fir forest soil

4.1 Introduction

The growth of a tree is limited ecologically by the niche it occupies. Temperate and boreal forest ecosystems are generally nitrogen (N) limited (Vitousek and Howarth, 1991). Plant available forms of N include ammonium (NH_4^+), naturally provided through ammonification of organic N, and, nitrate (NO_3^-) from nitrification. Fertilization with N can result in increasing carbon (C) sequestration (Aber et al., 1995; Aber et al., 1998). Studies have shown that the effects of N addition are positive on tree growth and also mostly positive on soil C sequestration in the Northern Hemisphere (Aber et al., 1995; Jassal et al., 2008; Liu and Greaver, 2009; Vitousek and Howarth, 1991).

In the N-limited Douglas-fir stands of the Pacific Northwest, N is mostly stored in soil organic matter (Chapell et al., 1991, Humphreys et al., 2006) and its availability to plants is largely dependent on the ammonification rate through to NH_4^+ as the typically high C/N ratios and low nitrification rates limit the availability of NO_3^- . Chapelle et al. (1991) note that fertilization programs have focussed predominantly on increasing stand growth, as nutrient deficiencies are not enough to prevent the establishment Douglas-fir stands. Because of the low rates of natural addition of N to the soils through symbiotic fixation and N deposition, it is of utmost importance to ensure that leaching losses enhanced by nitrification are kept to a minimum. In work done by Heilman and Gessel (1971), close to 30% of fertilizer N applied as

urea was found to be taken up by Douglas-fir trees. Jassal et al. (2008) concluded that fertilization of a 54-year-old Douglas-fir forest increased net ecosystem productivity (NEP) by 60%, from 326 to 535 g C m⁻² yr⁻¹ following fertilization. When accounting for changes to CH₄ and N₂O fluxes expressed in global warming potential (GWP) terms as CO₂ equivalents, fertilizer additions resulted in an additional uptake of 2.28 t CO₂ ha⁻¹ one year after fertilization.

Chen et al. (2011) concluded that urea-N fertilization increased NEP in a Douglas-fir forest by 83% after fertilization through increases in gross primary productivity (GPP) and reduced ecosystem respiration (R_e), largely through a reduction in soil respiration (R_s), where NEP = GPP - R_e. Clearly any opportunity to increase the low total uptake of applied urea-N (~30%) by the Douglas-fir trees could have financial benefits realized through further increased stand growth. Additionally this would increase C sequestration, reducing CO₂ concentrations in the atmosphere, helping to mitigate its contribution to climate change. Realizing this, British Columbia's Coastal Forest Action Plan offers fiscal incentives to increase productivity of second-growth coastal forests using fertilization to provide a potential benefit of reducing greenhouse gas (GHG) emissions through increased C sequestration while maintaining employment levels in the forest products sector (BCMFR, 2007).

Biochar, a C rich product resulting from pyrolysis of organic matter, has shown significant potential for use as a soil amendment that may increase tree growth, enhance the C sequestration potential of a fully managed forest cycle, and reduce nutrient loss after fertilization and harvesting while diversifying the forest economy (Clough and Condon, 2010; Jeffery et al., 2010; Lehman et al., 2006; Lehmann and Joseph, 2009; Thomas and Gale, 2015; IPCC, 2014). The properties of a particular biochar are largely determined by the feedstock and pyrolysis conditions (Sohi et al., 2010). The prevalence of aromatic structures containing few functional

groups enhances the resistance of biochar to decomposition in soils (Dai et al., 2005, Zimmerman, 2010). This is particularly true when the O:C ratio of the biochar is less than 0.2 (Spokas, 2010).

Compared to mineral soils, biochar has a lower particle density and larger surface area (Brewer et al., 2014). When added to soil, biochar alters the soil's physical structure, generally decreasing its bulk density (Major et al., 2010; Lim et al., 2016). This can serve to increase the exposure of chemically reactive surfaces to aqueous and gaseous exchange, and provide refugia for microbes (Lehmann et al., 2011).

The effect of biochar on dissolved organic carbon (DOC) is not well known, and could represent a significant loss of C when soil hydraulic conductivity is high. Major et al. (2009) used stable isotopes to demonstrate that biochar applied to a savanna Oxisol in Columbia resulted in increased biomass production and DOC leaching, but attributed enhanced DOC leaching to biochar-stimulated increases in below-ground net primary productivity rather than to leaching of biochar-derived DOC. In a soil column study without plants, Eykelbosh et al. (2015) found that biochar attenuated total DOC leached over the course of an experiment using filtercake-derived biochar on DOC and NO_3^- leaching from a vinasse-treated soil (5 % w/w). Hartley et al. (2016) determined that wood waste-derived biochar increased pore water DOC relative to controls in a sandy soil. Tang et al. (2016) showed that biochar increased dissolved organic matter and that DOC content and estimated aromaticity (SUVA_{254}) was dependent on the biochar feedstock.

In terms of N cycling, biochar could regulate ammonium-N (NH_4^+ -N) availability through increases in redox potential and CEC. The likely increase in CEC capacity over time resulting from biochar additions (Lehmann, 2007; Liang et al., 2006) and its subsequent

absorption of positively charged N based ions onto or into biochar amended soils could result in a reduction in dissolved N, leading to an initial decrease in plant N availability. However, as the biochar becomes saturated with positive ions, its ability to retain nutrients will decrease and an increased availability of N to plants over longer time periods could result. Specifically, NH_4^+ formation after urea-N fertilization and its subsequent adsorption onto the biochar could reduce the inorganic-N pool available for nitrifiers, and thus NO_3^- concentrations in leachate may be reduced.

It is important to note that results from biochar studies on N cycling have been contradicting. In a meta-analysis comparing 56 studies performed between 2010 and 2015, Nguyen et al. (2017) determined that biochar generally reduced soil inorganic nitrogen (SIN). They found that woody biochars reduce SIN less than other biochar types and that interaction between biochar and environmental factors, pyrolysis temperature and surface properties of biochar were the main factors affecting SIN. Some studies have reported increases in soil N mineralization and nitrification by as much as 269 % and 34 %, respectively in biochar mixtures with soil (Case et al., 2015). Singh et al. (2010) reported an increase in NO_3^- leaching from poultry manure derived biochar, as well as a decrease in NH_4^+ leaching from Eucalyptus and poultry-manure-derived biochar mixed with soil. Others have not detected any effect on NO_3^- leaching (Eykelbosh et al., 2015). Atanu and Zimmerman (2013) showed that for a range of biochar studied, $\text{NH}_4\text{-N}$ was generally the more abundant N form in leachates, with $\text{NO}_3\text{-N}$ also abundant in the biochar made from grass.

It is clear that applying biochar could have broad implications for DOC and total N (TN) in soil pore water and leachate. Complex interactions between applied biochar and biogeochemical cycles make it difficult to forecast the exact effects of biochar application at any

site, and so field-based studies are essential. Most work in this area has focused on either agricultural systems or on charcoal resulting from natural forest fires (Jeffreys et al., 2014; Thomas and Gale, 2015), as studies on the use of biochar as a silvicultural treatment are uncommon. Since field conditions in forest soils are typically highly spatially heterogeneous, controlled laboratory studies that investigate the dominant bulk soil contributing to components of the biogeochemical cycles can be highly informative.

Research Objectives

The objectives of this study were to investigate the effects of biochar application to a forest soil with and without N fertilization on soil pore water dissolved organic carbon (DOC) and total nitrogen (TN) in a Pacific Northwest Douglas-fir forest. Specifically, the research sought to determine the effects of differing biochar application rates on soil water DOC and TN concentrations, and to investigate differences in soil pore water quality using UV-Vis absorbance spectra. We hypothesized that biochar additions would (i) increase DOC in drainage water, (ii) decrease N in drainage water, with concentrations hypothesized to increase for larger biochar application rates and in response to fertilization additions.

The goal for the study was to determine whether biochar additions could reduce TN leaching losses without significantly contributing to DOC leaching. This information could assist in future efforts to maximize forest fertilization efficiency and improve carbon sequestration potential throughout the production cycle of these important forests.

4.2 Materials and methods

This chapter describes a study on water quality that is comprised of field and laboratory components that utilized the experimental plots described in Chapter 3 and the soil columns described in Chapter 2. Briefly, the field-based experiment was set up in previously unfertilized

area of the forest stand and consisted of sixteen 4 m x 4 m plots assigned in a randomized complete-block design with four blocks of the following four treatments: i) soil only (S; e.g. control), ii) 5 Mg ha⁻¹ biochar (BC), iii) 200 kg N ha⁻¹ urea fertilizer pellets (F), and iv) 5 Mg ha⁻¹ biochar with 200 kg N ha⁻¹ urea pellets (BC+F). Biochar was applied to plots assigned to BC and BC+F treatment in late February 2012. Urea-based fertilizer (N:P₂O₅:K₂O, 46:0:0) (Agrium Inc.) was applied in late March 2013 to plots assigned to F and BC+F treatments. These plots were utilized for water sampling in the present study, focusing on wet season conditions in the months following fertilizer application.

The laboratory component of this study (described fully in Chapter 2) consisted of mixtures of soil, biochar and fertilizer incubations in volumes of 200 cm³. Six experimental mixtures, consisting of combinations of soil, biochar (application rates of 0, 1% and 10% biochar on a mass basis) and fertilizer (application rates of 0 and 200 kg N ha⁻¹ equivalent of urea fertilizer, were replicated four times, yielding a total of 24 incubation units. The laboratory component of the present study utilized the incubations several months after the experiment described in Chapter 2. The present study thus followed several months of drying, with the wetting cycles described below simulating the rapid wet-up in late fall that follows the dry summer that is typical of the summer-fall weather pattern in the study region.

4.2.1 Field soil water sampling

Soil suction cup lysimeters (SCL) (model 1900, SoilMoisture Equipment Corp, Santa Barbara, CA) were installed at the 25-cm depth in each of the 16 field plots which were evenly allocated among the following treatments: biochar (BC, where soils were amended with 5 t ha⁻¹ Douglas-fir derived biochar), fertilized (F, where soils were amended with 200 kg ha⁻¹ urea-N fertilizer), biochar plus fertilizer (BC+F, where soils were amended with 5 t ha⁻¹ and 200 kg ha⁻¹

urea-N), and control plots (unamended soils, S). Full details on the experimental design and set-up of the plots is given in Chapter 3.

Each SCL consisted of a 25-cm long PVC tube with 4.8-cm outside diameter (OD) and a porous ceramic cup with a 2 bar (200 kPa) air-entry value. The PVC tube was capped with a Santoprene stopper assembly with compressible Neoprene access tubing (1/4" ID) and clamping ring (Z1900-200, SME, Santa Barbara). To install the SCL, a 7-cm diameter auger was used to bore the hole into which the SCL was placed. The space around the auger was then backfilled with a soil slurry (2-mm sieved) to well above the suction cup, capped with Bentonite, then backfilled with soil extracted during the excavation (SME, 2007).

The decreasing tension method (Titus, 1996) was used to collect mobile phase soil pore water using the SCL between site visits. Briefly, the SCL internal volume was evacuated using a Model 2005G2 Vacuum Hand Pump (1900, Soil Moisture Equipment Corp, Santa Barbara, CA) in the field. On the subsequent return visit, water samples were collected from the SCLs using the vacuum hand pump to create a negative pressure in the tubing thus transferring the sample from the SCL to a collection vessel. The SCL were evacuated monthly from November 2011 to March 2012 to their maximum vacuum (approximately -65 to -80 kPa) to allow the SCL body materials to reach chemical equilibrium with the surrounding soils. During this equilibration period, water samples were not analyzed. Sampling was conducted on two dates in spring 2012 following biochar application. Seven sampling campaigns were conducted in 2013, primarily in the spring following fertilizer application, but continuing as soil water contents and field logistical arrangements permitted.

For sampling, a negative pressure (-65 kPa) was applied to the internal volume and water accumulating in the volume between visits was collected for analysis. Samples were placed in brown PTFE containers (250 ml) and transported to the UBC Soil Water Atmosphere Laboratory (SWAL) for analysis. Before analysis, samples were refrigerated at 4 °C. Limited sample volumes were obtained over July through September due to dry soil conditions (< - 60 kPa) and a loss of hydraulic connectivity with the surrounding soil.

4.2.2 Laboratory Experimental Setup

Following the greenhouse gas experiment described in detail in Chapter 3, the incubations were left to air dry in the laboratory for three months, simulating the dry season. After this period, incubations were wet up with DDI water to saturation (visually confirmed by the appearance of surface pooling). This water was then allowed to freely drain until field capacity was reached. All incubations were then leached with 0.1 L de-ionized water (DDI) on Tuesdays and Wednesdays for two months, for a total 1.7 L of DDI water additions. After each 0.1 L wetting, the entire suite of 24 incubations was attached to a vacuum manifold and soil pore water was extracted at 30 kPa for 2 hrs. Between wettings, incubations were left uncovered at room temperature (23 °C) in the dark. Water samples were immediately analyzed with surplus water labeled and refrigerated in brown glass bottles at 4 °C in case repeated analysis was required.

4.2.3 Soil pore water analysis

All soil pore water samples from the field and laboratory were analyzed using a ultraviolet- visible (UV-VIS) spectrophotometer (Spectro::lyzer, s::can, Vienna, Austria). Laboratory samples were analyzed directly following collection, while field samples were analyzed on the spectrophotometer within 24 hours of collection. The instrument produces an

absorption spectrum from 200 to 750 nm that was used to calculate a range of spectral indices described below. The instrument applies a global calibration to the absorbance spectra to estimate DOC and NO_3^- , which were both useful for monitoring experimental progress. Since the calibration equation was developed for surface water rather than soil water these numbers were not used in analysis.

The spectral slope for the 275-295 nm wavelength band ($S_{275-295}$) was calculated after Helms et al., (2008). $S_{275-295}$ has been shown to increase with decreasing molecular weight of DOM. Specific UV absorbance at 254 nm (SUVA_{254}) has been used as an indicator of aromaticity. SUVA_{254} was calculated by dividing sample absorbance at 254 nm (m^{-1}) by the DOC concentration (mg L^{-1}) (Weishaar et al., 2003). Increasing SUVA_{254} indicates increasing aromaticity of DOM.

Following this analysis, samples were filtered through 0.7 μm glass fiber filters (Whatman Ltd. Kent, UK) to remove suspended solids and refrigerated at 4 °C in brown glass bottles until further analysis was performed.

The soil pore water dissolved organic carbon (DOC) and total nitrogen (TN) concentrations were analyzed on a TOC-Vcsh Total Carbon Analyzer (Shimadzu Corp, Japan) with an inline TNM-1 (Shimadzu Corp, Japan) system connected to a ASI-V autosampler (Shimadzu Corp, Japan).

Prior to sample injection, the autosampler performed sample acidification (7.5 μl 2N HCL) and sparging (ultra-zero compressed air) to remove any inorganic carbon (IC), allowing quantification of DOC as Non-Purgable Organic Carbon (NPOC), hereafter referred to as DOC_{SCL} when referring to SCL field samples and DOC_{lab} for laboratory incubation soil pore water samples. After sample injection (50 μl) into the system column (platinum beads), and

catalytic oxidation via dry combustion at 720 °C, the resulting CO₂ gas was picked up in the carrier gas stream (ultra-zero compressed air carrier gas) and passed through a highly sensitive non-dispersive infrared (NDIR) detector for measurement of CO₂ which was converted to DOC via a standards-based calibration curve.

Following the NDIR, the gas stream was carried to the TNM-1 system where a chemiluminescence detector determines TN in the sample, hereafter referred to as TN_{SCL} when referring to SCL field samples and TN_{lab} for laboratory incubation soil pore water samples. This combined system (TOC-vcsh + TNM-1) was configured to carry out 5 injections to achieve a within-sample coefficient of variation of 2%. Calibrations for all methods were performed after periodic maintenance and distilled DDI and 5 mg L⁻¹ standards were loaded with each sample run to determine the system detection threshold and to monitor calibration changes.

A Mettler Toledo benchtop meter fitted with pH and electrical conductivity (EC) probes was used to measure soil pore water pH and EC after transferring samples into 40 mL vials for analysis of DOC and TN. Hereafter pH and EC measurements for SCL field samples and laboratory incubation soil pore water samples are referred to as pH_{SCL} and EC_{SCL}, and pH_{lab} and EC_{lab}, respectively.

Following the laboratory flushing experiment soil incubations were destructively sampled and analysed for total organic carbon (TOC) using the loss on combustion technique and extractable NH₄⁺ and NO₃⁻ after KCL extraction using method version EE-SOP# A.04.01.

4.2.4 Soil moisture characterization

Field sensors

At the field site, additional instrumentation installed at 15-cm depth was used to monitor soil water conditions in twelve of the 16 plots (three replicates for each of the four treatments).

This instrumentation consisted of sensor clusters to measure volumetric water content (θ_{15}), bulk electrical conductivity (EC_{15}), and soil temperature (T_{15}) (model GS3, Decagon Devices Inc. Pullman, WA), and soil water matric potential (Ψ_{15} , model MPS-2 sensors, Decagon Devices Inc.). Signals were measured using a CR1000 data logger (Campbell Scientific Inc, Logan, UT) powered by a 12-V-DC 70-amp-hour lead-acid battery. Measurements were made at 5-min intervals and average output tabulated every 30 min. Furthermore, on each sample date a handheld GS3 sensor was used to measure surface volumetric water content (θ_s), bulk electrical conductivity (EC_s), and soil temperature (T_s).

4.2.5 Statistical analysis

4.2.5.1 Field experiment

To determine if there was any effect of biochar application on the EC_{SCL} , pH_{SCL} , DOC_{SCL} and TN_{SCL} in relation to fertilizer application, a two way ANOVA was first used to test the effect of location and time, followed by a one-way ANOVA to test treatment differences during specific times periods. Data were log-normalized prior to analysis and Tukey-adjusted differences of least square means (HSD) were used to compare treatments when significant differences were detected in the one-way ANOVA. Linear regression was used to investigate the relationship between DOC_{SCL} and TN_{SCL} for all data and between treatments, with the slope of significant relationships being used as an indicator of soil pore water C/N.

4.2.5.2 Laboratory experiment

To determine if there was any effect of biochar application on the EC_{lab} , pH_{lab} , DOC_{lab} , and TN_{lab} and in relation to fertilizer application, a one-way ANOVA was first used to test the effect of treatment on the first flushing date available, followed by a one-way ANOVA to test treatment differences during the period after signals had stabilized. When there was indication of non-

normal distributions of residuals during ANOVA, data were log-normalized prior to further analysis. Tukey-adjusted differences of least square means (HSD) were used to compare treatments when significant differences were detected in the one-way ANOVA. Linear regression was used to investigate relationships between DOC_{LAB} and TN_{LAB} for all data and between treatments, with the slope of significant relationships being used as an indicator of soil pore water C/N. Spectral indices ($S_{275-295}$ and SUVA_{254}) measured in the laboratory experiment were tested for treatment effects using a one-way analysis of variance.

4.3 Results

4.3.1 Field experiment

4.3.1.1 Soil climate

Cumulative precipitation for 2012 from January 1 up to the first day of sampling (date here) was 593 mm, equivalent to >40 % of the 1434 mm total for 2012. Total precipitation for 2013, however was only 840 mm, which was well distributed into the summer, keeping soil conditions moist through to the end of June (Figure 15). Following fertilization, there was an unexpectedly low amount of precipitation. During 2013, the maximum θ_{15} mean (\pm SD) measured was 36 (\pm 0.7)% and θ_{15} was above field capacity (21%, Appendix 1) 90% of the time (not shown) during 2013. Sampling of SCL always occurred when measured Ψ_{15} exceeded -15 kPa, which occurred 65% of the time in 2013.

The soil required more than 10 mm of precipitation in a daily rainfall event or cumulative over a period of days to replenish soil water conditions close the maximum measured at the site ($\theta_{15} \sim 36$ %). In figure 15 it can be seen that over the 16 days after fertilization (28 March 2013 - 11 April 2013), only 25 mm was recorded. Evidence of the fertilizer application was not detected in surface EC measurements until 9-days after fertilization, as indicated by significant increase in

measured surface EC for F and BC (Figure 15 and 16). Data shows that between 03 May 2013 and 31 May 2013 there was a brief period of decreased θ_{15} and Ψ_{15} , likely resulting from increasing evapotranspiration due to increasing temperatures (Figure 15), and clear sky conditions with increasing photosynthetic photon flux leading into the summer (not shown). Soil temperatures (T_{15}) followed an increasing trend throughout the sample period from a mean (\pm SD) value of 4.1 (0.2) °C on 26 March 2013 to a maximum of mean (\pm SD) of 13.5 (0.3) °C on 11 July 2013.

4.3.1.2 Field ancillary measurements of soil pore water quality

The mean (\pm 1 SE) soil pore water (EC_s) was highest for BC+F, 22.20 (\pm 1.80) μ S cm^{-1} (Table 4). There was a significant effect from SCL location ($F_{(15,344)} = 9.61$, $p < 0.001$) and date ($F_{(23,344)} = 15.55$, $p < 0.001$), as well as treatment ($F_{(3,222)} = 17.20$, $p < 0.001$). The order of increasing EC_s by treatment was S < BC < BC+F < F, with Tukey HSD analysis confirming the significant effect of the fertilization on both fertilized treatments (F & BC+F) compared to unfertilized treatments (S & BC).

The mean (\pm 1 SE) soil pore water (EC_{SCL}) was highest for BC+F, 91.44 (\pm 15.31) μ S cm^{-1} (Table 4). The soil extract EC was independently measured to be higher than the soil + biochar (1% w/w) soil extract EC at 46 (\pm 20) and 31 (\pm 15) μ S cm^{-1} , respectively. There was a highly significant effect from SCL location ($F_{(15, 123)} = 101.91$, $p < 0.001$), though data was inconsistent with assumptions needed for ANOVA and was log-normalized for further analysis. A closer look at the individual EC_{SCL} measurements for each SCL revealed that one BC+F plot had consistently higher values ($EC_{SCL} > 100$ μ S cm^{-1}) than all others with all measured ($EC_{SCL} < 75$ μ S cm^{-1}). The EC_{SCL} responded significantly to treatment ($F_{(3,135)} = 13.81$, $p < 0.01$). The order of increasing EC_{SCL} by treatment was BC < F < S < BC+F with HSD analysis detecting a

significant difference between BC and S, and, BC+F and BC suggesting that factors other than fertilization were determining the difference in contrast to results from EC_s.

The mean (± 1 SE) SCL soil pore water pH (pH_{SCL}) was lowest for BC, 6.2 (± 0.10) (Table 4). There was a highly significant effect from SCL location ($F_{(15,123)} = 28.23$, $p < 0.001$) though data was inconsistent with assumptions needed for ANOVA and log normalized for analysis hereafter. A closer look at the individual pH_{SCL} measurements for each SCL revealed that one BC plot (SCL 10) had consistently lower pH_{SCL} values (pH < 5.5) than all others (pH > 6). The order of increasing pH_{SCL} by treatment was S $<$ BC+F $<$ F $<$ BC, with no significant difference detected between treatments or sample date and no interactions between the two. The pH of soil at the 25-cm depth was 5.6 (± 0.05), which was lower than the pH of the biochar itself (6.86 ± 0.01). While it might have been expected that biochar would increase the bulk soil pH, the biochar was surface applied, and any impact on soil pH was difficult to discern in this study.

4.3.1.3 Field soil pore water DOC and TN

Data available for 2012 shows that BC generally had higher DOC_{SCL} concentrations in soil pore water (Figure 17), although these differences were not significant and the concentrations were similar to those measured in a near-by (500 m away) headwater catchment stream during peak flows (Jollymore et al., 2012) when soil pore water could be contributing significantly to surface water DOC fluxes. For 2013, the highest treatment mean (± 1 SE) soil pore water DOC_{SCL} was detected for BC on 20 June 2013, 8.5 (± 3.4) mg L⁻¹. There was a highly significant effect from SCL location ($F_{(15,188)} = 51.06$, $p < 0.01$) though data was inconsistent with assumptions needed for ANOVA and log normalized for analysis hereafter. A closer look at the individual DOC_{SCL} measurements for each SCL revealed that four of the SCLs (1,10,11 and 14), one in each of BC and F, and two S, had consistently higher DOC_{SCL} values (DOC_{SCL} > 10

mg L⁻¹) than all others (DOC_{SCL} < 5 mg L⁻¹) (Figure 17). The order of increasing DOC_{SCL} by treatment in 2013 was BC+F < S < F < BC, with no significant difference detected between treatments and significant differences detected over time ($F_{(3,178)} = 2.19, p < 0.04$).

There was no noticeable difference in treatment soil pore water TN_{SCL}, and values were low in this nitrogen-limited system in 2012 (Figure 18). Following fertilizer application in 2013, there was a highly significant effect from SCL location ($F_{(15,191)} = 24.83, p < 0.01$) on TN_{SCL} response, though data was inconsistent with assumptions needed for ANOVA and log normalized for statistical analysis hereafter. The highest mean (± 1 SE) soil pore water TN measured 0.24 (± 0.11) mg L⁻¹ for F on the 11 April 2013, 16 days after fertilization. A closer look at the individual TN_{SCL} measurements for each SCL revealed that three of the same SCL (1,10 and 11) identified to have above average for DOC_{SCL}, also had consistently higher TN_{SCL} values (TN_{SCL} > 0.2 mg L⁻¹) than all others (TN_{SCL} < 0.2 mg L⁻¹). On four of the seven sample days following fertilization, F plots recorded the highest TN_{SCL} values, only exceeded by S on two occasions, and exceeded by BC+F on one of the remaining sample dates (Figure 18). The overall order of increasing TN_{SCL} by treatment was BC < BC+F < F < S, with no significant difference detected between treatments or sample date. Unlike measurements at the surface (EC_S), there was surprisingly no significant response from fertilization detected at 25cm via the TN_{SCL} signal.

Linear regression analysis revealed a weak but significant correlation between DOC_{SCL} and TN_{SCL} data for the entire dataset ($R^2 = 0.54$; Table 5). Analyzing the data by individual treatment revealed much stronger and significant correlations for S ($R^2 = 0.86$), BC ($R^2 = 0.79$) and F ($R^2 = 0.98$) than for BC+F. By comparing the TN values to DOC in this way the slope of the linear regression can be used as a proxy for the C/N of the soil pore water, and it can be seen

that BC had a much higher C/N ratio than all other treatments, with BC+F having the lowest (Figure 19).

4.3.1.4 Field soil pore water spectral indices

The spectral indices $S_{275-295}$, S_R , and $SUVA_{254}$ were significantly different between SCL and over time ($p < 0.01$). A lower value for $S_{275-295}$ generally indicates higher molecular weights (MW) in DOM in freshwater samples (Helms et al. 2008). The $S_{275-295}$ measured for individual SCL show that SCL identified earlier to have high DOC_{SCL} and TN_{SCL} also tend to have low $S_{275-295}$ indicating that those samples had higher MW contributions to their DOM. After log normalization of the $SUVA_{254}$ data, a one-way ANOVA determined significant differences between treatments ($F_{(3,126)} = 3.01, p = 0.03$). The proceeding HSD analysis determined that $S > BC+F$ ($p = 0.07$). As $SUVA_{254}$ increases, the percentage of aromaticity increases (Chin et al. 1994; Fuentes et al. 2006) and this would suggest that there was a greater contribution of humic substances in S.

In summary there was no significant effect of biochar application on bulk DOC and TN in soil pore water measured during the first or second year after biochar application, when soil moisture conditions were favorable for downward percolation at the field site, although there were indications of differences in the composition of DOC as evidenced by the spectral indices. No effect was detected from fertilization in the second year on either DOC or TN at the 25-cm depth. The influence of fertilization was detected in electrical conductivity measurements at the surface close to the time of fertilization in plots with and without biochar application, suggesting that any fertilization responses diminished with increasing soil depth. Highly variable DOC/TN slope estimates between the treatments (13.02 to 114.86) were heavily influenced by outlying data identified to have increasing molecular weights using spectral indices.

4.3.2 Laboratory experiment

4.3.2.1 Laboratory ancillary soil pore water quality measurements

The EC_{lab} measurements remained above $25 \mu S cm^{-1}$ for all treatments throughout the flushing experiment, and differences can be noticed more clearly at the earlier stages of the experiment prior to the cumulative addition of 1 L of leachate volume (LV) (Figure 21). The mean (± 1 SE) EC values throughout the experiment were largest for BC1%+F and S+F starting at $489 (\pm 58.92) \mu S cm^{-1}$ and $481.5 (\pm 36.81) \mu S cm^{-1}$ respectively, with S and BC1% being approximately 35% smaller and BC10%+F and BC10%, being less than 25% of the magnitude of S and BC1%. During the period of flushing from 0 to 1 L, there were significant differences between treatments ($F_{(5,30)} = 30.69, p < 0.01$) and over time ($F_{(6,30)} = 25.68, p < 0.01$). The significant differences as determined by HSD analysis using the first available sampling were S+F > BC10%, S+F > BC10%+F, BC1%+F > BC10%. After 1.2 L of LV, all treatments were in the range of 50-75 $\mu S cm^{-1}$ and were not statistically different from each other.

The pH measurements were relatively stable throughout the experiment (Figure 21), and maintained significant differences between treatments throughout ($F_{(5,36)} = 3.843, p < 0.01$). HSD analysis detected significant differences between BC10% and all other treatments and BC10%+F and all other treatments ($p < 0.01$). The pH of the leachate was significantly higher (~10%) with high rates of biochar applications (Table 6).

4.3.2.2 Laboratory soil pore water DOC and TN

From the first flush, DOC_{lab} measurements exhibited significant differences between treatments ($F_{(5,17)} = 68.19, p < 0.01$), with all treatments exceeding $10 mg L^{-1}$ (Figure 22). The HSD analysis confirmed that BC10% and BC10+F were statistically similar and both were statistically greater ($p < 0.01$) than all other treatments (BC1%, BC1%+F, S, S+F). As was the

case for EC_{lab} , these differences diminished as more volume of water was flushed through, eventually reaching a rough equilibrium after 1 L. Regardless of this diminishing difference, treatments BC10% and BC10%+F remained statistically different from all other treatments ($F_{(5,34)} = 21.73, p < 0.01$) after more than 1L had been flushed through the incubations (Figure 23, Table 6). The cumulative loss of DOC from was largest for 10% mixtures. To investigate if the increase in DOC leaching detected at the higher rate biochar application was significant relative to the amount of biochar added (20 g x 78% C = 15 g C) we subtracted the mean cumulative loss of DOC of the control treatments (106 mg L^{-1}) from the 10% mixtures (180 mg L^{-1}) and multiplied this by the total amount of water leached (1.7 L). In this way we calculated that the total loss of DOC was <1% of the total amount of biochar-C added.

From the first flush, TN_{lab} measurements exhibited clear and significant differences between treatments ($F_{(5,16)} = 28.39, p < 0.01$), with all treatments, excluding BC10% and BC10%+F, exceeding 10 mg L^{-1} (Figure 22). The HSD analysis confirmed that BC10% and BC10%+F were statistically similar and, in contrast to DOC_{lab} , both were statistically smaller ($p < 0.01$) than all other treatments (BC1%, BC1%+F, S, S+F). Similar to EC_{lab} , these differences diminished as more water was flushed through, eventually reaching a rough equilibrium after 1 L. There was strong positive correlation between TN_{lab} and EC_{lab} ($R^2 = 0.96, F_{(1,225)} = 5781, p < 0.01$). Regardless of the diminishing difference between treatments, BC10% and BC10%+F remained statistically different from all other treatments ($F_{(5,36)} = 30.4, p < 0.01$) after more than 1L had been flushed through the incubations (Figure 23, Table 5).

Linear regression revealed a very weak but significant correlation between DOC_{SCL} and TN_{SCL} data ($R^2 = 0.04$, Table 7). Analyzing the data by treatment revealed strong and significant correlations with the addition of biochar, and more so for biochar in combination with fertilizer

(Table 7). It can be seen that BC10% with and without fertilizer had a much higher DOC/TN ratio than all other treatments, with the treatments listed in decreasing order as follows: BC10% > BC10%+F > BC1% > BC1%+F > S > S+F (Figure 23, Table 7). The application of fertilizer decreased the DOC/TNN slopes by as much as 20% for biochar treatments and less than 5% for S+F.

4.3.2.3 Laboratory soil pore water spectral indices

Values for $S_{275-295}$ ranged between 0.11 and 0.14 and were all below values measured from a biochar leaching experiment described by Jamieson et al., (2014) and below surface water measurements made by Helms et al., (2008). The HSD analysis confirmed that BC10% and BC10+F were statistically similar and both were statistically smaller ($p < 0.01$) than all other treatments (BC1%, BC1%+F, S, S+F). Over the course of the experiment, the $S_{275-295}$ values decreased in all treatments (Figure 24). Linear regression indicated that the slopes were significant and the correlation coefficients higher for increasing rates of biochar (Table 8). The $SUVA_{254}$ values ranged between mean (± 1 SE) of 0.54 (± 0.2) for BC10% and 1.72 (± 0.08) for BC1%, and were well below the range of values measured by Helms et al. (2008) and similar in range to those measured from the biochar leaching experiment described in Jamieson et al., (2014). There were significant differences detected between treatments ($F_{(5,30)} = 17.67$, $p < 0.01$), and the HSD analysis confirmed that BC10% and BC10%+F were statistically similar, and like $S_{275-295}$, both were statistically smaller ($p < 0.01$) than all other treatments (BC1%, BC1%+F, S, S+F).

4.3.2.4 Laboratory soil TOC, NO_3^- and NH_4^+ post experiment

At the end of the experiment, at which point the incubations had been subjected to several wetting and drying cycles and 1.7 L of water had been flushed through them, destructive

sampling and analysis indicated some interesting differences between treatments for TOC, extractable NH_4^+ , extractable NO_3^- and the ratio of $\text{NH}_4^+/\text{NO}_3^-$ (Figure 25). Significant differences were detected between treatments for TOC ($F_{(5,12)} = 33.83, p < 0.01$), NH_4^+ ($F_{(5,12)} = 10.10, p < 0.01$), NO_3^- ($F_{(5,12)} = 96.88, p < 0.01$) and $\text{NH}_4^+/\text{NO}_3^-$ ($F_{(5,12)} = 11.94, p < 0.01$) measurements. For TOC, Tukey HSD analysis confirmed that BC10% and BC10%+F were significantly greater than all other treatments, equivalent to about 46% more TOC (Table 6). For extractable NH_4^+ the HSD analysis confirmed that S+F had statistically higher amounts remaining than S and BC1% ($p < 0.02$). The same analysis also concluded that BC1%+F had statistically higher amounts of NH_4^+ remaining than S and BC1% ($p < 0.02$). Furthermore this analysis concluded that BC10%+F had statistically higher amounts remaining than S, BC1% ($p < 0.03$). For extractable NO_3^- HSD analysis concluded that BC10% had statistically ($p < 0.01$) higher amounts remaining than BC1% and S, and that BC1% also had statistically ($p < 0.01$) higher amounts remaining than S. Furthermore, this analysis concluded that BC10%+F had statistically ($p < 0.01$) higher amounts remaining than all other treatments. These results suggest that with fertilization biochar retained more extractable NH_4^+ . Even without fertilization, BC can help retain extractable NO_3^- during high flushing events and increasing rates of biochar increases retention of extractable NO_3^- , which could be directly related to surface charge density on the biochar and an affinity for negatively charged ions.

In summary, DOC leaching was greatly increased at the high rates of biochar application (10%), though not the low application rate of (1%), both with and without fertilization. Both EC and TN leaching decreased when biochar application rates were increased to 10% for both fertilized and unfertilized treatments. Also important for plant productivity is the increase in pH that was only found at higher rates of biochar application independent of fertilization status.

Using DOC/TN to infer differences in C/N ratios showed that the high biochar application rate increased the C/N ratio significantly. Fertilization was found to reduce this by up to 20% when applied to biochar treatments. The $S_{275-295}$ spectral index decreased as more water was flushed through the incubations, suggesting contributions of DOM with increasing molecular weight as the experiment continued.

4.4 Discussion

The results outlined in this chapter indicate that low rates of surface applied biochar did not impact soil pore water DOC at the field site during freely draining soil moisture conditions. Other field studies have detected low rates of biochar leaching as DOC. Major et al., (2010) found that in total, less than 1% of applied biochar was detected in percolating water over two growing seasons in a highly weathered tropical soil. Other studies have found that the magnitude of reported early flushes of bioavailable DOC leached from biochar soil mixtures is dependent on feedstock, production technique and soil temperature as well as soil type (Lin et al., 2012). In our study considering field and laboratory biochar application to the same soil, we found that the homogenized soil with no root activity showed increased DOC leaching at only the 10% application rate. Our field study was unable to detect differences related to a biochar application rate similar to that of the 1% application rate in the laboratory study. It is likely that a contribution to DOC from field-applied biochar was undetected; the rapidly flushed DOC in the laboratory experiment indicates that it could have moved quickly through the sample. It has been shown that biochar can promote soil organic carbon and that this was stored in the soil and not mineralized to CO₂ (Jaing et al., 2016), which could make it available for rapid leaching. The difficulty of obtaining field samples of mobile phase soil water from a remote site using suction cup lysimeters resulted in a lower sampling frequency than that of the laboratory study. This

difference in sampling frequency, plus the active root processes in the mature forest plots compared to root-free laboratory soil, makes the comparison between field and laboratory challenging.

The cumulative amount of DOC leached at the high rate application (10% w/w) in the laboratory study was much larger than for both the low (1% w/w) biochar application and the control treatments, and was similar for both fertilized and unfertilized applications. This suggests that the biochar application rate is the primary control on early flush DOC leaching here. Hartley et al. (2016) showed that DOC in soil pore water samples in a sandy agricultural soil was increased after application of biochar made from forest clearance operations. Liu et al. (2016) determined that increased DOC leaching measured after biochar applications to sand was affected by both the rate of application and particle size. Jaing et al. (2016) showed that biochar additions were less of an influence on SOC mineralization than N additions. In a batch experiment mixing two different biochars into an Acrisol at 10% w/w increased the soil pH from 4.9 to 8.7 and caused a 15-fold increase in DOC loss (Smebye et al., 2016). Liu et al. (2016) estimated an equivalent loss of 0.06 – 0.18 % by weight of biochar added C as DOC and as with this study (<1%) concluded that biochar-derived C would contribute little to surface and ground water C.

In the present laboratory study using the ratio of $\text{NH}_4^+/\text{NO}_3^-$, the HSD analysis concluded that S+F had significantly higher proportion of the N species left as NH_4^+ than NO_3^- , which suggests that biochar application increased nitrification rates in this study, which is in agreement with other findings (Case et al., 2015). Overall, however, we found that the higher rate of biochar application increased total N retention as NH_4^+ and NO_3^- in this soil, which could be due to increased physical entrapment in biochar pores (Jassal et al., 2015), and contradicts the

general finding in a meta-analysis by Nguyen et al. (2017), who found that biochar generally decreased SIN. Mukherjee and Zimmerman (2013) found that $\text{NH}_4\text{-N}$ was usually the more abundant inorganic N in leachate from most biochars they studied, which is in agreement with the increased retention of $\text{NO}_3\text{-N}$ relative to $\text{NH}_4\text{-N}$ retained in this study. It is likely that organic N contributed significantly to the total N lost in this study (Zimmerman, 2013) and that availability of any retained $\text{NO}_3\text{-N}$ would not be high (Lan et al., 2017).

We also found very strong correlations between DOC and TN in both the laboratory and field components, which suggests that to reduce the magnitude of N leaching relative to DOC leaching, a higher rate biochar application could be favorable. In our laboratory study the DOC and TN in leachate decreased quickly with successive DDI flushes. Lan et al. (2017) found DOC derived from biochar in a mixture with a ferrosol soil increased the DOC/ $\text{NO}_3\text{-}$ ratio early in their incubation experiment and this decreased quickly. In our field study, there would have been enough precipitation after ~11 days following fertilization (after considering interception from the canopy) to move the surface-applied fertilizer in solution past the depth of the SCL during sampling. However the effect of fertilization was only detected in surface electrical conductivity measurements, supporting findings that very little amounts of nitrogen species are lost through leaching in these podzol forest soils (Chapelle et al., 1991).

In the field study, the $S_{275-295}$ values were lower than those of water samples collected directly from biochar leachates by Jamieson et al. (2014), suggesting that the addition of biochar would tend to decrease the DOM MW (Eykelbosh et al. 2015). This effect was not clear in this study with BC having the lowest $S_{275-295}$ and BC+F the highest values (Table 4), which might suggest that the effect of the biochar application was masked by other soil processes at this depth in the field. The range of values for $S_{275-295}$ (Table 4) were comparable to “dark” freshwater

samples described in Helms et al. (2008) and to 23 freshwater samples collected from sites influenced by agriculture and vegetation as described in Chen et al. (2011). Furthermore, Chen et al., (2011) measured $S_{275-295}$ values in the range of 0.009-0.0130 from three humic acids over a pH range of 2-11, suggesting that the humic acid content in the forest soils could be masking the influence of biochar on the $S_{275-295}$ signal.

The $SUVA_{254}$ values measured from SCL were similar to all Helms et al. (2008) tidally influenced samples in Chesapeake Bay water. Contrastingly, the $SUVA_{254}$ from our field samples were higher than those from free-draining leachate collected from root-free column study using a mineral soil collected from a Brazilian sugar cane field and mixed with filtercake biochar (Eykelbosh et al., 2015). In our laboratory study, $SUVA_{254}$ values were well below the range of values measured by Helms et al. (2008) and similar in range to those measured from the biochar leaching experiment described in Jamieson et al., (2014).

Here, we compared differences between treatments for both field and laboratory findings since all treatments used the same soil. In the field, highly variable DOC/TN slope estimates between the treatments (13.02 to 114.86) were heavily influenced by apparent outliers, which were identified to have optical indices values indicative of increasing molecular weights. This supports the idea that treatment effects were not observed due to other stronger influences in soil humification processes. The $SUVA_{254}$ values in the laboratory component were lower for higher biochar application rates, without any influence from fertilization, in line with results from Eykelbosch et al. (2015), which showed that biochar preferentially retained high-molecular weight, more humified DOC species. Our results suggest that labile components contributed significantly to leachate DOC. This can be inferred by observing that there was no slope change

in the $SUVA_{254}$ over time in the laboratory, while $S_{275-294}$ decreased with increasing flushing volume.

4.5 Conclusions

These results suggest that the high and low rate of Douglas-fir derived biochar application to this forest soil could be beneficial for both increasing C-sequestration and N-retention in this context, despite higher rates of DOC leaching at the high rate of biochar application in the laboratory. The increased retention of TN as both NH_4^+ -N and NO_3^- -N in 10% biochar applications with and without fertilization suggests there could be an added benefit to stand productivity through high rates of biochar application. Stronger correlations between DOC and TN were observed in the laboratory leaching experiment for the higher rate of biochar addition compared to lower rate of biochar addition. Based on optical characteristics of leachate in the laboratory experiment, it appears that labile components contributed significantly to leachate DOC. Furthermore, that there was no significant effect of biochar application on DOC and TN leaching measured in the field after biochar application provides further evidence that there is a net carbon sequestration and N retention benefit at the 5 t ha^{-1} field application rate.

4.6 Tables

Table 4. Field EC_s and EC_{SCL}, pH_{SCL} and spectral indices. All values given are mean (± 1 standard error) of all available data in 2013

| Variable | Treatment | | | |
|--|------------------------|------------------------|------------------------|------------------------|
| | S | BC | F | BC+F |
| EC _s ($\mu\text{S cm}^{-1}$) | 11.65 (0.60) <i>a</i> | 16.08 (0.98) <i>a</i> | 22.66 (2.23) <i>b</i> | 22.20 (1.80) <i>b</i> |
| EC _{SCL} ($\mu\text{S cm}^{-1}$) | 38 (2.5) <i>a</i> | 27.42 (1.65) <i>b</i> | 33.45 (1.98) <i>a</i> | 91.44 (15.31) <i>a</i> |
| pH _{SCL} | 6.5 (0.04) <i>a</i> | 6.2 (0.10) <i>a</i> | 6.6 (0.03) <i>a</i> | 6.5 (0.03) <i>a</i> |
| DOC _{SCL} (mg L^{-1}) | 4.47 (0.57) <i>a</i> | 6.62 (1.19) <i>a</i> | 5.29 (0.86) <i>a</i> | 2.99 (0.30) <i>a</i> |
| TN _{SCL} (mg L^{-1}) | 0.18 (0.01) <i>a</i> | 0.15 (0.01) <i>a</i> | 0.17 (0.02) <i>a</i> | 0.16 (0.01) <i>a</i> |
| S ₂₇₅₋₂₉₅ | 0.015 (0.000) <i>a</i> | 0.012 (0.001) <i>a</i> | 0.014 (0.000) <i>a</i> | 0.016 (0.000) <i>a</i> |
| SUVA ₂₅₄ ($\text{L m}^{-1} \text{mg}^{-1}$) | 5.73 (0.55) <i>a</i> | 5.53 (0.58) <i>ab</i> | 4.43 (0.35) <i>ab</i> | 3.86 (0.38) <i>b</i> |

Data points with differing italic lowercase letters are significantly different from each other at $p < 0.05$

Table 5. DOC_{SCL} vs TN_{SCL} linear regression analysis output

| Treatment | df | <i>F</i> | <i>p</i> | <i>R</i> ² | Equation |
|-----------|---------|----------|----------|-----------------------|-----------------------|
| All | (1,130) | 145.70 | <0.01 | 0.53 | $y = 47.64x - 2.94$ |
| S | (1,28) | 180.89 | <0.01 | 0.86 | $y = 36.69x - 2.21$ |
| BC | (1,34) | 131.31 | <0.01 | 0.31 | $y = 114.86x - 10.43$ |
| F | (1,34) | 2296.37 | <0.01 | 0.79 | $y = 55.89x - 4.43$ |
| BC+F | (1,28) | 12.34 | <0.01 | 0.99 | $y = 13.02x + 1.09$ |

Table 6. Laboratory EC, pH and spectral indices. All values given are mean (± 1 standard error) of all data collected after more than 1 L of DDI had been flushed through each incubation.

| Variable | Treatment | | | | | |
|---|----------------------------|----------------------------|----------------------------|----------------------------|----------------------------|----------------------------|
| | S | BC1% | BC10% | S+F | BC1%+F | BC10%+F |
| EC _{lab} ($\mu\text{S cm}^{-1}$) | 64.17 (8.33) <i>abc</i> | 69.33 (8.22) <i>abc</i> | 53.5 (2.57) <i>a</i> | 56.5 (4.82) <i>b</i> | 59.67 (2.32) <i>bc</i> | 51.33 (3.4) <i>ac</i> |
| pH _{lab} | 6.35(0.06) <i>a</i> | 6.15 (0.12) <i>a</i> | 6.93 (0.05) <i>b</i> | 6.33 (0.09) <i>a</i> | 6.2 (0.1) <i>a</i> | 6.87 (0.06) <i>b</i> |
| DOC _{lab} (mg L ⁻¹) | 22.1 (1.08) <i>a</i> | 19.47 (1.40) <i>a</i> | 67.31 (10.35) <i>b</i> | 18.30 (3.29) <i>a</i> | 24.14 (2.57) <i>a</i> | 75.32 (4.22) <i>b</i> |
| TN _{lab} (mg L ⁻¹) | 2.76 (0.45) <i>a</i> | 3.64 (0.36) <i>a</i> | 0.82 (0.07) <i>b</i> | 3.11 (0.51) <i>a</i> | 3.79 (0.33) <i>a</i> | 0.99 (0.07) <i>b</i> |
| S ₂₇₅₋₂₉₅ | 0.0133 (0.002) <i>a</i> | 0.0134 (0.002) <i>a</i> | 0.0116 (0.001) <i>b</i> | 0.0138 (0.001) <i>a</i> | 0.0136 (0.001) <i>a</i> | 0.0117 (0.001) <i>b</i> |
| SUVA ₂₅₄ (L m ⁻¹ mg ⁻¹) | 1.7 (0.09) <i>a</i> | 1.72 (0.08) <i>a</i> | 0.54 (0.02) <i>b</i> | 1.62 (0.08) <i>a</i> | 1.54 (0.08) <i>a</i> | 0.55 (0.02) <i>b</i> |
| TOC (mg g ⁻¹) | 0.09 (0.00) <i>a</i> | 0.11 (0.00) <i>a</i> | 0.16 (0.00) <i>b</i> | 0.10 (0.01) <i>a</i> | 0.11 (0.00) <i>a</i> | 0.16 (0.01) <i>b</i> |
| NH ₄ ⁺ (mg g ⁻¹) | 0 (0.00) <i>a</i> | 0 (0.00) <i>a</i> | 0.02 (0.01) <i>a</i> | 0.05 (0.01) <i>b</i> | 0.07 (0.02) <i>b</i> | 0.05 (0.01) <i>b</i> |
| NO ₃ ⁻ (mg g ⁻¹) | 0.13 (0.01) <i>a</i> | 0.39 (0.05) <i>b</i> | 0.82 (0.04) <i>c</i> | 0.23 (0.08) <i>abc</i> | 0.44 (0.05) <i>abc</i> | 1.39 (0.01) <i>d</i> |

Data points with differing italic lowercase letters are significantly different from each other at $p < 0.05$

Table 7. DOC_{LAB} vs TN_{LAB} linear regression analysis output

| Treatment | df | F | p | R ² | Equation |
|-----------|-------|--------|--------|----------------|---------------------|
| All | 1,273 | 13.67 | < 0.01 | 0.04 | y = -0.194x + 27.67 |
| S | 1,44 | 12.94 | < 0.01 | 0.23 | y = 0.156x + 14.171 |
| BC1% | 1,45 | 31.49 | < 0.01 | 0.41 | y = 0.260x + 12.173 |
| BC10% | 1,42 | 786.47 | < 0.01 | 0.95 | y = 20.52x + 8.285 |
| S+F | 1,45 | 39.43 | < 0.01 | 0.47 | y = 0.162x + 11.82 |
| BC1%+F | 1,44 | 66.13 | < 0.01 | 0.60 | y = 0.213x + 13.71 |
| BC10%+F | 1,43 | 193.54 | < 0.01 | 0.82 | y = 16.38x + 3.061 |

Table 8. S₂₇₅₋₂₉₅ vs leachate volume linear regression analysis output

| Treatment | df | <i>F</i> | <i>p</i> | <i>R</i> ² | Equation |
|-----------|------|----------|----------|-----------------------|---------------------------|
| All | 1,64 | 5.34 | 0.02 | 0.06 | $y = -0.00073x + 0.01389$ |
| S | 1,9 | 13.62 | <0.01 | 0.60 | $y = -0.00086x + 0.01448$ |
| BC1% | 1,9 | 12.03 | <0.01 | 0.57 | $y = -0.00091x + 0.01459$ |
| BC10% | 1,9 | 90.28 | <0.01 | 0.91 | $y = -0.00144x + 0.01359$ |
| S+F | 1,9 | 3.19 | 0.11 | 0.26 | $y = 0.00045x + 0.01320$ |
| BC1%+F | 1,9 | 1.79 | 0.21 | 0.17 | $y = -0.00035x + 0.01410$ |
| BC10%+F | 1,9 | 92.82 | <0.01 | 0.91 | $y = -0.00127x + 0.01345$ |

4.7 Figures

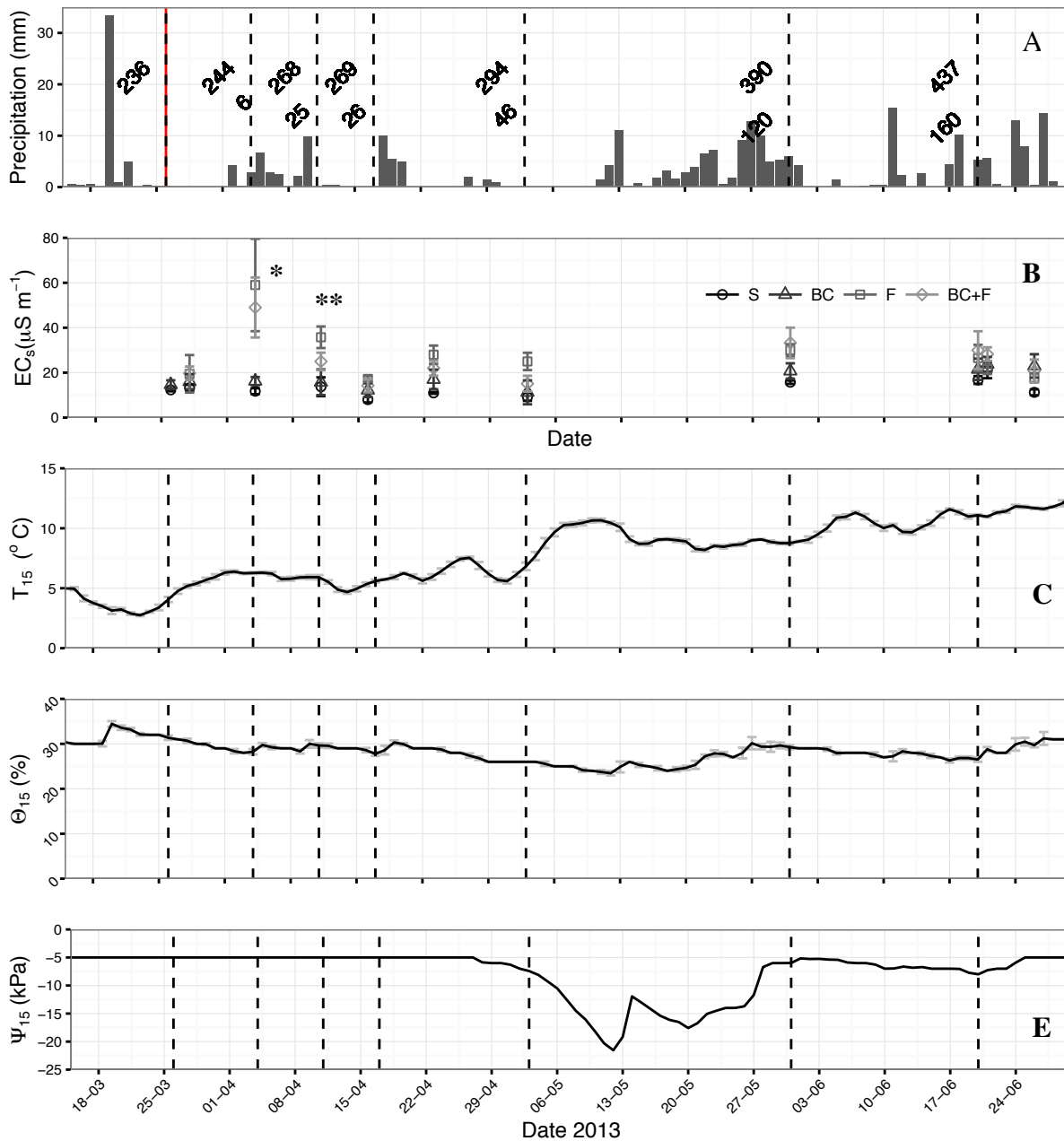


Figure 15. Suction cup lysimeter (SCL) sample date (dashed lines) daily (month-day) soil climate at 15-cm depth. (A) Daily precipitation with cumulative precipitation prior to each sample date is provided above and below this the cumulative amount of precipitation since fertilization; (B) Treatment EC_s , mean (± 1 SE), 1 and 2 asterisks indicates where one way ANOVA detected statistical differences between treatments at $p < 0.01$ and $p < 0.5$ respectively; (C) Soil temperature, site mean (± 1 standard deviation); (D) Volumetric soil water content site mean (± 1 SD); (E) Soil water matric potential, site mean (± 1 SD). In plots B-E values shown are the mean values from soil sensors with one in each of 12 plots, evenly distributed between treatments. The red dashed line indicates timing of fertilization.

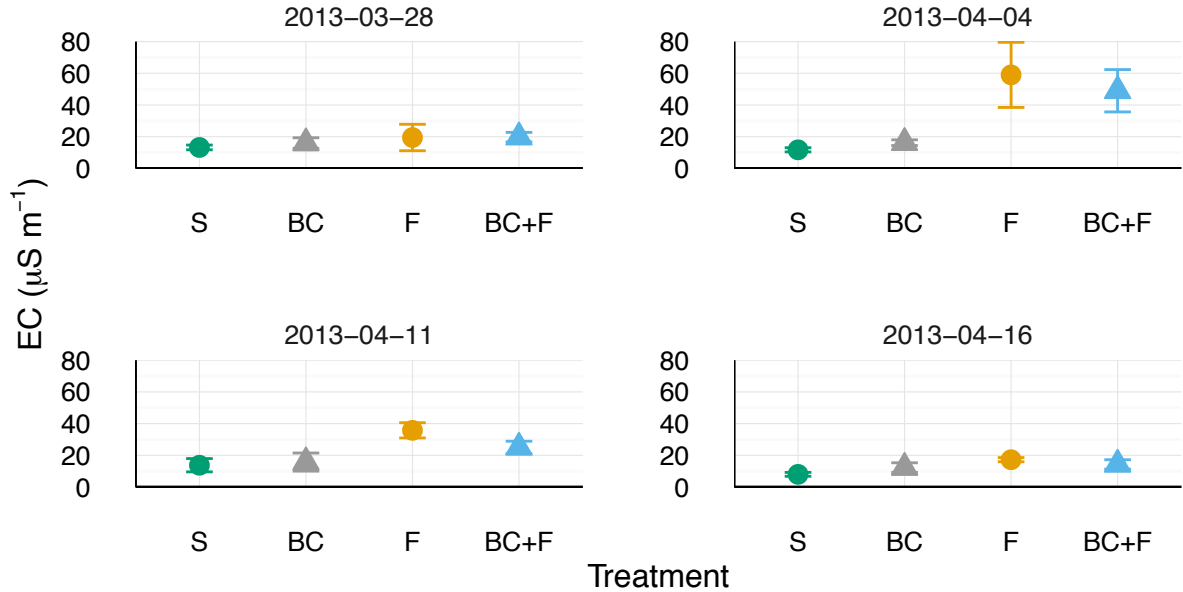


Figure 16. Field sample date treatment surface EC measurements, mean (± 1 standard error). (i) 2-days. (ii) 9-days. (iii) 16-days and (iv) 21-days after fertilization on 26 March 2013. There is a significant response to fertilization in F and BC+F treatment plots 9-days and less so 16-days after fertilization.

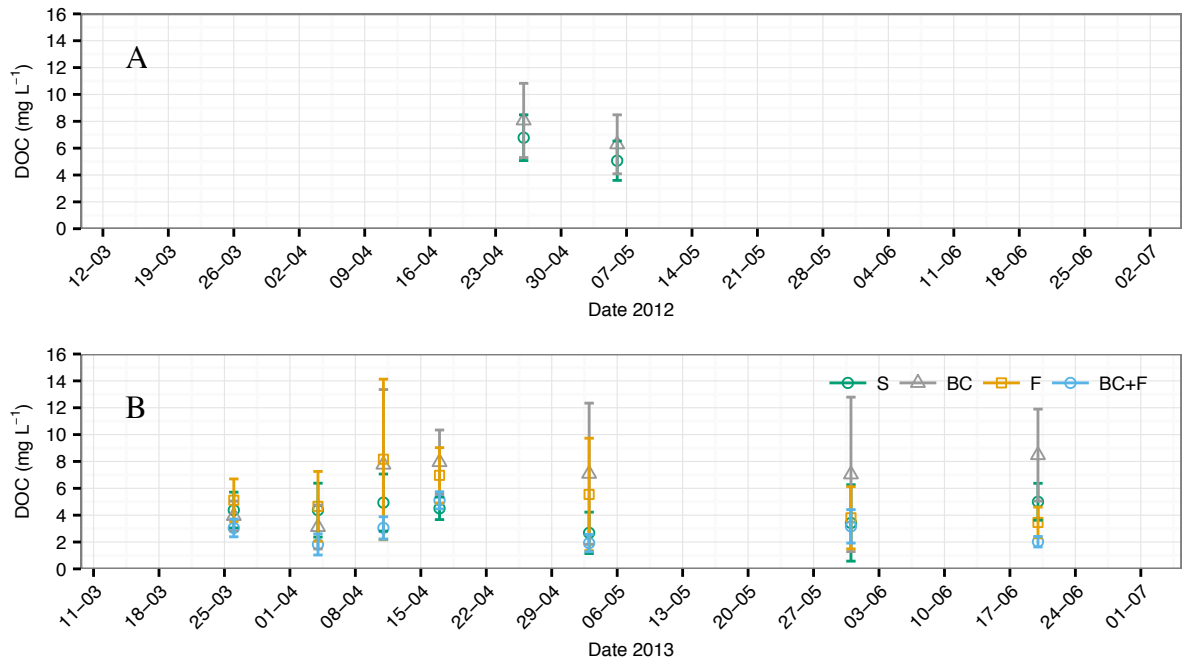


Figure 17. Field sample date treatment mean DOC_{SCL} (± 1 standard error). (A) 2012; (B) 2013

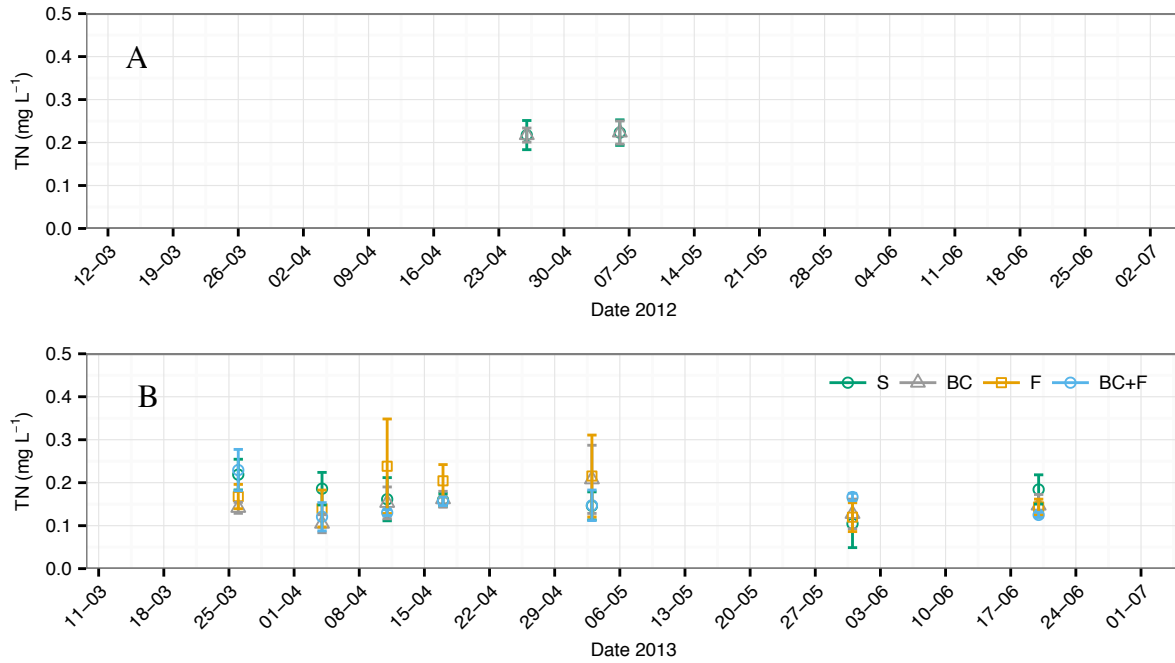


Figure 18. Field sample date (month-day) treatment mean TN (± 1 standard error). (A) 2012; (B) 2013

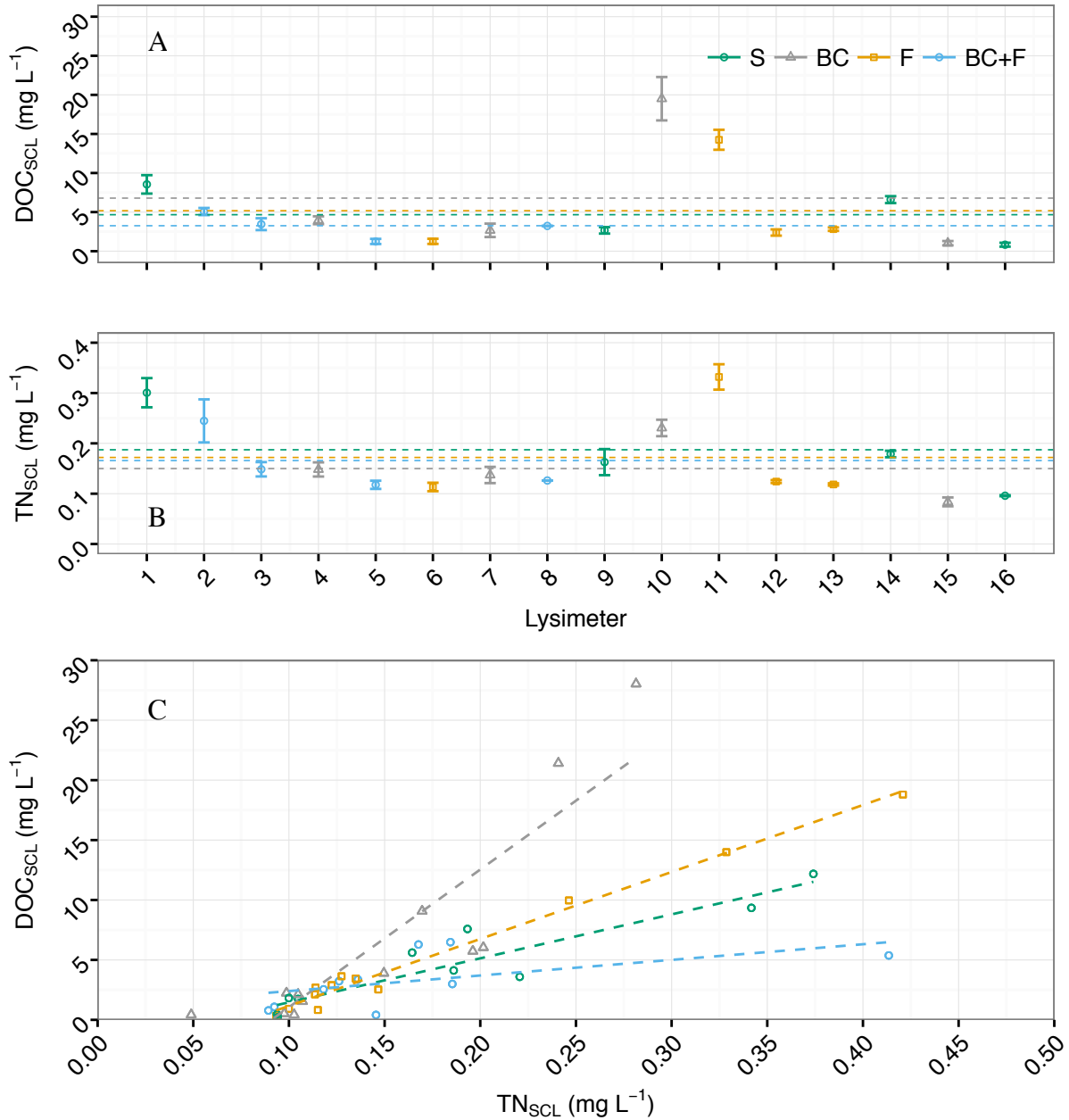


Figure 19. Suction cup lysimeter mean (± 1 standard error) DOC and TN observations from data collected during 2013 (A) DOC_{SCL}; (B) TN_{SCL}; (C) Treatment DOC vs TN analysis. Colored dashed lines in panels (A) and (B) indicate the treatment to be used as an aid to identifying dataset outliers.

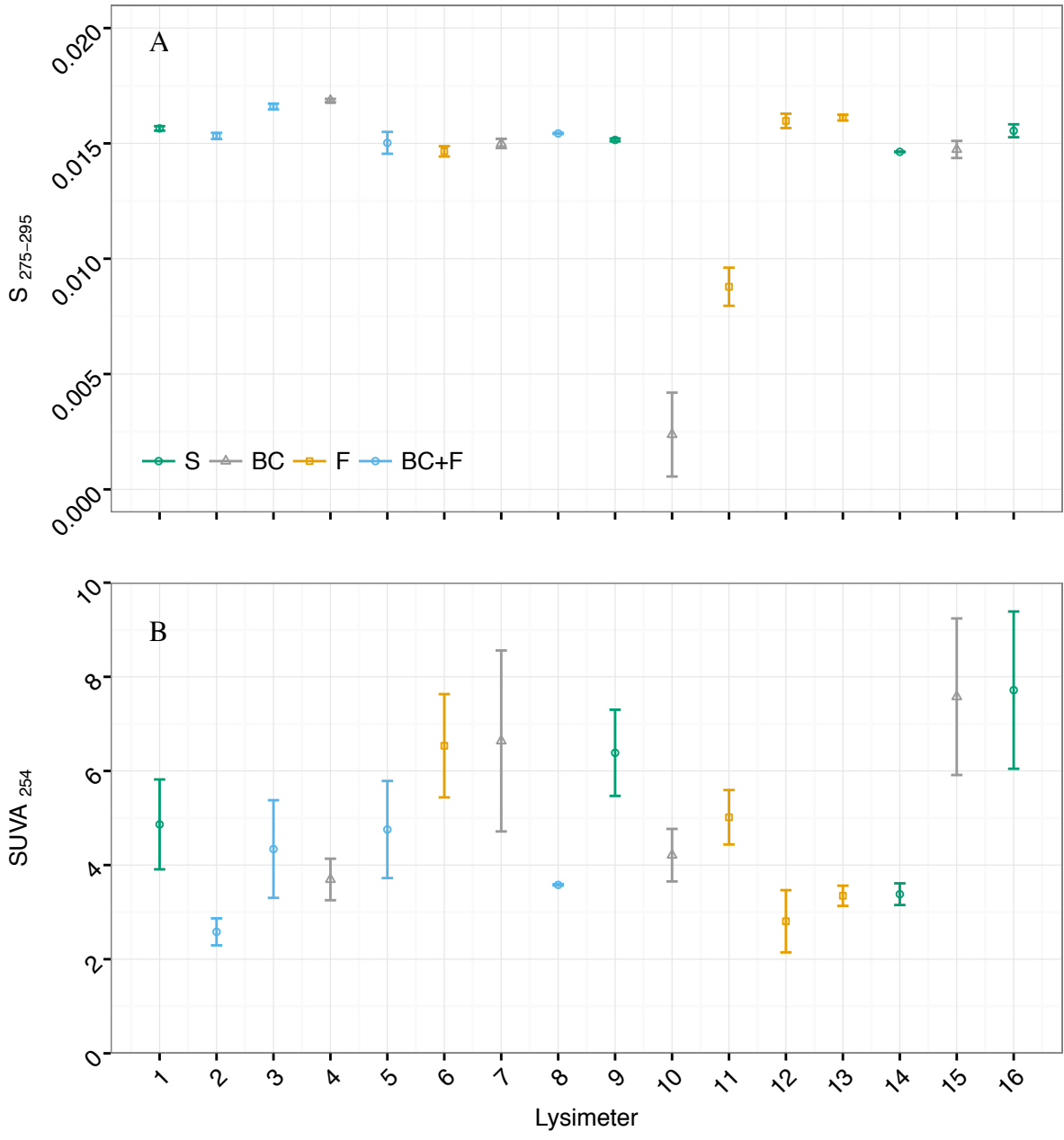


Figure 20. Suction cup lysimeter mean (± 1 standard error) (A) $S_{275-295}$; (B) $SUVA_{254}$

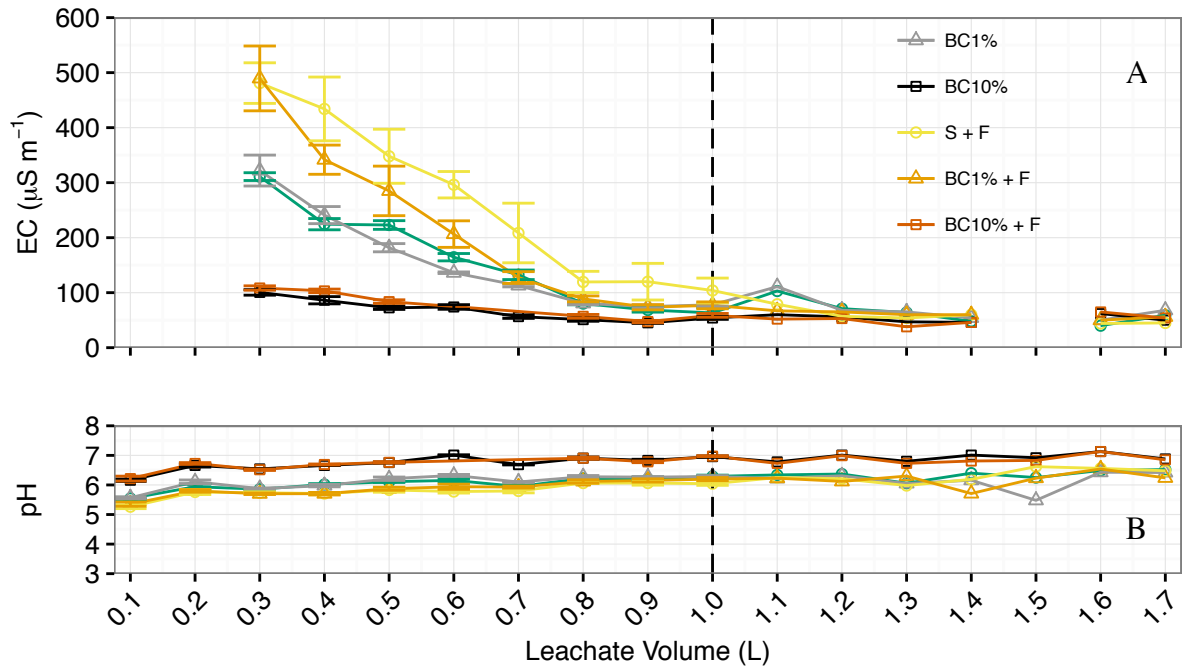


Figure 21. Soil incubation pore water treatment mean EC (A) and pH (B) measurements over the course of the leaching experiment. Error bars indicate one standard error.

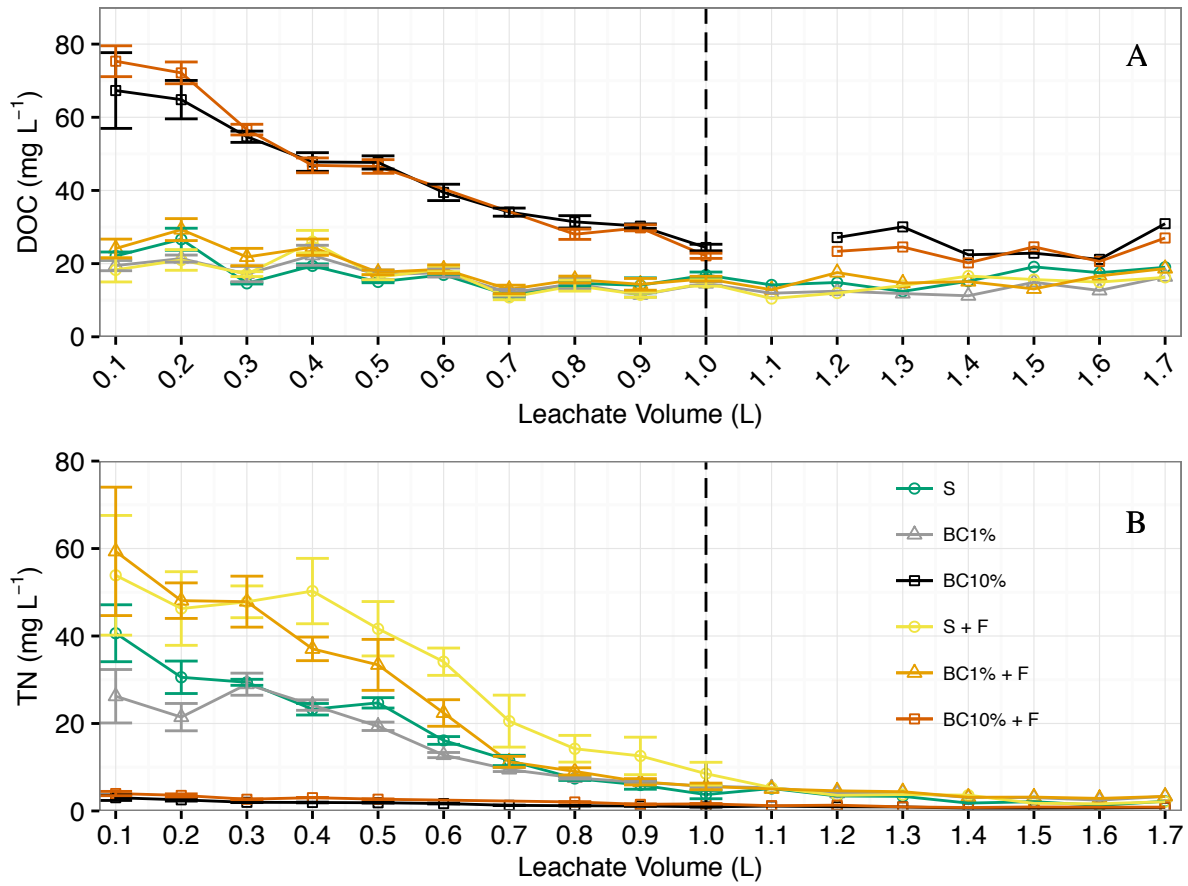


Figure 22. Soil incubation pore water treatment mean DOC (A) and TN (B) measurements over the course of the leaching experiment. Error bars indicate one standard error.

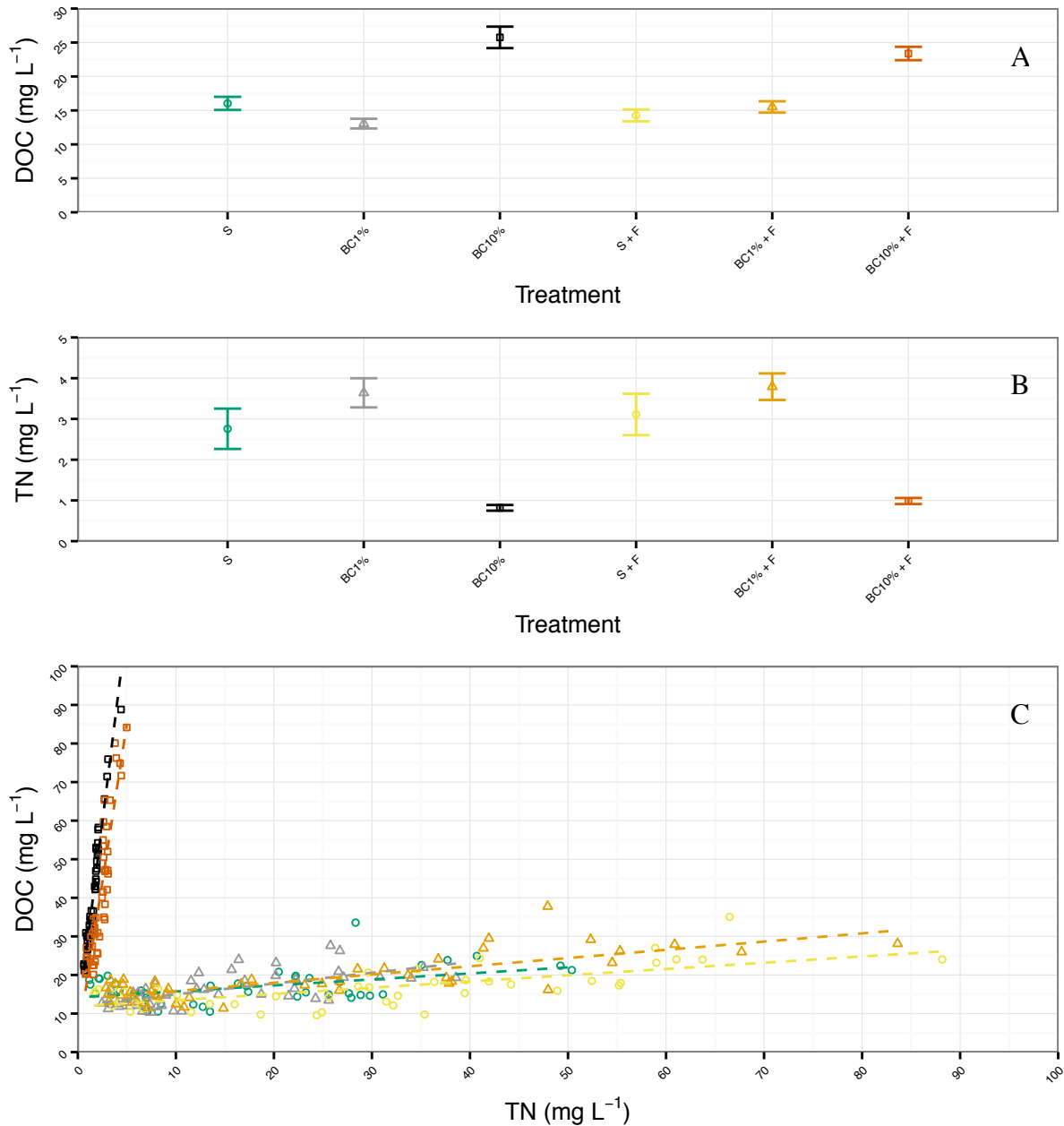


Figure 23. Soil incubation pore water treatment boxplots of (A) DOC and (B) TN after >1 L volume of leachate collected. Error bars are one standard error. (C) Relationship between DOC and TN. The coloured dashed lines are the lines of best fit for each treatment following treatment color conventions in (A) and (B).

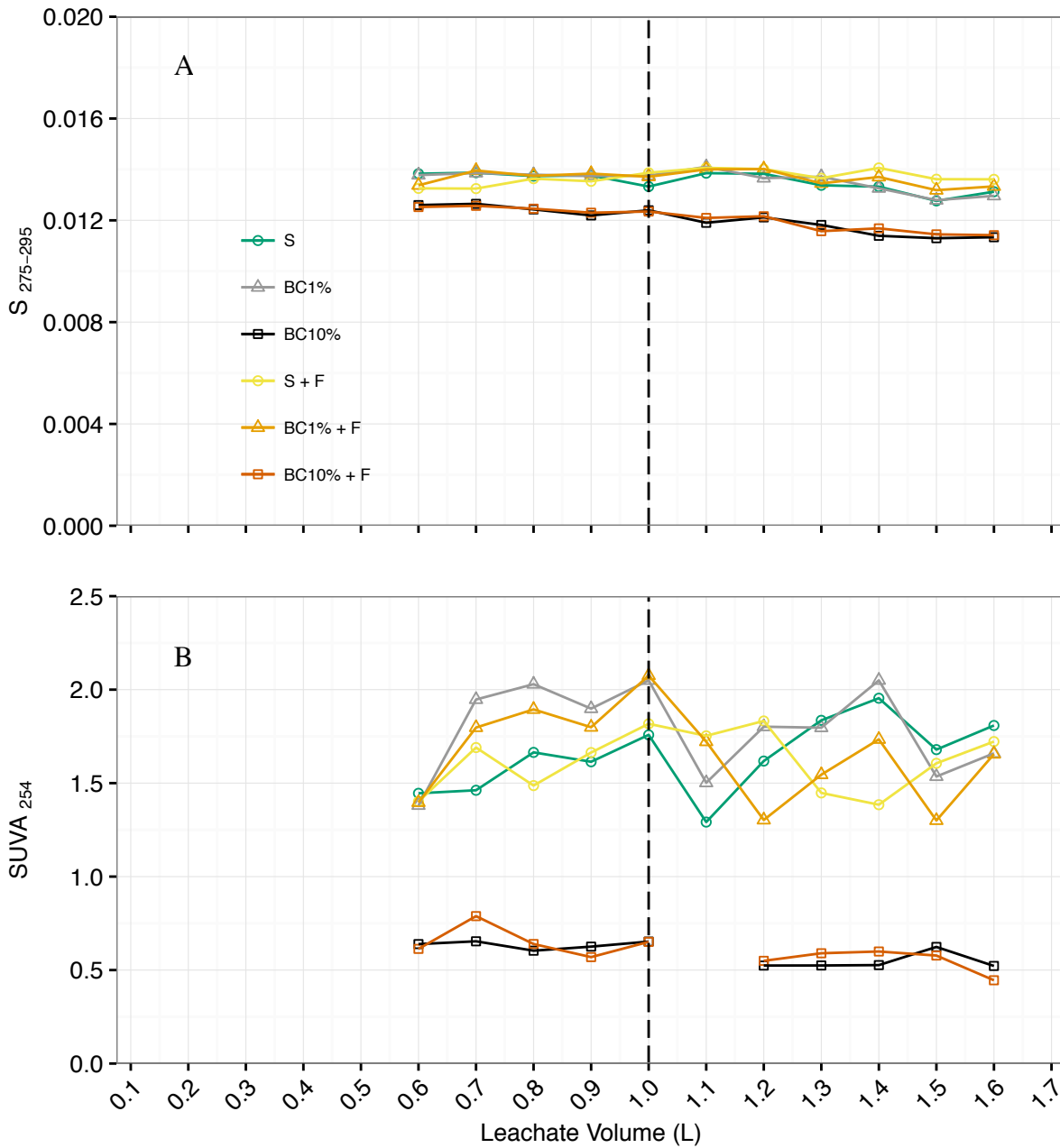


Figure 24. Soil incubation pore water treatment UV-Vis spectroscopy-based indicators of DOC quality (A) $S_{275-295}$ and (B) $SUVA_{254}$

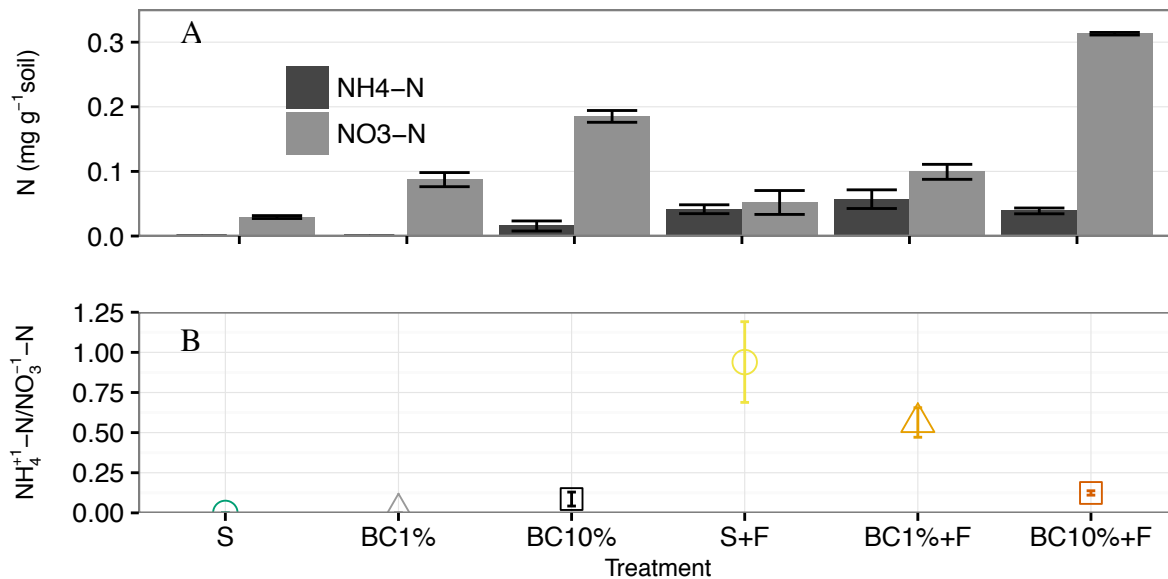


Figure 25. (A) Amount of nitrogen species (NH₄⁺-N and NO₃⁻-N) remaining in soil following the soil incubation experiment for each treatment; (B) Mean treatment ratio of nitrogen species (NH₄-N/NO₃-N). Error bars are one standard error.

Chapter 5: Summary and conclusions

This thesis describes the effects of biochar application on CH₄, N₂O and CO₂ fluxes for a forest soil on the west coast of Canada in relation to fertilizer use. In the laboratory soil incubation study described in Chapter 2, biochar application at high (10%) application rates increased CO₂ and N₂O emissions when applied without urea-N fertilizer, and decreased CH₄ uptake with and without fertilization. Furthermore, biochar application with urea-N fertilization did not increase CO₂ emissions compared to biochar-amended soil without fertilization. This is important given that CO₂ contributed > 97% of the CO_{2e} measured in the laboratory experiment. Regardless of the increased CO₂ emissions detected after biochar application, the treatment with the longest time interval for which C sequestration resulting from biochar additions would be negated by increased total CO_{2e} of GHG emissions from the soil was the BC10%+F at 17.7 years. This was slightly longer than the value calculated for the BC10% treatment (16.3 years), suggesting that biochar helps reduce soil CO₂ emission when fertilizer is applied.

As a result of the low impact on CO_{2e} from N₂O and CH₄ in this system, these results did not significantly change when using the stronger global warming potentials (GWPs) for the 20-year residency time period compared to the GWP over a 100-year period. It should be noted that the short-term laboratory incubation study did not account for important effects from changing climatic conditions, changes in biochar and soil interactions over time, or plant-root interactions. The field study (Chapter 3) was conducted to better understand these influences. As a result of CO₂ fluxes remaining high, the low rates of biochar application in the field study did not appear to significantly improve the climate benefit of C sequestration in this soil (6.7 years), and with fertilization (BC1%+F), the climate benefit of biochar to soil was reduced to just 3.9 years of equivalent C sequestration, when using mean CO₂ flux values from all of the data.

In the field study, soil CO₂ emissions were strongly controlled by soil temperature. This relationship was found to be stronger after fertilization, suggesting that the partitioning between autotrophic and heterotrophic respiration can vary with different treatments. It was determined that the effect of adding low amounts of Douglas-fir derived biochar to the surface of the dominant soil type (humoferric podzol) supporting Douglas-fir stand growth on the west coast of Canada would have little effect on GHG emissions and their total CO₂e fluxes. It was concluded over all that low rates of biochar addition to this forest soil would improve soil C sequestration in the soil, with or without fertilization.

The carbon sequestration potentials discussed in this work do not take into account the amount of direct CO₂ loss to the atmosphere that were avoided through biochar conversion rather than on site burning or any improvements to stand productivity that could be realized from liming of the acidic soils and N-species (NH₄⁺ and NO₃⁻) retention favourable for Douglas-fir growth possibly realized when higher rates of biochar are applied.

Combining studies in the field and in the laboratory (Chapter 4) was a productive way to determine the effects of biochar application on dissolved organic concentrations of C and total N in leachate in relation to fertilizer application. Regardless of increased CO₂ and DOC losses in the laboratory incubation experiment with higher biochar additions, there was still 50% more TOC remaining in the soil/biochar mixture after the incubation experiment, with or without fertilization, when compared to the lower biochar treatment. From the laboratory study it was concluded that carbon sequestration potential is increased by adding biochar to a disturbed forest soil of this kind. The results for TN presented were interesting as they showed that higher rates of biochar application likely suppress TN leaching and over time, although it may also increase

nitrification rates leading to more loss of applied N during periods of heavy rain and rapid percolation.

From the laboratory soil greenhouse gas emission and flushing experiments, it was concluded that gains could be small with regards to carbon sequestration potential by adding biochar in a single large application to a disturbed forest soil of this kind, as the net CO₂ efflux rates were increased along with DOC losses, although the latter was very small, and was less than 1% loss over the course of the experiment.

Recommendations for field application resulting from this study are to apply multiple small amounts, perhaps 10 x 5 t ha⁻¹, of biochar spaced out over time, while monitoring DOC leaching to minimize early flush losses and maximize carbon retention resulting from biochar applications. Given that the fertilization in the field was only detected as an increase in soil surface electrical conductivity and not in leachate C and N measurements suggests that managing biochar applications more specifically for carbon sequestration through direct increases in soil carbon and not leachate reduction may be a relevant focus when working in N-deficient undisturbed soils.

5.1 Future work

Voltaire is reported to have said, “it is not the answer you give, but the questions you ask”, which the author takes as the premise that we are never finished scientific research. In Chapter 3 a disparity between N₂O and CH₄ fluxes measured at the field site in this work and those measured by Jassal et al. (2008, 2010, 2011) at another research site close-by (200 m away) after fertilization were identified. The N₂O fluxes measured by the author were considerably smaller and did not indicate any increase following fertilization, regardless of a clear spike in EC_s after fertilization documented in Chapter 4. Also, no fertilization effect was

observed when analyzing TN data from field leachate, which suggests that it did not percolate down to this depth or was lost to deeper percolation or as gaseous N.

To properly address this, the author believes that another independent study directly investigating N₂O and CH₄ fluxes after fertilization utilizing an improved automated chamber system capable of high frequency measurements, supplemented with careful soil microbial population profiling could help to discern treatment effects. Additionally, there is a need to better understand the effect of increasing the rate of application of biochar on the measured greenhouse gas fluxes in this study.

It was stated in Chapter 3 that without a more thorough knowledge of the impact on stand productivity, it is difficult to ascertain through investigation of soils alone whether the effects of biochar application in combination with fertilization on stand productivity resulted in an increase in C sequestration. Based on the results of this investigation, it is possible that biochar would increase C-sequestration by 15% during the first year after fertilization compared to fertilization in the absence of biochar application. That is, the increase in stand C sequestration of a Douglas-fir forest resulting from fertilization estimated by Jassal et al. (2008) of 64% (3.3 to 5.3 Mg-C ha⁻¹ yr⁻¹) following fertilization could be increased by applying biochar to result in a total annual C sequestration of 5.9 Mg-C ha⁻¹. Ideally, this would be confirmed through the adoption of suitable methodologies such as eddy covariance and a larger scale application of biochar.

5.2 Overall significance

In this thesis, a fast effective laboratory method for quantifying fluxes of CO₂, CH₄ and N₂O resulting from different biochar application rates with and without N fertilization was developed. Furthermore, this technique allowed quantification of differences in soil pore water DOC and TN. The method was described at the Western Silvicultural Contractors Association

Annual General Meeting (Feb 2017) where private companies and government agencies expressed interest in using it.

The results presented herein show promise for incorporating biochar production and application into the current forest economy of BC, and of Canada as a whole. First Nations, private companies and government land managers have expressed interest in using this information to guide large-scale pilot studies in British Columbia. The author has been invited to participate in a working group to assemble this information.

This thesis provides the first study of a potential holistic biochar system, evaluating the potential to make environmentally beneficial uses of residual materials remaining following forest harvest. At present, forest harvest residues are typically burned in British Columbia, reducing air quality, diminishing soil carbon stocks, and increasing the greenhouse gas loading to the atmosphere. As an alternative, these forest harvest residual materials can be converted via pyrolysis to biochar, and returned to forest soils when incorporated into existing silvicultural techniques along with ongoing forest fertilization practices.

References

- Aber, J. D., Magill, A., McNulty, S. G., Boone, R. D., Nadelhoffer, K. J., Downs, M., & Hallett, R. (1995). Forest biogeochemistry and primary production altered by nitrogen saturation. *Water, Air, and Soil Pollution*, 85(3), 1665-1670, doi: 10.1007/BF00477219
- Aber, J., McDowell, W., Nadelhoffer, K., Magill, A., Berntson, G., Kamakea, M., McNulty, S., Currie, W., Rustad, L., and Fernandez, I., (1998), Nitrogen Saturation in Temperate Forest Ecosystems, *BioScience* 48, no. 11: 921-34, doi:10.2307/1313296.
- Barton, L., B. Wolf, D. Rowlings, C. Scheer, R. Kiese, P. Grace, K. Stefanova, and K. Butterbach-Bahl (2015), Sampling frequency affects estimates of annual nitrous oxide fluxes, *Scientific Reports*, 5, 15912, doi:10.1038/srep15912
- British Columbia Ministry of Forests and Range (BCMFR) (2007), Coastal Forest Action Plan, BC Min. For. Range, Victoria, BC. www.for.gov.bc.ca/mof/CoastalPlan/cap07.pdf (Last accessed 10 Jan 2011).
- Bodelier, P. L.E. and Laanbroek, H. J. (2004), Nitrogen as a regulatory factor of methane oxidation in soils and sediments. *FEMS Microbiology Ecology*, 47: 265–277. doi:10.1016/S0168-6496(03)00304-0.
- Bodelier, P. L. E., P. Rosley, T. Henckel, and P. Frenzel (2000), Stimulation by ammonium-based fertilizers of methane oxidation in soil around rice roots, *Nature*, 403(6768), 421-424. Doi:10.1038/35000193.
- Brewer, C. E., V. J. Chuang, C. A. Masiello, H. Gonnermann, X. Gao, B. Dugan, L. E. Driver, P. Panzacchi, K. Zygourakis, and C. A. Davies (2014), New approaches to measuring biochar density and porosity, *Biomass and Bioenergy*, 66, 176-185, doi:10.1016/j.biombioe.2014.03.059.
- British Columbia. Ministry of Environment (2012), British Columbia Greenhouse Gas Inventory Report 2012. Retrieved from: www2.gov.bc.ca/assets/gov/environment/climate-change/reports-and-data/provincial-ghg-inventory-report-bcs-pir/pir-2012-full-report.pdf (Last accessed 8 Feb 2017).

- Brodowski, S., John, B., Flessa, H & Amelung, W (2006), Aggregate-occluded black carbon in soil. *European Journal of Soil Science*, 57, 539-546. doi:10.1111/j.1365-2389.2006.00807.x.
- Case, S. D. C., N. P. McNamara, D. S. Reay, A. W. Stott, H. K. Grant, and J. Whitaker (2015), Biochar suppresses N₂O emissions while maintaining N availability in a sandy loam soil, *Soil Biology & Biochemistry*, 81, 178-185, doi:10.1016/j.soilbio.2014.11.012.
- Cayuela, M. L., L. van Zwieten, B. P. Singh, S. Jeffery, A. Roig, and M. A. Sánchez-Monedero (2014), Biochar's role in mitigating soil nitrous oxide emissions: A review and meta-analysis, *Agriculture, Ecosystems & Environment*, 191, 5-16, doi: 10.1016/j.agee.2013.10.009.
- Cayuela, M. L., O. Oenema, P. J. Kuikman, R. R. Bakker, and J. W. Van Groenigen (2010), Bioenergy by-products as soil amendments? Implications for carbon sequestration and greenhouse gas emissions, *GCB Bioenergy*, 2(4), 201-213, doi:10.1111/j.1757-1707.2010.01055.x.
- Cayuela, M. L., M. A. Sánchez-Monedero, A. Roig, K. Hanley, A. Enders, and J. Lehmann (2013), Biochar and denitrification in soils: when, how much and why does biochar reduce N₂O emissions?, *Scientific Reports*, 3, 1732, doi:10.1038/srep01732
- Cayuela, M. L., L. van Zwieten, B. P. Singh, S. Jeffery, A. Roig, and M. A. Sánchez-Monedero (2014), Biochar's role in mitigating soil nitrous oxide emissions: A review and meta-analysis, *Agriculture, Ecosystems & Environment*, 191, 5-16, doi: 10.1016/j.agee.2013.10.009.
- Chapuis-Lardy, L., Wrage, N., Metay, A., Chotte, J-L. and Bernoux, M. 2007. Soils, a sink for N₂O? A review. *Global Change Biology*, 13,1-17. doi: 10.1111/j.1365-2486.2006.01280.x.
- Chappell, H. N., D. W. Cole, S. P. Gessel, and R. B. Walker (1991), Forest fertilization research and practice in the Pacific Northwest, *Fertilizer research*, 27(1), 129-140, doi:10.1007/bf01048615.

- Chen, H., B. Zheng, Y. Song, and Y. Qin (2011), Correlation between molecular absorption spectral slope ratios and fluorescence humification indices in characterizing CDOM, *Aquatic Sciences*, 73(1), 103-112, doi:10.1007/s00027-010-0164-5.
- Chen, J. M., A. Govind, O. Sonnentag, Y. Zhang, A. Barr, and B. Amiro (2006), Leaf area index measurements at Fluxnet-Canada forest sites, *Agricultural and Forest Meteorology*, 140(1–4), 257-268, doi: 10.1016/j.agrformet.2006.08.005.
- Chin, Y.P., G. Aiken, and E. O'Loughlin (1994), Molecular Weight, Polydispersity, and Spectroscopic Properties of Aquatic Humic Substances, *Environmental Science & Technology*, 28(11), 1853-1858, doi:10.1021/es00060a015.
- Chintala, R., et al. (2014), Molecular characterization of biochars and their influence on microbiological properties of soil, *Journal of Hazardous Materials*, 279, 244-256, doi:10.1016/j.jhazmat.2014.06.074.
- Christiansen, J. R., J. Outhwaite, and S. M. Smukler (2015), Comparison of CO₂, CH₄ and N₂O soil-atmosphere exchange measured in static chambers with cavity ring-down spectroscopy and gas chromatography, *Agricultural and Forest Meteorology*, 211–212, 48-57, doi:10.1016/j.agrformet.2015.06.004.
- Cleveland, C. C., and D. Liptzin. (2007), C:N:P stoichiometry in soil: is there a “Redfield ratio” for the microbial biomass? *Biogeochemistry* 85:235–252, doi: 10.1007/s10533-007-9132-0.
- Clough, T. J., and Condon, L. M. (2010), Biochar and the nitrogen cycle: introduction. *Journal of Environmental Quality*, 39(4):1218-23, doi:10.2134/jeq2010.0204.
- Cross, A., and S. P. Sohi (2011), The priming potential of biochar products in relation to labile carbon contents and soil organic matter status, *Soil Biology and Biochemistry*, 43(10), 2127-2134, doi:10.1016/j.soilbio.2011.06.016.
- Dai, X., T. W. Boutton, B. Glaser, R. J. Ansley, and W. Zech (2005), Black carbon in a temperate mixed-grass savanna, *Soil Biology and Biochemistry*, 37(10), 1879-1881, doi:10.1016/j.soilbio.2005.02.021.
- Davidson, E. A., and I. A. Janssens (2006), Temperature sensitivity of soil carbon decomposition and feedbacks to climate change, *Nature*, 440(7081), 165-173, doi:10.1038/nature04514

- Davidson EA, Belk E, and Boone RD (1998), Soil water content and temperature as independent or confounded factors controlling soil respiration in a temperate mixed hardwood forest, *Global Change Biology*, 4, 217–227, doi:10.1046/j.1365-2486.1998.00128.x.
- de Ruiter G, S. H. a. M. R. (2014), Industrial and Market Development of Biochar in British Columbia, *White Paper series of the Pacific Institute for Climate Solutions Rep.*, 21 pp.
- Del Grosso, S. J., et al. (2000), General CH₄ oxidation model and comparisons of CH₄ oxidation in natural and managed systems, *Global Biogeochemical Cycles*, 14(4), 999-1019, doi:10.1029/1999GB001226.
- Diaz-Ravina, M., Acea, M. J., and Carballas, T. (1995), Seasonal changes in microbial biomass and nutrient flush in forest soils. *Biology and Fertility of Soils*, 199:220-226, doi:10.1007/BF00336163.
- Downie A., Munroe, P. & Crosky, A. (2012) Chapter 2: Characteristics of Biochar-Physical and Structural Properties. In J. Lehmann & S. Joseph (Eds.), *Biochar for Environmental Management: Science and Technology*. Earthscan. Pg. 13-29. ISBN: 978-1-84407-658-1.
- Drewitt, G. B., T. A. Black, Z. Nesic, E. R. Humphreys, E. M. Jork, R. Swanson, G. J. Ethier, T. Griffis, and K. Morgenstern (2002), Measuring forest floor CO₂ fluxes in a Douglas-fir forest, *Agricultural and Forest Meteorology*, 110(4), 299-317, doi:10.1016/S0168-1923(01)00294-5.
- Eberwein, J. R., P. Y. Oikawa, L. A. Allsman, and G. D. Jenerette (2015), Carbon availability regulates soil respiration response to nitrogen and temperature, *Soil Biology and Biochemistry*, 88, 158-164, doi:10.1016/j.soilbio.2015.05.014.
- Evans, L. J., and W. G. Wilson (1985), Extractable Fe, Al, Si and C in B Horizons of Podzolic and Brunisolic soils from Ontario, *Canadian Journal of Soil Science*, 65(3), 489-496, doi:10.4141/cjss85-052.
- Eykelbosh, A. J., M. S. Johnson, E. S. de Queiroz, H. J. Dalmagro, and E. G. Couto (2014), Biochar from Sugarcane Filtercake Reduces Soil CO₂ Emissions Relative to Raw Residue and Improves Water Retention and Nutrient Availability in a Highly-Weathered Tropical Soil, *Plos One*, 9(6), doi:10.1371/journal.pone.0098523.

- Fang, Y., B. P. Singh, and B. Singh (2014), Temperature sensitivity of biochar and native carbon mineralisation in biochar-amended soils, *Agriculture, Ecosystems & Environment*, 191, 158-167, doi:10.1016/j.agee.2014.02.018.
- Fleck, D., He, Y., Alexander, C., Jacobson, G., Cunningham, K.L. (2013), AN034: Simultaneous soil flux measurements of five gases – N₂O, CH₄, CO₂, NH₃, and H₂O – with the Picarro G2508 1–11. Picarro Inc., Santa Clara, CA, USA. Retrieved from: <https://picarro.app.box.com/s/z2gpj3hpl11xye9csz6mdpixltcli5hl> (Last accessed 8 Feb 2017)
- Foley, J. A., DeFries, R., Asner, G. P., Barford, C., Bonan, G., Carpenter, S. R., Chapin, F. S., Coe, M. T., Daily, G. C., Gibbs, H. K., Helkowski, J. H., Holloway, T., Howard, E. A., Kucharik, C. J., Monfreda, C., Patz, J. A., Prentice, I. C., Ramankutty, N., Snyder, P. K. (2005), Global Consequences of Land Use, *Science*, 309(5734), 570-574, doi:10.1126/science.1111772.
- Fox, R.H., and L.D. Hoffman. 1981. The effect of N fertilizer source on grain yield, N uptake, soil pH, and lime requirement in no till corn, *Journal of Agronomy*, 73:891-895, doi:10.2134/agronj1981.00021962007300050032x
- Frey, S. D., M. Knorr, J. L. Parrent, and R. T. Simpson (2004), Chronic nitrogen enrichment affects the structure and function of the soil microbial community in temperate hardwood and pine forests, *Forest Ecology and Management*, 196(1), 159-171, doi: 10.1016/j.foreco.2004.03.018.
- Fuentes, M., G. González-Gaitano, and J. M. García-Mina (2006), The usefulness of UV–visible and fluorescence spectroscopies to study the chemical nature of humic substances from soils and composts, *Organic Geochemistry*, 37(12), 1949-1959, doi:10.1016/j.orggeochem.2006.07.024.
- Goldman, M. B., P. M. Groffman, R. V. Pouyat, M. J. McDonnell, and S. T. A. Pickett (1995), CH₄ uptake and N availability in forest soils along an urban to rural gradient, *Soil Biology and Biochemistry*, 27(3), 281-286, doi:10.1016/0038-0717(94)00185-4.

- Gundale, M. J., and T. H. DeLuca (2006), Temperature and source material influence ecological attributes of ponderosa pine and Douglas-fir charcoal, *Forest Ecology and Management*, 231(1–3), 86-93, doi:10.1016/j.foreco.2006.05.004.
- Gurwick, N. P., L. A. Moore, C. Kelly, and P. Elias (2013), A systematic review of biochar research, with a focus on its stability in situ and its promise as a climate mitigation strategy, *PLoS ONE*, 8(9), e75932, doi:10.1371/journal.pone.0075932.
- Hanley, D. P., H. N. Chappell, and E. H. Nadelhoffer (1996), Fertilizing coastal Douglas-fir forests, Bull. 1800, Wash. State Univ. Ext., Pullman, Wash.
- Harter, J., H.-M. Krause, S. Schuettler, R. Ruser, M. Fromme, T. Scholten, A. Kappler, and S. Behrens (2014), Linking N₂O emissions from biochar-amended soil to the structure and function of the N-cycling microbial community, *The ISME Journal*, 8(3), 660-674, doi:10.1038/ismej.2013.160.
- Hartley, W., P. Riby, and J. Waterson (2016), Effects of three different biochars on aggregate stability, organic carbon mobility and micronutrient bioavailability, *Journal of Environmental Management*, 181, 770-778, doi:10.1016/j.jenvman.2016.07.023.
- Helms John R. Stubbins Aron Ritchie Jason D. Minor Elizabeth C. Kieber David J. Mopper Kenneth, (2008), Absorption spectral slopes and slope ratios as indicators of molecular weight, source, and photobleaching of chromophoric dissolved organic matter, *Limnology and Oceanography*, 53, doi:10.4319/lo.2008.53.3.0955.
- Hiltbrunner, D., Zimmermann, S., Karbin, S., Hagedorn, F., & Niklaus, P. A. (2012). Increasing soil methane sink along a 120-year afforestation chronosequence is driven by soil moisture. *Global Change Biology*, 18(12), 3664-3671. doi:10.1111/j.1365-2486.2012.02798.x.
- Houghton, R. A. (2000), Interannual variability in the global carbon cycle, *Journal of Geophysical Research*, 105(D15), 20121–20130, doi:10.1029/2000JD900041.
- Howard, J.A. and Howard, D.M. (1979) Respiration of decomposing litter in relation to temperature and moisture. *Oikos*, 33, 457-465. doi: 10.2307/3544334
- Hutchinson, G. L., and G. P. Livingston (2001), Vents and seals in non-steady-state chambers used for measuring gas exchange between soil and the atmosphere, *European Journal of*

- Soil Science*, 52(4), 675-682, doi:10.1046/j.1365-2389.2001.00415.x. Hu, H.-W., D. Chen, and J.-Z. He (2015), Microbial regulation of terrestrial nitrous oxide formation: understanding the biological pathways for prediction of emission rates, *Fems Microbiology Reviews*, 39(5), 729-749, doi:10.1093/femsre/fuv021.
- Humphreys, E. R., T. A. Black, K. Morgenstern, T. Cai, G. B. Drewitt, Z. Nestic, and J. A. Trofymow (2006), Carbon dioxide fluxes in coastal Douglas-fir stands at different stages of development after clearcut harvesting, *Agricultural and Forest Meteorology*, 140(1-4), 6-22, doi:10.1016/j.agrformet.2006.03.018.
- International Biochar Initiative (2012), International Biochar Initiative (IBI) Standardized Product Definition and Testing Guidelines for Biochar that is used in Soil, IBI (2012), p. 47
- Inubushi, K., S. Otake, Y. Furukawa, N. Shibasaki, M. Ali, A. M. Itang, and H. Tsuruta (2005), Factors influencing methane emission from peat soils: Comparison of tropical and temperate wetlands, *Nutrient Cycling in Agroecosystems*, 71(1), 93-99, doi:10.1007/s10705-004-5283-8.
- IPCC (2014), Climate Change 2014: Synthesis Report. Contribution of Working Groups I, II and III to the Fifth Assessment Report of the Intergovernmental Panel on Climate Change Rep., 151 pp, IPCC, Geneva, Switzerland.
- Jiang, X., M. L. Haddix, and M. F. Cotrufo (2016), Interactions between biochar and soil organic carbon decomposition: Effects of nitrogen and low molecular weight carbon compound addition, *Soil Biology and Biochemistry*, 100, 92-101, doi: 10.1016/j.soilbio.2016.05.020.
- Jamieson, T., E. Sager, and C. Guéguen (2014), Characterization of biochar-derived dissolved organic matter using UV-visible absorption and excitation-emission fluorescence spectroscopies, *Chemosphere*, 103, 197-204, doi: 10.1016/j.chemosphere.2013.11.066.
- Jassal, R., A. Black, M. Novak, K. Morgenstern, Z. Nestic, and D. Gaumont-Guay (2005), Relationship between soil CO₂ concentrations and forest-floor CO₂ effluxes, *Agricultural and Forest Meteorology*, 130(3-4), 176-192, doi:10.1016/j.agrformet.2005.03.005.

- Jassal, R. S., T. A. Black, T. Cai, K. Morgenstern, Z. Li, D. Gaumont-Guay, and Z. Nestic (2007), Components of ecosystem respiration and an estimate of net primary productivity of an intermediate-aged Douglas-fir stand, *Agricultural and Forest Meteorology*, 144(1–2), 44–57, doi:10.1016/j.agrformet.2007.01.011.
- Jassal, R. S., T. A. Black, B. Z. Chen, R. Roy, Z. Nestic, D. L. Spittlehouse, and J. A. Trofymow (2008), N₂O emissions and carbon sequestration in a nitrogen-fertilized Douglas fir stand, *Journal of Geophysical Research-Biogeosciences*, 113(G4), doi:10.1029/2008jg000764.
- Jassal, R. S., T. A. Black, J. A. Trofymow, R. Roy, and Z. Nestic (2010), Soil CO₂ and N₂O flux dynamics in a nitrogen-fertilized Pacific Northwest Douglas-fir stand, *Geoderma*, 157(3–4), 118–125, doi:10.1016/j.geoderma.2010.04.002.
- Jassal, R. S., T. A. Black, T. Cai, G. Ethier, S. Pepin, C. Brümmer, Z. Nestic, D. L. Spittlehouse, and J. A. Trofymow (2010), Impact of nitrogen fertilization on carbon and water balances in a chronosequence of three Douglas-fir stands in the Pacific Northwest, *Agricultural and Forest Meteorology*, 150(2), 208–218, doi:10.1016/j.agrformet.2009.10.005.
- Jassal, R. S., T. A. Black, R. Roy, and G. Ethier (2011), Effect of nitrogen fertilization on soil CH₄ and N₂O fluxes, and soil and bole respiration, *Geoderma*, 162(1–2), 182–186, doi:10.1016/j.geoderma.2011.02.002.
- Jassal, R. S., T. A. Black, Z. Nestic, and D. Gaumont-Guay (2012), Using automated non-steady-state chamber systems for making continuous long-term measurements of soil CO₂ efflux in forest ecosystems, *Agricultural and Forest Meteorology*, 161, 57–65, doi:10.1016/j.agrformet.2012.03.009.
- Jassal, R. S., M. S. Johnson, M. Molodovskaya, T. A. Black, A. Jollymore, and K. Sveinson (2015), Nitrogen enrichment potential of biochar in relation to pyrolysis temperature and feedstock quality, *Journal of Environmental Management*, 152, 140–144, doi:10.1016/j.jenvman.2015.01.021.
- Jeffery, S., F. G. A. Verheijen, C. Kammann, and D. Abalos (2016), Biochar effects on methane emissions from soils: A meta-analysis, *Soil Biology and Biochemistry*, 101, 251–258, doi:10.1016/j.soilbio.2016.07.021.

- Jollymore, A., M. S. Johnson, and I. Hawthorne (2012), Submersible UV-Vis Spectroscopy for Quantifying Streamwater Organic Carbon Dynamics: Implementation and Challenges before and after Forest Harvest in a Headwater Stream, *Sensors*, 12(4), 3798.
- Karhu, K., T. Mattila, I. Bergström, and K. Regina (2011), Biochar addition to agricultural soil increased CH₄ uptake and water holding capacity – Results from a short-term pilot field study, *Agriculture, Ecosystems & Environment*, 140(1–2), 309-313, doi:10.1016/j.agee.2010.12.005.
- μKnorr, M., Frey, S. D. and Curtis, P. S. (2005), Nitrogen additions and litter decomposition: A meta-analysis, *Ecology*, 86: 3252–3257. doi:10.1890/05-0150
- Koehler, B., M. D. Corre, E. Veldkamp, and J. P. Sueta (2009), Chronic nitrogen addition causes a reduction in soil carbon dioxide efflux during the high stem-growth period in a tropical montane forest but no response from a tropical lowland forest on a decadal time scale, *Biogeosciences*, 6(12), 2973-2983, doi:10.5194/bg-6-2973-2009.
- Kolb, S. E., K. J. Fermanich, and M. E. Dornbush (2009), Effect of Charcoal Quantity on Microbial Biomass and Activity in Temperate Soils. *Soil Science Society of America Journal*, 73(4), 1173-1181, doi:10.2136/sssaj2008.0232.
- Kruse, C. W., and N. Iversen (1995), Effect of plant succession, ploughing, and fertilization on the microbiological oxidation of atmospheric methane in a heathland soil, *FEMS Microbiology Ecology*, 18(2), 121-128, doi:10.1016/0168-6496(95)00048-F.
- Kuzyakov, Y. (2006), Sources of CO₂ efflux from soil and review of partitioning methods, *Soil Biology and Biochemistry*, 38(3), 425-448, doi:10.1016/j.soilbio.2005.08.020.
- Lal, R. (2004), Soil Carbon Sequestration Impacts on Global Climate Change and Food Security, *Science*, 304(5677), 1623-1627, doi:10.1126/science.1097396.
- Lan, Z. M., C. R. Chen, M. R. Rashti, H. Yang, and D. K. Zhang (2017), Stoichiometric ratio of dissolved organic carbon to nitrate regulates nitrous oxide emission from the biochar-amended soils, *Science of The Total Environment*, 576, 559-571, doi:10.1016/j.scitotenv.2016.10.119.
- Lashof, D.A. and Ahuja, D.R., 1990. Relative contributions of greenhouse gas emissions to global warming. *Nature*, 344(6266), doi:10.1038/344529a0

- Lehmann, J., and S. Joseph (2012), Biochar for Environmental Management: Science and Technology. Earthscan. Pg. 13-29. ISBN: 978-1-84407-658-1.
- Lehmann, J., M. C. Rillig, J. Thies, C. A. Masiello, W. C. Hockaday, and D. Crowley (2011), Biochar effects on soil biota - A review, *Soil Biology & Biochemistry*, 43(9), 1812-1836, doi:10.1016/j.soilbio.2011.04.022.
- Lehmann, J. (2007), A handful of carbon, *Nature*, 447(7141), 143-144, doi:10.1038/447143a.
- Levy-Booth, D. J., C. E. Prescott, J. R. Christiansen, and S. J. Grayston (2016), Site preparation and fertilization of wet forests alter soil bacterial and fungal abundance, community profiles and CO₂ fluxes, *Forest Ecology and Management*, 375, 159-171, doi:10.1016/j.foreco.2016.05.033.
- Liang, B., et al. (2006), Black Carbon Increases Cation Exchange Capacity in Soils, *Soil Science Society of America Journal*, 70(5), 1719-1730, doi:10.2136/sssaj2005.0383.
- Lim, T. J., K. A. Spokas, G. Feyereisen, and J. M. Novak (2016), Predicting the impact of biochar additions on soil hydraulic properties, *Chemosphere*, 142, 136-144, doi:10.1016/j.chemosphere.2015.06.069.
- Lin, Y., P. Munroe, S. Joseph, and R. Henderson (2012), Migration of dissolved organic carbon in biochars and biochar-mineral complexes, *Pesquisa Agropecuária Brasileira*, 47, 677-686, doi:10.1590/S0100-204X2012000500007
- Liu, L. and Greaver, T.L., (2009). A review of nitrogen enrichment effects on three biogenic GHGs: the CO₂ sink may be largely offset by stimulated N₂O and CH₄ emission. *Ecology Letters*, 12(10): 1103-1117, doi:10.1111/j.1461-0248.2009.01351.x.
- Liu, Y., M. Yang, Y. Wu, H. Wang, Y. Chen, and W. Wu (2011), Reducing CH₄ and CO₂ emissions from waterlogged paddy soil with biochar, *Journal of Soils and Sediments*, 11(6), 930-939, doi:10.1007/s11368-011-0376-x.
- Liu, L., Y. Wang, X. Yan, J. Li, N. Jiao, and S. Hu (2017), Biochar amendments increase the yield advantage of legume-based intercropping systems over monoculture, *Agriculture, Ecosystems & Environment*, 237, 16-23, doi:10.1016/j.agee.2016.12.026.

- Liu, S. W., Y. J. Zhang, Y. J. Zong, Z. Q. Hu, S. Wu, J. Zhou, Y. G. Jin, and J. W. Zou (2016), Response of soil carbon dioxide fluxes, soil organic carbon and microbial biomass carbon to biochar amendment: a meta-analysis, *Global Change Biology Bioenergy*, 8(2), 392-406, doi:10.1111/gcbb.12265.
- Lloyd, J., & Taylor, J. (1994), On the Temperature Dependence of Soil Respiration, *Functional Ecology*, 8(3), 315-323. doi:10.2307/2389824.
- Lousier, J. Daniel, Holger Brix, Rob Brockley, Reid Carter and Valin Marshall (1991) Improving Forest Fertilization Decision-Making in British Columbia. Published by Research Branch, Ministry of Forests, Victoria, BC, Canada.
- Major, J., J. Lehmann, M. Rondon, and C. Goodale (2010), Fate of soil-applied black carbon: downward migration, leaching and soil respiration, *Global Change Biology*, 16(4), 1366-1379, doi:10.1111/j.1365-2486.2009.02044.x.
- Masiello, C. A., Y. Chen, X. Gao, S. Liu, H.-Y. Cheng, M. R. Bennett, J. A. Rudgers, D. S. Wagner, K. Zygourakis, and J. J. Silberg (2013), Biochar and Microbial Signaling: Production Conditions Determine Effects on Microbial Communication, *Environmental Science & Technology*, 47(20), 11496-11503, doi:10.1021/es401458s.
- Montzka, S.A., Dlugokencky, E.J. and Butler, J.H. (2011), Non-CO₂ greenhouse gases and climate change. *Nature*, 476(7358): 43-50, doi:10.1038/nature10322.
- Morgenstern, K., Black, T.A., Humphreys, E.R., Griffis, T.J., Drewitt, G.B., Cai, T., Nesic, Z., Spittlehouse, D.L., Livingston N.J., (2004), Sensitivity and uncertainty of the carbon balance of a Pacific Northwest Douglas-fir forest during an El Niño/La Niña cycle, *Agricultural and Forest Meteorology*. 123: 201-219, doi:10.1016/j.agrformet.2003.12.003
- Mukherjee, A., A. R. Zimmerman, and W. Harris (2011), Surface chemistry variations among a series of laboratory-produced biochars, *Geoderma*, 163(3-4), 247-255, doi:10.1016/j.geoderma.2011.04.021.
- Mukherjee, A., and A. R. Zimmerman (2013), Organic carbon and nutrient release from a range of laboratory-produced biochars and biochar-soil mixtures, *Geoderma*, 193-194(0), 122-130, doi:10.1016/j.geoderma.2012.10.002.

- Natural Resources Canada. (2017, April 14). Infographic: Canada's forest by numbers. Retrieved from <http://www.nrcan.gc.ca/forests/report/17563>.
- Nguyen, T. T. N., C.-Y. Xu, I. Tahmasbian, R. Che, Z. Xu, X. Zhou, H. M. Wallace, and S. H. Bai (2017), Effects of biochar on soil available inorganic nitrogen: A review and meta-analysis, *Geoderma*, 288, 79-96, doi:10.1016/j.geoderma.2016.11.004.
- Novak, J. M., I. Lima, B. Xing, J. W. Gaskin, C. Steiner, K. Das, M. Ahmedna, D. Rehrh, D. W. Watts, and W. J. Busscher (2009), Characterization of designer biochar produced at different temperatures and their effects on a loamy sand, *Annals of Environmental Science*, 3(1), 2. Retrieved from <http://openjournals.neu.edu/aes/journal/article/view/v3art5>.
- Pan, Y., et al. (2011), A Large and Persistent Carbon Sink in the World's Forests, *Science*, 333(6045), 988-993, doi:10.1126/science.1201609.
- Papen H., Daum M., Steinkamp R. and Butterbach-Bahl K. (2001), N₂O and CH₄-fluxes from soils of a N-limited and N-fertilized spruce forest ecosystem of the temperate zone. *Journal of Applied Botany= Angewandte Botanik* 75: 159–163. Retrieved from <http://publica.fraunhofer.de/documents/N-38130.html>.
- Parton, W. J., A. R. Mosier, D. S. Ojima, D. W. Valentine, D. S. Schimel, K. Weier, and A. E. Kulmala (1996), Generalized model for N₂ and N₂O production from nitrification and denitrification, *Global Biogeochemical Cycles*, 10(3), 401-412, doi:10.1029/96gb01455.
- Paul-Limoges, E., T. A. Black, A. Christen, Z. Nestic, and R. S. Jassal (2015), Effect of clearcut harvesting on the carbon balance of a Douglas-fir forest, *Agricultural and Forest Meteorology*, 203, 30-42, doi:10.1016/j.agrformet.2014.12.010.
- Pedersen, A. R., S. O. Petersen, and K. Schelde (2010), A comprehensive approach to soil-atmosphere trace-gas flux estimation with static chambers, *European Journal of Soil Science*, 61(6), 888-902, doi:10.1111/j.1365-2389.2010.01291.x.
- Peng, Q., Y. Qi, Y. Dong, S. Xiao, and Y. He (2011), Soil nitrous oxide emissions from a typical semiarid temperate steppe in inner Mongolia: effects of mineral nitrogen fertilizer levels and forms, *Plant and Soil*, 342(1), 345-357, doi:10.1007/s11104-010-0699-1.

- Peterson St-Laurent, G., S. Hagerman, and G. Hoberg (2017), Emergence and influence of a new policy regime: The case of forest carbon offsets in British Columbia, *Land Use Policy*, 60, 169-180, doi:10.1016/j.landusepol.2016.10.025.
- Pojar, J., K. Klinka, and D. Meidinger, (1987), Biogeoclimatic ecosystem classification in British Columbia, *Forest Ecology and Management*, 22: 119-154.
- Prescott, C.E., McDonald, M.A., Gessel, S.P., Kimmins, J.P., (1993), Long-term effects of sewage sludge and inorganic fertilizers on nutrient turnover in litter in a coastal Douglas-fir forest, *Forest Ecology and Management* 59, 149–164, doi:10.1016/0378-1127(93)90076-Y.
- Prommer, J., et al. (2014), Biochar Decelerates Soil Organic Nitrogen Cycling but Stimulates Soil Nitrification in a Temperate Arable Field Trial, *PLoS ONE*, 9(1), e86388, doi:10.1371/journal.pone.0086388.
- Raich, J. W., and C. S. Potter (1995), Global patterns of carbon dioxide emissions from soils, *Global Biogeochemical Cycles*, 9(1), 23-36, doi:10.1029/94GB02723\
- R Core Team (2016). R: A language and environment for statistical computing. R Foundation for Statistical Computing, Vienna, Austria. URL <https://www.R-project.org/>.
- Ryan, M. G., and B. E. Law (2005), Interpreting, measuring, and modeling soil respiration, *Biogeochemistry*, 73(1), 3-27, doi:10.1007/s10533-004-5167-7.
- Sackett, T. E., N. Basiliko, G. L. Noyce, C. Winsborough, J. Schurman, C. Ikeda, and S. C. Thomas (2015), Soil and greenhouse gas responses to biochar additions in a temperate hardwood forest, *Global Change Biology Bioenergy*, 7(5), 1062-1074, doi:10.1111/gcbb.12211.
- Sagrilo, E., S. Jeffery, E. Hoffland, and T. W. Kuyper (2015), Emission of CO₂ from biochar-amended soils and implications for soil organic carbon, *Global Change Biology Bioenergy*, 7(6), 1294-1304, doi:10.1111/gcbb.12234.
- Schiller, C. L., and D. R. Hastie (1996), Nitrous oxide and methane fluxes from perturbed and unperturbed boreal forest sites in northern Ontario, *Journal of Geophysical Research: Atmospheres*, 101(D17), 22767-22774, doi:10.1029/96JD01620.

- Shrestha, R. K., B. D. Strahm, E. B. Sucre, S. M. Holub, and N. Meehan (2014), Fertilizer Management, Parent Material, and Stand Age Influence Forest Soil Greenhouse Gas Fluxes, *Soil Science Society of America journal*, 78(6), 2041-2053, doi:10.2136/sssaj2014.03.0118.
- Singh, B., B. P. Singh, and A. L. Cowie (2010), Characterisation and evaluation of biochars for their application as a soil amendment, *Australian Journal of Soil Research*, 48(6-7), 516-525, doi:10.1071/sr10058.
- Sloan, S., and J. A. Sayer (2015), Forest Resources Assessment of 2015 shows positive global trends but forest loss and degradation persist in poor tropical countries, *Forest Ecology and Management*, 352, 134-145, doi:10.1016/j.foreco.2015.06.013.
- Smebye, A., V. Alling, R. D. Vogt, T. C. Gadmar, J. Mulder, G. Cornelissen, and S. E. Hale (2016), Biochar amendment to soil changes dissolved organic matter content and composition, *Chemosphere*, 142, 100-105, doi:10.1016/j.chemosphere.2015.04.087.
- Smith, K. A., T. Ball, F. Conen, K. E. Dobbie, J. Massheder, and A. Rey (2003), Exchange of greenhouse gases between soil and atmosphere: interactions of soil physical factors and biological processes, *European Journal of Soil Science*, 54(4), 779-791, doi:10.1046/j.1351-0754.2003.0567.x.
- Sohi, S. P., E. Krull, E. Lopez-Capel, and R. Bol (2010), A review of biochar and its use and function in soil, in *Advances in Agronomy, Vol 105*, edited by D. L. Sparks, pp. 47-82, doi:10.1016/s0065-2113(10)05002-9.
- Spittlehouse, D. L. (2003), Water Availability, Climate Change and the Growth of Douglas-Fir in the Georgia Basin, *Canadian water resources journal*, 28(4), 673-688, doi:10.4296/cwrj2804673.
- Spokas, K. A., and D. C. Reicosky (2009), Impacts of sixteen different biochars on soil greenhouse gas production, *Annals of Environmental Science*, 3(1), 4. Retrieved from <http://openjournals.neu.edu/aes/journal/article/view/v3art4>.
- Spokas, K. A., W. C. Koskinen, J. M. Baker, and D. C. Reicosky (2009), Impacts of woodchip biochar additions on greenhouse gas production and sorption/degradation of two

- herbicides in a Minnesota soil, *Chemosphere*, 77(4), 574-581, doi:10.1016/j.chemosphere.2009.06.053.
- Spokas, K. A. (2010), Review of the stability of biochar in soils: predictability of O:C molar ratios, *Carbon Management*, 1(2), 289-303, doi:10.4155/cmt.10.32.
- Spokas, K. A. (2013), Impact of biochar field aging on laboratory greenhouse gas production potentials, *Global Change Biology Bioenergy*, 5(2), 165-176, doi:10.1111/gcbb.12005.
- Steinbeiss, S., G. Gleixner, and M. Antonietti (2009), Effect of biochar amendment on soil carbon balance and soil microbial activity, *Soil Biology and Biochemistry*, 41(6), 1301-1310, doi:10.1016/j.soilbio.2009.03.016.
- Thomas, S. C., and N. Gale (2015), Biochar and forest restoration: a review and meta-analysis of tree growth responses, *New Forests*, 46(5), 931-946, doi:10.1007/s11056-015-9491-7.
- Thomazini, A., K. Spokas, K. Hall, J. Ippolito, R. Lentz, and J. Novak (2015), GHG impacts of biochar: Predictability for the same biochar, *Agriculture, Ecosystems & Environment*, 207, 183-191, doi:10.1016/j.agee.2015.04.012.
- Usowicz, B., J. Lipiec, M. Łukowski, W. Marczewski, and J. Usowicz (2016), The effect of biochar application on thermal properties and albedo of loess soil under grassland and fallow, *Soil and Tillage Research*, 164, 45-51, doi:10.1016/j.still.2016.03.009.
- Van Zwieten, L., Kammann, C, MariaLuz Cayuela, Singh, B-P, Joseph S, Kimber, S, Clough, T, Spokas, K. (2009), Biochar effects emissions of non-CO2 GHGs from soil, in *Biochar for Environmental Management: Science and Technology*, edited by L. J. a. J. S., pp. 227-249, Earthscan, Washington, DC.
- Van Zwieten, L., S. Kimber, S. Morris, K. Y. Chan, A. Downie, J. Rust, S. Joseph, and A. Cowie (2010), Effects of biochar from slow pyrolysis of papermill waste on agronomic performance and soil fertility, *Plant and Soil*, 327(1-2), 235-246, doi:10.1007/s11104-009-0050-x.
- Van Zwieten, L., S. Kimber, S. Morris, A. Downie, E. Berger, J. Rust, and C. Scheer (2010), Influence of biochars on flux of N2O and CO2 from Ferrosol, *Australian Journal of Soil Research*, 48(6-7), 555-568, doi:10.1071/sr10004.

- Wang, L. W., et al. (2015), The influence of nitrogen fertiliser rate and crop rotation on soil methane flux in rain-fed potato fields in Wuchuan County, China, *Science of the Total Environment*, 537, 93-99, doi:10.1016/j.scitotenv.2015.08.003.
- Weishaar, J. L., G. R. Aiken, B. A. Bergamaschi, M. S. Fram, R. Fujii, and K. Mopper (2003), Evaluation of Specific Ultraviolet Absorbance as an Indicator of the Chemical Composition and Reactivity of Dissolved Organic Carbon, *Environmental Science & Technology*, 37(20), 4702-4708, doi:10.1021/es030360x.
- Yanai, Y., K. Toyota, and M. Okazaki (2007), Effects of charcoal addition on N₂O emissions from soil resulting from rewetting air-dried soil in short-term laboratory experiments, *Soil Science & Plant Nutrition*, 53(2), 181-188, doi:10.1111/j.1747-0765.2007.00123.x.
- Yang, L., and Z. Cai (2005), The effect of growing soybean (*Glycine max. L.*) on N₂O emission from soil, *Soil Biology and Biochemistry*, 37(6), 1205-1209, doi:10.1016/j.soilbio.2004.08.027.
- Zhang, X., E. A. Davidson, D. L. Mauzerall, T. D. Searchinger, P. Dumas, and Y. Shen (2015), Managing nitrogen for sustainable development, *Nature*, 528(7580), 51-59, doi:10.1038/nature15743
- Zimmerman, A. R. (2010), Abiotic and Microbial Oxidation of Laboratory-Produced Black Carbon (Biochar), *Environmental Science & Technology*, 44(4), 1295-1301, doi:10.1021/es903140c.
- Zimmerman, A. R., B. Gao, and M.-Y. Ahn (2011), Positive and negative carbon mineralization priming effects among a variety of biochar-amended soils, *Soil Biology and Biochemistry*, 43(6), 1169-1179, doi:10.1016/j.soilbio.2011.02.005.

Appendices

Appendix 1 Site soil description

The site soil is classified as duric humo-ferric podzol from morainal origin with a Quimper gravelly-sandy-loam texture commencing below a variable litter-fermenting- humified (LFH) organic layer (0.09-0.193 cm).

Table 9. Soil characteristics literature review

| | |
|---|---------------------|
| Humphreys (1999) | |
| Bulk density (\pm SE) (upper 10 cm, kg m ⁻³) | 971 (\pm 221) |
| Drewitt (2002) | |
| Bulk density (\pm SE) (10-80 cm) (kg m ⁻³) | 1353 (\pm 51) |
| Soil porosity (10-80 cm, %) | 49.0 |
| Coarse fraction (> 2mm) | 31 |
| Jassal <i>et al.</i> , (2005) | |
| Bulk density (0-10 cm) (kg m ⁻³) | 1050 |
| Bulk density (50 cm) (kg m ⁻³) | 1500 |
| Humphreys <i>et al.</i> , (2006) | |
| Soil mineral fraction (m) | 0-1 |
| Texture | Gravelly loamy sand |
| Wilting point (m ³ m ⁻³) | 0.06 |
| Field capacity (m ³ m ⁻³) | 0.21 |
| Available water content (mm) | 150 |
| Soil mineral fraction (m) | 0 - 0.15 |
| C (mg g ⁻¹ dry soil) | 18-74 |
| N (mg g ⁻¹ dry soil) | 0.4-4.4 |
| ratio (L,M,H) | 45,19,17 |
| Surface organic horizons | |
| C (mg g ⁻¹ dry soil) | 244-527 |
| N (mg g ⁻¹ dry soil) | 6.8-16.5 |
| % (L,M,H) | 36,33,32 |
| Average thickness (m) | 0.09-0.193 |

A total of 12 soil core were taken from 3 locations spread around the perimeter of the biochar plots. At each location a trench approximately 30 cm x 30 cm was dug to 15 cm deep. From each of the four walls of the pit one bulk density core (7.3 cm diam. x 3.8 cm depth) was inserted horizontally 2-3 cm below the organic-mineral transition. Results of the measured soil characteristics are shown in Table 10, 11 and 12.

Table 10. Soil characteristics

| Bulk Density (kg m ⁻³) | Fine Fraction (<2mm) | Percent Coarse Fraction (>2mm) | Organic Matter Content (%) | Carbon Content (%) | Volume- weighted particle density (kg m ⁻³) | Porosity (m ⁻³ m ⁻³) |
|---------------------------------------|-------------------------|---|-------------------------------------|--------------------------|--|--|
| 1133.1 (133.6) | 46.1 (9.2) | 53.9 (9.2) | 6.8 (1.8) | 3.1 (0.8) | 2570.7 (17.4) | 0.559 (0.053) |

Table 11 Fine mineral fraction %

| Sand | Silt | Clay |
|------------|------------|-----------|
| 74.5(3.7) | 18.5 (3.5) | 7.0 (1.5) |

Table 12. Textural class soil organic matter content

| Textural Class | Soil Organic Matter (%) |
|----------------|-------------------------|
| Sand: | 5.1 |
| Silt: | 6.1 |
| Clay: | 12.5 |

Two additional soil pits (50 cm depth) were excavated at the site and two differing soil types thought to be associated with topography were identified. On flat areas the soil (S1) was found to be higher in organic matter and have a more gravelly-loamy-sand texture (27% coarse fraction (> 2 mm diameter)), less easily drained than that found on more sloping locations (S2) (53% coarse fraction > 2mm).

Additional soil was also collected from the same depth described above and brought back to the lab for use in an incubation experiment. This soil was analyzed for total organic carbon, cation exchange capacity, nitrate and ammonia concentrations and microbial abundance.

Appendix 2 Biochar details

The biochar particle size distribution described in Table 1 was produced using 1 cm chipped Douglas-fir woody materials from British Columbia heated in a pyrolysis oven to 420 °C for 32 min (Diacarbon Energy Inc. Canada). The resulting biochar has high carbon content (78.8%), low volatiles and ash content (18.8 & 2.4%, respectively). After production the char was transported to UBC in 55 gallon steel drums sealed from the atmosphere.

Table 13. Diacarbon Douglas-fir derived biochar particle size distribution

| Size Fraction (µm) | Average % of Sample (± 1Standard Deviation) |
|--------------------|---|
| >2000 | 5 (2) |
| 991-2000 | 17 (1) |
| 425-991 | 32 (4) |
| 250-425 | 13 (1) |
| 105-250 | 19 (2) |
| 53-105 | 7 (1) |
| <53 | 7 (4) |

Values in table 13 were determined after sieving four 100 g samples taken from three incremental depths in the biochar supply containers.

Appendix 3 Minimum detectable flux estimation

Using methodology outlined in Christiansen et al., (2015), the minimum detectable flux (*MDF*) was estimated for each gas. Briefly, the sensitivity of the sample collection and measurement procedure as characterized by the *MDF* is quantified by defining the minimum quantification limit (*MQL*), following Corley et al., (2003), where analytical accuracy is determined from multiple standard assessment as 3 x standard deviation x $t_{99\%}$ ($t_{99\%}$ taken from t-table at respective degrees of freedom) and the *MDF* was defined as the flux equivalent to the analytical precision of raw output divided by closure time:

$$MDF = \frac{A_a}{t_c} \times \frac{V \times P}{S \times R \times T} \quad (4)$$

where A_a is the analytical accuracy of the instrument (ppm), t_c is the closure time of the chamber in hours, V is the chamber volume (m^3) P is the atmospheric pressure (Pa), S is the chamber surface area (m^2), R is the ideal gas constant ($m^3 \text{ Pa K}^{-1} \text{ mol}^{-1}$) and T is the ambient air temperature (K).

The largest contribution to error in this study was likely due to sampling, storage and vial sampling and injection into the GC. Currently, following Christiansen et al., 2015 we were able to achieve an A_a of 13 ppm CO_2 , 0.0998 ppm for CH_4 and 0.013 ppm for N_2O from GC autosampler vial analysis. The A_a for our system from direct GC injections was 6 ppm CO_2 , 0.096 ppm CH_4 and 0.036 ppm N_2O . Notice the increase in A_a for direct injections compared to the autosampler for N_2O . This can be attributed to human error, due to unavoidable differences between manual injections (e.g., pace and force).

None of the CH₄ and N₂O emissions measured in the field were calculated to be above the MDF. Consequences in regards to the conclusions drawn from this thesis are inconsequential given their small contribution to the total CO_{2e} estimations. Methods for improving future studies would need to involve in-situ estimation using sensitive flow through detectors as mentioned in Chapter 5.

Appendix 4 Project instrumentation

Table 14. Field and laboratory equipment

| Manufacturer | Name | Detector/Hardware | Measurement | Symbol/acronym | Range | Units |
|--|--|--|---|----------------|----------------|-------|
| Decagon Devices Inc. | GS3 | Electrode resistance | Matric Potential | θ | | % |
| | | Electrode resistance | Bulk Electrical Conductivity | EC | | dS/m |
| | | Thermistor | Temperature | T | | °C |
| Decagon Devices Inc. | MPS-2 | Electrode resistance | Soil water potential | ψ | -5 to -500 | kPa |
| | | Thermistor | Temperature | T | -40 to +50 | °C |
| SoilMoisture Equipment Corp | L1900 | Suction cup lysimeter | Soil water sampler | SCL | 0 to 250 ml | ml |
| Campbell Scientific | CR1000 | Datalogger | Controls measurements and stores data | | | |
| University of British Columbia | Static Non- steady state chamber | PVC collar + Lid | Greenhouse gas in headspace (CH ₄ , CO ₂ , N ₂ O) | SNSS | | |
| EMD Millipore, Darmstadt, Germany | Soil incubation | Steri-fil® Aseptic filtration units | | | | |
| Agilent | 7890A GC | Flame ionisation detector + methanizer | [CH ₄], [CO ₂] | | | ppm |
| Agilent | 7890A GC | Electron Capture | N ₂ O | | | ppm |
| Shimadzu | TOC-V CSH | Nondispersive Infrared | TOC, NPOC IC = TC-NPOC | | | mg/l |
| Shimadzu | TNM-1 | Chemiluminescence | TN | | | mg/l |

Appendix 5 Site images



Figure 26. This image shows a slash piles in the foreground, with eight more visible in the background at a near-by (within 500 m of research location) harvested forest location that could have been feedstock for biochar production.



Figure 27. This image shows the slash piles burned to improve access for replanting and reduce forest fire hazard.



Figure 28. Research site soil profile.



Figure 29. This image shows a static non-steady state chamber between two large trees with the chamber lid on during a site greenhouse gas flux measurement campaign.



Figure 30. This image shows the ancillary GS3 instrument in use for surface soil electrical conductivity (EC_s), volumetric water content and temperature measurements in close proximity to a static non-steady state chamber collar. Also seen are 5 vials used for greenhouse gas sample storage in preparation for chamber flux measurements.



Figure 31. Biochar being hand applied on date of application (27th Feb 2012).



Figure 32. Completed biochar application, showing contrasting color with untreated surrounding area.